Identification of Molecular Targets for Brucein D and Metastasis Suppressor Genes in Cancer through MicroRNA and RNAi Screening

XIA, Tian

A Thesis Submitted in Partial Fulfilment

of the Requirements for the Degree of

Master of Philosophy

in

Medical Sciences

The Chinese University of Hong Kong

April 2012

Abstract of thesis entitled:

Identification of Molecular Targets for Brucein D and Metastasis Suppressor Genes in Cancer through MicroRNA and RNAi Screening

Submitted by XIA Tian

for the degree of Master of Philosophy in Medical Sciences

at The Chinese University of Hong Kong in April 2012

Abstract

MicroRNAs (miRNAs) are endogenous small non-coding RNAs that have been shown to play important roles in tumorigenesis. Brucein D (BD), a chemical compound isolated from Brucea javanica fruit, has previously been reported to have anti-cancer effect in pancreatic cancer. In this study, we showed that BD also inhibited the growth of liver cancer cells both in vitro and in vivo. To investigate whether BD exerts its anti-cancer effect through regulation of miRNAs, we performed a cancer miRNA qPCR array profiling. From the profiling, miR-95 was found to be significantly down-regulated after BD treatment. Subsequently, a pro-apoptotic gene CUGBP2 was identified as a direct downstream target of miR-95. These findings suggested BD suppressed liver cancer cell growth through down-regulation of miR-95 and reinforcing CUGBP2.

Pancreatic cancer is an aggressive malignancy with extremely poor prognosis. It is usually diagnosed when metastases are already present. To identify genes that play

critical roles in the processes of pancreatic cancer metastasis, a whole genome RNAi screening was performed. An shRNA library targeting all human genes was introduced into a human pancreatic cancer cell line capan-2. The infected cells were then transplanted into the pancreas of nude mice. Because capan-2 is of low metastatic potential, we hypothesized that knocking down of metastasis suppressor genes would facilitate capan-2 cells to spread to the liver. By retrieving shRNA templates from the liver metastatic nodules, several candidate genes were found. One of them, SOX9, has been validated as metastasis suppressor gene in vivo, implying that loss of expression of SOX9 promotes pancreatic cancer metastasis.

Chemotherapy is recommended for patients of pancreatic cancer in advanced stage. However, their response to the first-line chemotherapy drug gemcitabine is not satisfactory. A genome-wide RNAi screening was conducted to identify genes that were critical in chemotherapy resistance. Capan-2 cells containing the above shRNA library were applied for the screening under gemcitabine treatment. Through microarray analysis, a number of genes were screened as potential gemcitabine sensitivity genes. Validation experiments implied that the gene LLGL1 may play an important role in modulating pancreatic cancer cells' sensitivity to gemcitabine.

摘要

微小 RNA 是内源性小非编码 RNA，在肿瘤生成中扮演重要角色。Brucein D(BD)是一种 B. javanica 果实提取物，已被报道在胰腺癌中具有抗肿瘤作用。在此研究中，我们证明了 BD 在体内和体外均可抑制肝癌细胞生长。为了研究 BD 是否通过调节微小 RNA 来执行其抗肿瘤功能，我们进行了一个肿瘤微小 RNA 定量 PCR 阵列谱分析。此阵列包括 95 个已被报道与肿瘤有关的微小 RNA。通过对比 BD 处理前后微小 RNA 谱的变化，我们发现微小 RNA-95 在 BD 处理后被显著下调了。其后促凋亡的 CUGBP2 被确定为微小 RNA-95 的下游靶基因。

胰腺癌是一种预后很差的恶性肿瘤，常常在确诊时已发生转移。为了找出在胰腺癌转移过程中发挥决定性作用的基因，我们进行了全基因组范围的 RNA 干扰筛选。一个包含针对全部人类基因的 shRNA 文库被导入胰腺癌细胞系 capan-2.然后将这些细胞移植到裸鼠的胰腺中来建立一个原位胰腺癌小鼠模型。我们的假设是下调某个基因会促使低转移潜力的 capan-2 细胞转移到肝脏。通过从肝转移结节中回收 shRNA 模板，我们找到了几个推定的转移抑制基因。其中之一，SOX9，通过体内实验验证，证明下调 SOX9 基因的表达可促进胰腺癌转移。

化疗适用于进展期胰腺癌病人。然而他们对一线化疗药吉西他滨的反应并不乐观，这进一步使胰腺癌的预后变差。我们展开了一个全基因组范围的 RNA 干扰筛选来确定一些在化疗耐药过程中起关键作用的基因。携带上述 shRNA 文库的 capan-2 细胞被用于吉西他滨药物处理之下的筛选。通过微阵列分析，一些

基因被筛选成为可影响癌细胞对药物敏感性的潜在的靶基因。通过进一步验证，LLGL1 基因被确定为在调节癌细胞对化疗敏感性过程中起重要作用的基因。

Acknowledgements

I would like to take this opportunity to acknowledge the support of many people who made this dissertation possible. First of all, I would like to express my honest gratitude to my supervisor Prof. CHEN Yangchao in School of Biomedical Sciences for his excellent guidance and support to my work throughout these academic years. I specially appreciate for his marvelous patience, kindness, and forgiveness in guiding me through the mistakes I made during my study.

I would like to thank Prof. LIN Zhixiu for providing Brucein D as a key reagent in my project and for his valuable advice on the thesis revision.

I also want to deliver my sincere appreciation to all my wonderful team members. Special thanks to Wong Gigi who spent a lot of time helping me to prepare paraffin embedded sections, to Zhu Yinxin who kindly assisted me to conduct animal studies, to Wang Yi who spared valuable time with my IHC works, to Xiao Zhangang who offered great help in my molecular cloning works, and to Li Samson who shared useful ideas on designing screening scheme. Additionally, I would like to thank all the labmates in CSLB 214/218 who encouraged me when I came across difficulties and treasure every moment we were together.

Last but not the least, I would like to express my profound gratitude to my family for their support along the way and I shall dedicate my work to them.

Abbreviations

Abbreviation	Full name
AFB1	aflatoxin B1
APS	ammonium persulfate
ATP	adenosine 5’-triphosphate
BCA	bicinchoninic acid
BD	Brucein D
bp	base pair
BSA	bovine serum albumin
cDNA	complementary DNA
CpG	CpG island
CRC	Colorectal Cancer
Ctrl	Control
DAB	diaminobenzidine
DISC	death-inducing signaling complex
DMEM	Dulbecco’s modified Eagle’s medium
DMSO	dimethyl sulfoside
DNA	deoxyribonucleic acid
dNTP	deoxyribonucleoside 5’-triphosphate
dsRNA	double strand RNA
E. coli	*Escherichea coli*
EDTA	ethylenediaminetetracetic acid
EMT	epithelial-to-mesenchymal transition
ER	Endoplasmic Reticulum
Exp-5	Exportin-5
FBS	fetal bovine serum
HCC	hepatocellular carcinoma
HBV	hepatitis B virus
HCV	hepatitis C virus
HMG	high mobility group
ICC	intrahepatic cholangiocellular carcinoma
IHC	immunohistochemistry
i.p.	intraperitoneal
Kd	knockdown
KSFM	keratinocyte serum free medium
LB	Luria-Bertani medium
miRISC	miRNA-containing RNA-induced silencing complex

miRNA	microRNA
MOI	multiplicity of infection
mRNA	messenger RNA
MTT	3-(4,5-Dimethylthiazol-2-yl)-2,5-diphenyltetrazolium bromide
NC	negative control
NP water	Nano Pure® water
OD	optical density
p	p arm of a chromosome
PAGE	polyacrylamide gel electrophoresis
PBS	phosphate buffered saline
PCR	polymerase chain reaction
PDAC	pancreatic ductal adenocarcinoma
PI	propidium iodide
pre-miRNA	precursor miRNA
pri-miRNA	primary miRNA
PS	phosphatidylserine
PVDF	polyvinylidene fluoride
q	q arm of a chromosome
qPCR	quantitative PCR
RNA	ribonucleic acid
RNAi	RNA interference
rpm	rotation per minute
RT	reverse transcription
s.c.	subcutaneous
SDS	sodium dodecyl sulfate
shRNA	small hairpin RNA or short hairpin RNA
siRNA	small interfering RNA
SNP	single nucleotide polymorphism
TAE	Tris-acetate-EDTA
TBS	Tris-buffered saline
TBST	Tris-buffered saline with Tween 20
TEMED	N,N,N',N'-tetramethyl-ethylenediamine
TSG	tumor suppressor genes
Tween 20	polyoxyethylene-sorbitan monolaurate
UTR	untranslated region
UV	Ultraviolet
WT	wild-type

Abbreviation of gene products

Abbreviation	Full name
ABCE1	ATP-binding cassette, sub-family E (OABP), member 1
ACTA1	actin, alpha 1, skeletal muscle
APC	adenomatosis polyposis coli
BAK	BCL2-antagonist/killer
BAX	Bcl-2-associated X protein
Bcl-2	B-cell CLL/lymphoma 2
CTNNB1	catenin (cadherin associated protein), beta 1
BRCA2	breast cancer 2, early onset
CDH1	cadherin 1, type 1, E-cadherin (epithelial)
CDH2	cadherin 2, type 1, N-cadherin (neuronal)
CDKN2A	cyclin-dependent kinase inhibitor 2A
CEA	carcinoembryonic antigen
CEACAM1	carcinoembryonic antigen-related cell adhesion molecule 1
CUGBP2	CUGBP, Elav-like family member 2
CTNNB1	β-catenin
dCK	deoxycytidine kinase
EGF	epidermal growth factor
FasL	Fas ligand
FGFR	fibroblast growth factor receptor
FN1	fibronectin 1
GNAI2	guanine nucleotide binding protein (G protein), alpha inhibiting activity polypeptide 2
Gp130	glycoprotein-130
GSK-3B	glycogen synthase kinase-3β
hCNT	human concentrative nucleoside transporter
hENT1	human equilibrative nucleoside transporter-1
IAPs	inhibitor of apoptosis proteins
IGF-2R	insulin-like growth factor-2 receptor
IL-6	interleukin-6
KRAS	v-Ki-ras2 Kirsten rat sarcoma viral oncogene homolog
LLGL1	lethal giant larvae homolog 1 (Drosophila)
MAPK	mitogen-activated protein kinase
NF- κB	nuclear factor kappa-light-chain-enhancer of activated B cells
NR4A2	nuclear receptor subfamily 4, group A, member 2
OAZ2	ornithine decarboxylase antizyme 2

PI3K	phosphatidylinositol 3-kinases
PTEN	phosphatase and tensin homolog
RB	retinoblastoma *RB1*
TGF-β	transforming growth factor-β
TNF	tumor necrosis factor
TP53	tumor protein 53
TRAF2	TNF receptor associated factor 2
SELS	selenoprotein S
SHOX2	short stature homeobox 2
SMAD	SMAD family member
SNX1	Sorting nexin-1
SOX9	sex determining region Y-box 9
TGF- β	Transforming growth factor beta
VIM	Vimentin
Wnt	wingless-related MMTV integration
XIAP	X-linked inhibitor of apoptosis protein
ZO-1	tight junction protein 1 (zona occludens 1)

Table of Contents

List of Figures

Part I:

Part II:

List of Tables

Part I:

Part II:

Part I: Brucein D-modulated microRNA-95 expression inhibits hepatocellular carcinoma cell growth

Introduction

Hepatocellular carcinoma

Definition and classification

Liver cancers or hepatic cancers refer to all the malignant tumors growing in the liver. Cancers that originate from liver tissues are primary liver cancer. Comparatively, cancers that derive from other organs of the body and spread to the liver are metastatic liver cancer.

According to the cellular origin of cancer, primary liver cancer can be classified as several subtypes. The cancer develops from hepatocytes is named hepatocellular carcinoma (HCC), which represents the majority of primary liver cancer. The second most common type is intrahepatic cholangiocellular carcinoma (ICC), which arises from biliary epithelium. Other rarer types include angiosarcoma (or heamangiosarcoma), which starts in the blood vessels of the liver, hepatoblastoma, and lymphoma of liver.

Epidemiology

By world area, liver cancer is the fourth most common cancer and the second leading cause of cancer related death in men (Jemal, 2007). The annually rising number of new cases and cancer deaths puts liver cancer as an important health issue. In 2008, there were approximately 748,300 new cases diagnosed and 695,900 cases died from it (Ferlay, 2010). The distribution of HCC by geography is noticeably uneven. It is higher in less developed areas than in more developed areas. Approximately 80% of HCC occurs in eastern Asia and sub-Saharan Africa (Parkin 2006). Specially, China accounts for about half of the cases.

In the high-risk regions, the age of liver cancer incidence shifts towards younger persons. In southeast Asia and west Africa, the incidence rate starts to rise at the age of 20 to 30 years and reaches the peak at 50 years old. In the US and European countries, the rate increases after 45 and stabilizes at around 65 years old (Parkin 1992). Men are more likely to be affected by liver cancer, which is consistent worldwide. The ratio of gender-specific incidence ranges from 1.4 to 3.3 (man/woman). In the more prevalent districts, higher gender ratios are observed (Ferlay, 2001).

HCC is the most common type of primary liver cancer, which accounts for about 80% of all primary liver cancer cases globally (Perz, 2006). About one or two out of ten cases of primary liver cancer is diagnosed as ICC (Shin, 2010). This

pattern is similar across different gender or ethnic groups. In Chinese population, however, the proportion of HCC among all primary liver cancer cases can reach 95**%.**

Etiology

HCC is one of the few cancers whose risk factors and causal factors are relatively clearly established. The geographic variance of incidence reflects several different causes of HCC (Bosch, 1999). In developing countries, hepatitis B virus (HBV) infection is proved to be the major cause. Higher HBV infection prevalence accompanies with higher incidence rate of HCC. In endemic areas where the carrier rate can be as high as 10–20% of the whole population, over 60% HCC is responsible for chronic HBV infection (Parkin, 2006). HBV carriers have 100-fold higher probability than non-carriers to develop HCC. Infection of HBV at birth or childhood results in HCC at early age. Additionally, introduction of HBV vaccine into infants successfully prevented the cases of HBV infection and incidence of HCC in Taiwan (Beasley, 1981). Aflatoxin B1 (AFB) intake from diet also contributes to HCC in less developed areas (Ming, 2002).

In western countries and Japan, where HBV infection is rare, hepatitis C virus (HCV) infection is proved to be the main risk factor(Bosetti, 2008; Altekruse, 2009). The recently elevated incidence of HCC in the low-risk areas is probably due to the

dissemination of HCV through blood transfusion by drug abusers. Causes of cirrhosis such as alcohol and non-alcohol fatty liver disease associated with obesity are also closely linked with HCC in developed countries. (El-Serag, 2007)

Given the prevalence of HBV infection and continuously high HCC incidence rate in Africa and Asia, and the growing number of new cases of HCC in US and Europe, the prevention and management of HCC are always urgent problems that need intensive investigation (Schwartz, 2011).

Molecular pathogenesis of HCC

Our current understanding of the molecular mechanisms that give rise to HCC mainly concludes the genetic alteration, deregulation of signaling pathways, and aberrant epigenetic modifications. In general, HCC is a result of both genetic and epigenetic changes that accumulatively lead to the transformation of normal hepatocytes into malignant cells. Additionally, two diverse yet complimentary models of HCC tumorigenesis have been established, which will improve our understanding in this field as well (Kumar, 2011).

Genomic instability

It has been shown that regions of 1p, 4q, 6q, 8p, 9p, 13q, 16p, 16q and 17p are most frequently lost and regions of 1q, 6p, 8q and 17q are most commonly gained by comparing large scale of HCC tumors and non-tumorous tissue (Homayounfar,

2009). The deleted chromosome regions correlate with mutation or deletion of tumor suppressor genes (TSG) such as TP53, insulin-like growth factor-2 receptor IGF-2R, CDKN2A (p16INK4A), and retinoblastoma *RB1* (Rb) (Kumar, 2011).

TP53 gene encoding the p53 protein actively exerts its tumor suppressive function in the presence of varies cellular stress, resulting in cell cycle arrest, apoptosis, or senescence. HCC is commonly linked with TP53 deletion or loss of function mutation in chromosome 17p (Hussain, 2006). A particular mutagen of TP53 is AFB1, whose intake from food is highly correlated with HCC incidence (Aguilar, 1993). A viral protein HBx coding by HBV can specifically bind to p53 and thus blocks p53-mediated apoptosis (Wang, 1994).

Deregulation of key signaling pathways

Several signaling pathways that are important in carcinogenesis are found to be activated in HCC. Deregulation of these pathways plays an important role in HCC pathogenesis**.**

Inactivation of the transforming growth factor-β (TGF-β) signaling is another common molecular event in HCC. The role of TGF- β is controversial. It induces apoptosis and cell cycle arrest in normal conditions and early stages of cancer. In advanced stages, TGF- β in return losses its control of cell proliferation. It has been observed that HCC is associated with disrupted TGF-β signaling together with

interleukin-6 (IL-6) signaling activation (Tang, 2008). And alteration of glycoprotein-130 (gp130), a co-receptor of IL-6, is also accompanied with β-catenin activating mutation in HCC (Rebouissou, 2009). All of these factors interplay with each other to contribute to HCC tumorigenesis.

The Wnt/ β-catenin pathway plays an important part in development, cell differentiation, and proliferation. Without Wnt signaling, β-catenin binds with the tumor suppressor adenomatosis polyposis coli (APC), Axin1, and glycogen synthase kinase-3β (GSK-3β) in cytoplasm. GSK-3B sends β-catenin to ubiquitin for degradation. When Wnt signaling participates, conformational change of Axin releases β-catenin. Subsequently β-catenin translocates into nucleus and activates oncogenic Myc, which bypasses cell senescence through induction of telomerase. An elevated level of Wnt signaling is observed in HCC. Probably these pathways are also responsible for carcinogenesis of HCC (Cavard, 2008). Wnt/ β-catenin signaling also activates PI3K/PTEN/Akt pathway. Activation of Akt signaling is associated with more aggressive HCC (Nakanishi, 2005). There may be some interaction between PI3K/PTEN/Akt and Wnt/β-catenin pathways to promote HCC progression.

Epigenetic changes of HCC

In addition to genetic abnormalities, epigenetic changes contribute to HCC

occurrence as well. In the past decade, growing evidence supports that altered DNA methylation is responsible for human HCC. DNA methylation refers to a methyl group (-CH3) being covalently bonded to the 5-carbon of a cytosine. In human 90% cytosine methylation is found at dinucleotide CpG sequences (Tykocinski, 1984). Among them, promoter CpG islands, which is defined as regions larger than 200bp with more than 50% GC content, are the most frequent sites (Jones, 2002). Expression of a gene is controlled by its promoter DNA methylation status. Basically, promoter methylation silences the expression of a gene, and vice versa (Larsen, 1992). Thus hypermethylation of a TSG may lead to malignant development. On the contrary, hypomethylation of oncogenes favors tumorigenesis. Accumulative studies show that aberrant DNA methylation is found in various types of cancer, including HCC (Jones, 2002).

Two models of HCC pathogenesis

The pathogenesis of HCC can be explained by two prevalent models (Kumar, 2011). The first model illustrates the development of HCC as a stepwise process. Malignancy occurs from normal hepatocytes to dysplastic nodules, and precancerous lesions, and finally tumor cells. The process is a consequence of accumulative genetic and epigenetic alterations. The previous described etiological factors such as hepatitis viruses and AFB1 contributes to these changes. And every single tumor cell

is regarded as monoclonal origination. This model is fine except that it could not to be efficiently translated into useful approaches to address the problems in current HCC therapies.

More recently another model sheds new lights on our understanding of HCC development. Given that liver is a regenerative organ, the self-renewal and unlimited dividing progenitor liver cells that differentiate into hepatocytes can also develop into HCC. It is hypothesized that HCC is possibly derived from transformed progenitor cells. This cancer stem cell model does not conflict the multistep hypothesis. In turn, it offers a more comprehensive explanation of the generation of HCC. What's more, based on this model, clinical treatments targeting hepatocytes possessing stemness nature will be a more beneficial choice.

Therapeutic methods and prognosis of HCC

Current management for HCC includes curative treatment and palliative treatment (Llovet, 2003). Generally 30% to 40% HCC patients receive curative treatment. The methods of curative treatment contain surgical resection, percutaneous ablation and liver transplantation. Surgery is considered the treatment of choice for HCC, and a considerable number of patients get satisfactory responses after resection. But only a limited number of cases are surgical resectable. More common situations are that diagnosis is made when metastasis is already present.

Patients who should be given curative treatment must be carefully selected regarding their disease staging. On the other hand, good as liver transplantation is, the long waiting time for a donor liver restrains the application of liver transplantation to cure HCC. However, tumor recurrence always exists, further rendering the disease complicated to eradicate. If no better option comes out, current methods only benefit a small population.

Palliative treatment, such as arterial embolization, chemotherapy and oestrogen blockade, is for advanced stages. Patients who are not suitable to receive curative treatment will be given palliative treatment. Nevertheless, the inclusion criteria should also be strictly defined. From several randomized control trials, no significant survival benefit was observed among these methods.

In general, current therapeutic methods are far from satisfactory to meet our needs. Developing novel effective strategies for HCC treatment is of great concern.

Apoptosis

Types of cell death

When a cell is going to die, there are some molecular and morphological changes occurring: loss of membrane integrity, fragmentation of the cell, and engulfment of the fragments by adjacent cells. According to the morphological characteristics, cell death can be divided as apoptosis, necrosis, autophage, and

mitosis. Based on the functional criteria, there are programmed cell death and accidental cell death.

Apoptosis

The term “apoptosis” described a specific type of cell death in its morphological aspects. Defects occurring at any point of the regulatory pathways of apoptosis cause a variety of problems. For instance, too much apoptosis results in degenerative diseases, while too little leads to uncontrolled cell growth including cancer. Complicated as the mechanisms are, unraveling the control of apoptosis will extend its significance for not only understand the pathogenesis of a disease, but also novel strategies for cancer therapies.

Morphological features of apoptosis

In contrast to necrosis, cells undergo apoptosis actively switch on a course towards death. Morphological changes of apoptosis includes rounding up of cells, retraction of pseudopods, reduced cell volume, and, the most importantly, chromatin condensation and nuclear fragmentation (Kroemer, 2005). On the biochemical bases, membrane changes, breakdown of DNA and proteins, and activation of caspases are three hallmarks of apoptosis (Robbins, 2009). In early stage of apoptosis, phosphatidylserine (PS) translocates from the inner layers of the cell membrane to the outer layer, allowing recognition by macrophages for phagocytosis without

inflammation reactions (Hengartner, 2001). Later on, it comes to the breakdown of DNA into large fragments and then the cleavage of DNA into multiple small pieces of 180 to 200 bp by endonucleases (McCarthy, 1998). But DNA fragmentation is not specific to apoptosis, which can also be seen in necrosis. Another feature of apoptosis is the activation of caspases, which are a group of cysteine protease catalyzing aspartic acid residues. They destroy many pivotal proteins of the cell and activates DNAase for DNA degradation(Lavrik, 2005). However, apoptosis could be caspase-independent as well.

Molecular mechanisms of apoptosis

Caspases are the central players of apoptosis for they initiate and guide the process of apoptosis. Three pathways that activate caspases are (1) intrinsic pathway or mitochondrial pathway; (2) extrinsic pathway or death receptor pathway; and (3) intrinsic endoplasmic reticulum (ER) pathway (Wong, 2011).

The extrinsic death receptor pathway is activated upon external damage stimuli by the binding of death ligands, such as Fas ligand (FasL) and TNF, to their death receptor (Hengartner 2001). This binding induces the formation of death-inducing signaling complex (DISC), which then assembles and activates pro-caspase 8. Subsequently, the caspase initiator, caspase-8, starts the progression of apoptosis by activating other downstream caspases (Reed, 2000)

Intrinsic mitochondrial pathway is triggered by internal stimuli, for example genetic damage, hypoxia, and oxidative stress. Mitochondrial permeability initiates the pathway (Danial, 2004). Bcl-2 family proteins play a major part in the process. Bcl-2 family can be divided into two groups, the pro-apoptotic proteins (Bax,Bak, Bad, Bcl-Xs, Bid, Bik, Bim, and Hrk) and the anti-apoptotic proteins (Bcl-2, Bcl-Xl, Bcl-W, Bfl-1, and Mcl-1) (Reed, 1997). Pro-apoptotic proteins promote the release of cytochrome-c from mitochondrial. On the other hand, anti-apoptotic proteins block the release. The balance between the two groups of proteins controls the initiation of intrinsic apoptosis. The release of cytochrome c induces the formation of apoptosome, which contains cytochrome c, Apaf-1, and caspase-9, and then activates of caspase-3 (Kroemer, 2007).

The activation of upstream caspases, caspase-8 and caspase-9 of extrinsic and intrinsic pathways respectively, converge to activate caspas-3. Caspase-3 then induces the cleavages of the inhibitor of the caspase-activated deoxyribonuclease for nuclear apoptosis. Other downstream proteins catalyzes more vital cellular proteins relating with cytoskeleton and cell cycle, finally leading to the apoptotic morphological changes (Ghobrial, 2005).

The intrinsic endoplasmic reticulum pathway is not well studied. When cellular stresses pose injuries to the ER, protein synthesis reduces and some proteins unfold.

TNF receptor associated factor 2 (TRAF2) leaves pro-caspase-12. Here comes the activation of intrinsic ER pathway (Szegezdi, 2003).

Apoptosis and cancer

Basically, decreased level of apoptosis leads to tumorigenesis. Cells that are less apoptotic or resistant to apoptosis and thus acquiring malignant transformation can be accessed by several ways. In general there are three ways: (1) breakdown of the balance between pro-apoptotic preteins and anti-apoptotic proteins; (2) loss of functional caspases; and (3) disruption of death receptor signaling pathways.

Imbalance of pro-apoptotic proteins and anti-apoptotic proteins

Based on their functions in cells, some proteins are regarded as pro-apoptotic proteins or anti-apoptotic proteins. The normal ratio of these proteins plays a vital role in determining cell proliferation or cell death. Overexpression of anti-apoptotic proteins and under-expression of pro-apoptotic proteins lead to reduction of apoptosis, and thus confer to carcinogenesis.

The Bcl-2 protein family contains both pro-apoptotic and anti-apoptotic proteins. They mainly act through the intrinsic pathway due to their location on the outer layer of mitochondrial membrane (Gross, 1999). Disrupted balance between anti-apoptotic and pro-apoptotic proteins of the Bcl-2 family has frequently been reported to result in deregulated apoptosis. Overexpression of Bcl-2 protected cells

from apoptosis in prostate cancer (Raffo, 1995), neuroblastoma, and breast cancer(Fulda, 2000). Overexpression of Bcl-xL is reported to associate with drug resistance (Fulda, 2002). Mutation of bax is common in colorectal cancers and endows colorectal cells resistance to anticancer therapy (Miquel, 2005).

The protein p53 or tumor protein 53 (TP53) is another key player in apoptosis. Activation of tumor suppressive p53 promotes transcription of pro-apoptosis proteins and suppresses the transcription of anti-apoptotic proteins. Mutation of this tumor suppressor gene renders the affected cells oncogenic (Okada, 2006).

The inhibitor of apoptosis proteins (IAPs) are another group of proteins mediating apoptosis, cytokinesis and signal transduction. IAPs are endogenous inhibitors of caspases to degrade activated caspases or prevent caspases from binding to their substrates. IAPs implication has been reported in many cancers, for instance, pancreatic cancer (Lopes, 2007), non-small cell lung carcinomas resistance (Krepela, 2009), and melanoma (Vucic, 2000).

Impaired caspases activity

Apoptosis associated caspases can be divided as initiator caspases (such as caspase-2, -8, -9, and -10) and effector caspases (such as caspase-3, -6, and -7) which direct the cleavage of cellular components. Loss of functional caspases could lead to eliminated apoptosis and promotes carcinogenesis. Examples are

downregulation of caspase-9 in colorectal cancer (Shen, 2010), decreased caspase-3 level in breast, ovarian and cervical tumors (Devarajan, 2002), and low expression of caspase-8 and -10 in choriocarcinoma (Fong, 2006).

Deregulated death receptor signaling

In the extrinsic pathway, death receptor pathway plays an important part. Triggered by a death signal, the death receptors (such as TNFR1 or DR1, Fas or DR2) attract a variety of cellular molecules to their death domains and thus initiate the signaling cascade. Any abnormalities involved in the death signaling can result in a reduction of apoptosis and may be responsible for carcinogenesis.

Cancer therapy targeting apoptotic defects

Fortunately, the mechanisms of defects in apoptosis just provide us therapeutic target for cancer treatment. Any strategies that can revise the balance of apoptotic signaling exert the potential to treat cancer. Currently, several methods targeting defects in apoptosis have been investigated. In general, gene therapy, immunotherapy and drug therapy are the novel options. The most popular molecules being the targets include the anti-apoptotic proteins in the Bcl-2 family, the p53 gene, Survivn, XIAP, and caspases. A number of them achieve benefits in cell-based experiments and animal models. Some of them have already entered different stages of clinical trials. The problems to be considered mainly focus on whether the

treatment causes massive death of normal cells, whether resistance will be induced. If the therapy specifically targets a single protein or only one pathway, it would be more beneficial. The combination of molecular therapy and conventional therapy may possess broader applications. Nevertheless, long-term clinical observation is needed and future investigations should aim at the selectivity of the treatment to induce apoptosis in cancer cells but not normal cells.

microRNA

Overview

Implications of microRNA (miRNA) in biological processes and diseases have drawn increasing attention from scientists. They are a collection of endogenous small RNAs. They are generated from endogenous transcripts. The mature form of miRNAs are of about 19 – 25 nucleotides in length. They bind to their target mRNAs in a sequence specific manner and then mediate gene silencing at post-transcriptional and translational levels. Since the first two miRNAs, lin-4 and let-7, were discovered in Caenorhabditis elegans, hundreds of thousands of miRNAs have been identified in various species. Bioinformatic analysis predicts more than 1000 miRNAs existing in human genome. Subsequent studies have revealed that miRNAs are involved in most biological processes and the aberrant expression pattern of miRNAs has been implicated in numerous diseases. The discovery of the

mechanisms of miRNAs' part taking in gene regulation has opened up exciting era for future researches.

Biogenesis and maturation of microRNA

Most human miRNA genes locate within introns of protein-coding genes or intergenic regions of non-protein-coding genes in chromosomes. Their transcription can be regulated by their host gene promoters. A large number of miRNAs are found in clusters and are transcribed as polycistronic transcripts (Lagos-Quintana, 2003). The first step of miRNA biogenesis is the generation of primary miRNAs (pri-miRNAs). This process is transcribed by RNA Polymerase II (Pol II). Pri-miRNAs are about hundreds to thousands nucleotides in length containing stem-loop structures together with the unique 7-methylguanosine caps and poly A tails. (Cai, 2004; Lee, 2004). In the next step, pri-miRNAs are processed by two RNase-III enzymes, Drosha and Dicer. Both of the two enzymes are double strand RNA (dsRNA) specific. Localized in the nucleus, Drosha cleaves pri-miRNAs into about 70 bp fragments consisting of imperfect stem-loop structures, generating precursor miRNAs (pre-miRNAs)(Lee, 2004). Following the cleavage by Drosha, pre-miRNAs are transported from nucleus into cytoplasm by Exportin-5 (Exp-5) (Lund, 2004). As soon as the arrival in cytoplasm, pre-miRNAs are catalyzed by the cytoplasmic RNase III, Dicer. They are then cleavage into small imperfect dsRNAs,

which is a miRNA : miRNA* duplex containing both the mature miRNA and its complementary strand miRNA*. It is believed that miRNA* also takes part in gene regulation, although the mature miRNA plays a more active role in gene silencing (Tang, 2005).

Gene silencing by microRNA

Gene silencing mediated by miRNAs requires the formation of the miRNA-containing RNA-induced silencing complex (miRISC). The mature miRNA strand released from the miRNA : miRNA* duplex incorporate into the miRISC complex, while the miRNA* is rapidly degraded. The mature miRNA helps miRISC to recognize its target genes by complementary binding to the 3' untranslated regions (3' UTR) of target mRNAs (Bartel, 2004).

Suppression of gene expressions by miRNAs is carried out at post-transcriptional level and translational level. A well-studied model is illustrated by lin-4 and lin-14. Perfect base-pairing between lin-4 and lin-14 is crucial for the negative regulation. Lin-4 only inhibits lin-14 protein synthesis but fails to affect the mRNA abundance of lin-14, implying a repression effect at translational levels (Olsen, 1999). This mechanism is common among miRNAs in animals. Another model that has been established indicates that miRNA can directly induce its target gene mRNA destruction (Yekta, 2004). However, the mechanism of post-transcriptional suppression still needs to be elucidated.

The miRISC mediated gene suppression also depends on the degree of complementarity between the miRNA and its target sequences. Basically, perfect base-pairing between the mature miRNA and target gene 3'UTR sequences favors cleavage of the target mRNA. Inhibition of translation can be processed in partial complementary cases (Bartel, 2004).

The sequence-specific recognition of miRNA to its target mRNA is determined by a crucial region of miRNA. This region locates at 2 to 7 nucleotides from the 5' end of mature miRNA and is named "seed sequence" (Xie, 2005). Genomic analysis showed that the seed sequences of a large number of miRNAs are complementary to the 3'UTRs of various mRNAs. Moreover, it is found that one miRNA is able to target different 3'UTRs. Meanwhile, the 3'UTR of an mRNA may also be targeted by numerous miRNAs. Thus it is reasonable to imagine gene regulation on miRNA-mRNA basis must be quite a complicated, yet precisely orchestrated, network of gene regulation. In general, miRNA mediated gene silencing relies on the complementarity between the seed sequence of miRNAs and the 3'UTRs of target mRNAs (Gregory, 2006).

MicroRNA and cancers

MiRNAs participate in many biological processes, including development, differentiation, proliferation, and apoptosis (Bartel, 2004). Aberrant expression of miRNAs has been implicated in numerous diseases, including cancer. Abnormal

expression patterns of miRNAs have been detected in a number of types of human cancers. For example, reduced expression of miR-15 and miR-16-1 is tightly linked with chronic lymphocytic leukemia (CLL) (Cimmino, 2005). A single nucleotide polymorphism (SNP) is associated with poor outcome of non-small cell lung cancer (Hu, 2008). MiRNAs' association with cancer can be either oncogenesis or tumor suppressive. On the one hand, miRNAs' location in genomic regions determines its nature of carcinogenesis. When it locates in regions that are frequently amplified in cancers, it functions as oncogenic miRNA. Conversely, if a miRNA locates in chromosomes that are deleted in cancers, it acts as a tumor suppressor. On the other hand, the function of a miRNA can be determined by its target gene that may be either oncogenic or tumor suppressive.

The use of miRNA in cancer management has been intensively explored recently. Based on the changed pattern of miRNA expression in cancers, miRNA profiles may assist to diagnose cancer types. Based on its endogenous antisense interaction with target genes, it is proposed that miRNAs could be used for cancer treatments. Administration of ectopic miRNAs to suppress oncogene is also promising (McLaughlin, 2007; Liu, 2009) However, many problems are still needed to be tackled. Besides the mechanisms of miRNA in cancer, some studies have focused on how to enhance life time and efficiency of miRNAs in human body, such as modification of

miRNA molecules. To bring theoretical concepts to bedside practice, there is still a long way to go. Nevertheless, advances in understanding the miRNA mechanisms in cancer will extend its potential application significance in cancer therapy.

MicroRNA's involvement in HCC

Several miRNAs have been reported to have implications in HCC. For example, miR-181 expression has been proved to be negatively correlated with Wnt/β-catenin signaling in HCC. Elevated Wnt/β-catenin signaling is accompanied with increased miR-181 expression. Knocking down of TGF- β is associated with reduced expression of miR-181 (Wang, 2010; Ji, 2009). Loss of let-7g favors HCC metastasis (Ji, 2010), while some other miRNA expression profile is identified to be related with venous metastasis (Budhu, 2008). Cancer cells with silenced miR-26 undergo more active signaling pathways related to inflammation and have better response to interferon therapy (Ji, 2009). MiR-21 expression is linked with loss of heterozygosity of PTEN. As a consequence, Akt signaling pathway is activated, thus enhancing tumorigenesis (Meng, 2007). MiRNA induced cell cycle deregulation and prohibition of apoptosis have also been reported (Varnholt, 2008).

Involvement of miR-95 in cancer

Increasing findings support the notion that miR-95 functions as an oncogene in cancers. From a miRNA profiling study comparing pancreatic cancer tissue samples

with normal tissues, miR-95 was found to be up-regulated in both pancreatic cancer surgical specimens and pancreatic cancer cell lines (Zhang, 2009). In colorectal cancer (CRC), miR-95 also has increased expression. (Huang, 2011) Inhibition of miR-95 prohibited Hela cell growth (Cheng, 2005). Ectopic introduction of miR-95 in human CRC cell lines enhances both in vitro cell growth and in vivo tumorigenesis. A tumor suppressor gene, SNX1 is identified as the down-stream target of miR-95, further implying the oncogenesis nature of miR-95 (Huang, 2011). However, to date, there has been relatively little research conducted on miR-95's implication in liver cancer.

Brucein D

Brucein D (BD) is a naturally occurring chemical compound isolated from Brucea javanica fruit, which is commonly used in Chinese medicine to treat cancer. The chemical structure of BD is demonstrated below (adapted from S.T. Lau, 2009).

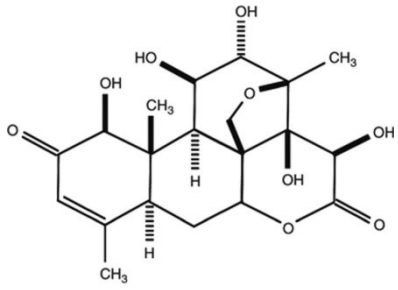

Previous studies demonstrate that BD exerts cytotoxic effect on pancreatic cancer cell lines by inducing apoptosis and cell cycle arrest (Lau, 2009). The mechanisms of BD's being an apoptogenic agent of pancreatic cancer involve

activation of p38-MAPK pathway and inhibition of NF-κB anti-apoptotic activity (Lau, 2010) . However, the mechanism of BD's anti-cancer effect is largely unknown.

Aims of study

We hypothesized that

(1) BD had anti-cancer effect on HCC cells;

(2) BD could induce apoptosis to inhibit cell growth;

(3) BD could change expression pattern of miRNAs in HCC cells;

(4) BD could modulate cell growth by regulating expression of a specific miRNA which executed its function through its downstream target gene.

Our objectives were to

(1) Investigate whether BD exhibits anti-cancer effect for HCC cells;

(2) Examine whether BD induces apoptosis;

(3) Find different expression patterns of miRNAs before and after BD treatment in HCC cells;

(4) Identify miRNA targets of BD and downstream genes of the targeted miRNAs

(5) Understand how BD inhibits HCC cell growth.

Materials and Methods

Cell Culture

Mammalian Cell Culture

293T, MIHA, HepG2, Hep3B, Huh7, Bel7404 and PLC cells were obtained from the American Type Culture Collection (Rockville, MD, USA). The cells were cultured in Dulbecco's modified Eagle's medium supplemented with 50 unit/ml penicillin-streptomycin (GibcoBRL, USA) and 10% (v/v) fetal bovine serum (Hyclone) in a humidified incubator at 37°C in 5% CO_2. After the cells reached about 80% confluence, the medium was removed and the cells were trypsinized with 1 ml of 0.05% trypsin-EDTA (Gibco, USA) for 2 mins. Then cell suspension was transferred to a 15-ml centrifuge tube containing 10 ml of PBS and centrifuged at 1,000 rpm at room temperature for 5 min. The cell pellet was resuspended with fresh medium and transferred to new plates and incubated as described above.

Preparation of cell stock

When reached about 80% confluent, the cells were washed with PBS twice and trypsinized as described above. After centrifugation, the cell pellet was resuspended in a freezing medium (20% v/v FBS and 10% DMSO in DMEM) 450 μl of DMEM supplemented with 10% v/v fetal bovine serum and transferred into a 2-ml freezing

tube containing 450 µl of fetal bovine serum and 100 µl of DMSO. The medium was transferred to a 2-ml freezing tube and put in an isopropanol filled freezing. Finally, the pot was put into a -80°C freezer so that the cell stock was frozen at a constant rate of about 1°C/min. Cell stocks were stored at -80°C or liquid nitrogen.

Cell recovery from liquid nitrogen stock

The cell stock tube was taken out from the liquid nitrogen tank or -80°C freezer which was immediately thawed in a 37°C water bath. To remove the DMSO, the cell stock was diluted with 10 ml of DMEM with 10% v/v FBS. The cell suspension was centrifuged as described above and the supernatant was discarded. The cell pellet was resuspended in 10 ml of DMEM containing 10% FBS and plated on a 10-cm tissue culture plate. One day after cell recovery, the medium was changed.

Preparation of drugs for treatments

Brucein D was provided by Professor Lin Zhixiu of the Chinese University of Hong Kong. Its purity was above 98%. It was dissolved in steriled DMSO (Sigma-Aldrich, USA) at the concentration of 100 mM and stored at 4°C. Right before use, stock solution was further diluted in sterile DMEM to different final concentrations. Stock solution of BD was aliquot as small volume to avoid freeze and thaw cycles and was used within 3 months.

Drug treatment

Single cell suspensions were counted and seeded in 12-well plates or 96-well plates the day before drug treatment. On the day of treatment, cells were cultured to approximately 50-70% confluence. Stock solutions of drugs were diluted in culture medium to desired concentrations. Control solutions were prepared by diluting the same volume of dissolving reagent used in drug stocks to culture medium. Culture medium of cells was replaced by the medium containing drugs. Cells were cultured for additional 72 hours.

Transfection of siRNA

DharmaFECT was purchased from Thermo Scientific. The transfection procedure was done according to the product protocol. In brief, 3000 cells were plated to each well of a 96-well plate and cultured in a 37°C overnight. On the next day, 5 μl of 2 μM siRNA was mixed with 5μl of plain DMEM medium in a 1.5-ml eppendorf tube. In a separated tube, 0.5 μl of DharmaFECT transfection reagent was added to 49.5 μl of plain DMEM. The mixtures were gently mixed by pipetting up and down which were followed by 5 minutes of incubation at room temperature. The diluted siRNA was then added to the diluted DharmaFECT transfection reagent, mixed and incubated for another 20 minutes. When incubation was completed, 80 μl of antibiotic-free complete medium was added to the mixture for a final siRNA

concentration of 100 nM. The medium from the wells of the 96-well plate was removed and replaced by the 100 μl transfection mixtures. Transfection medium was replaced with fresh culture medium 8-16 hours post transfection. The cells were incubated at 37°C for additional 24 to 72 hours before harvest. Drug treatment could start 24 hours after transfection.

MTT Assay

MTT (3-(4,5-Dimethylthiazol-2-yl)-2,5-diphenyltetrazolium bromide) was purchased from USB Chemicals Corporation. The MTT powder was dissolved in sterile NP Water to a final concentration of 5mg/ml and sterilized by passage through a 0.22 μm pore PVDF filter. Before treatments, $1x10^3$ to $5x10^3$ cells were plated on a 96-well plate. When the treatment was completed, the cells were cultured in a medium containing 1mg/ml of MTT for 3 hours. Following that, the medium was discarded and 100ul of DMSO was added to each well in a 96-well plate. The plate was shaken at a speed of 120 rpm for 15 minutes. Finally, absorbance was measure at λ490 nm. For each treatment, the samples were repeated in triplicates. Cell viability was calculated as $OD_{treatment}/OD_{control}$.

Luciferase reporter assays

The putative miRNA binding site was subcloned in the pMIR-REPORT™ reporter (Invitogen) to detect endogenous miRNA expression. Before transfection,

appropriate number of cells was seeded in a 24-well plate. 200 ng of the pMIR reporter together with 1ng of the pRenilla reporter (Promega) were co-transfected into the cells by lipofectamine 2000 (Invitrogen) according to standard protocols. After 48 hours of incubation, the cells were harvested for measuring luciferase activity. Firstly, the cells were rinsed in ice-cold PBS twice and lysed in 1X Passive Lysis Buffer (PLB) (Promega) for 15 minutes. Then the cells were scraped off and transferred to a 1.5 ml microfuge tube. To clear the cell debris, the samples were centrifuged in 13000 rpm at 4°C for 15 minutes. Then the activities of the firefly luciferase and Renilla luciferase were measured by using the Dual-Luciferase Reporter Assay System (Promega).

Annexin V Assay

When treatments were finished, the cells and the culture medium were collected as described above. Then 5 x 10^5 cells were re-suspended in 500 μl of 1x Annexin V binding buffer (Biovision). Thereafter, the cell suspension was incubated with 5μl of Annexin V-Cy5 antibody and 0.25 μg of propidium iodide (PI) at room temperature for 5 minutes in the dark. Finally, the samples were analyzed with BD LSRFortessa Cell Analyzer.

In vivo mouse model

Male nude mice at the age of 4-6 weeks old were provided by the Laboratory

Animal Services Center (LASEC) of the Chinese University of Hong Kong (CUHK). They were kept in pathogen-free, air-controlled conditions with 12-hour light-dark cycles. Food and water supplied were sterilized. All experiments were approved by the Animal Experimental Ethics Committee of the CUHK. 5 x 10^6 cells re-suspended in 100 μl sterilized PBS containing 10% matrigel (BD) were subcutaneously injected into the left flank of nude mice to generate subcutaneous (s.c.) xenografts. When tumors reached 5-10 mm in diameter, mice were randomly allocated into different groups and drug treatment got started. Stock solution of Brucein D dissolved in DMSO was diluted in sterilized PBS and administrated to mice at the concentration of 1.5 mg/kg body weight through intraperitoneal (i.p.) injections. Mice of control group received i.p. injections of the solvent only. Tumor volumes and body weight were measured every 2 to 3 days. Tumor volumes were calculated as length(mm)*width(mm)*height(mm)/2.

Tunel Assay (Terminal deoxynucleotide transferase dUTP Nick End Labeli ng Assay)

Apo-BrdU-IHC™ was used for detecting apoptotic cells on Paraffin Embedded Tissue. The subcutaneous tumor samples were harvested and fixed by methanol at 4°C for 24 hours. And then they were dehydrated and embedded in paraffin. Paraffin blocks were sectioned as 5 um in thick onto glass slides. Samples were

deparaffinized and rehydrated by immersing the slide in following solutions and order: twice in xylene for 5 minutes, twice in 100% ethanol for 5 minutes, once in 90% ethanol for 3 minutes, once in 80% ethanol for 3 minutes, once in 70% ethanol for 3 minutes and finally in 1X PBS for 1 minutes before drying the slide. Then, the samples were digested with proteinase K at room temperature for 20 minutes for permeabilization which was followed by inactivating the endogenous peroxidase as described above. After this, the samples were equilibrated in 1X reaction buffer at room temperature for 10 to 30 minutes. Sequentially, 1x complete labeling reaction mixture was added to the sample and kept at 37°C for 1.5 hours. Following the incubation with blocking buffer, the samples were probed with 100 µl antibody solution. Then 100 µl of DAB solution was applied to the samples at room temperature for 15 minutes. At the end, the samples were counterstained with Mtheyl Green.

RNA manipulation

RNA Isolation

TRIzol® Reagent (Invitrogen) was used for RNA isolation. The samples, tissue or cells, were firstly homogenized with Trizol and incubated at room temperature for 5 minutes. For 1ml of Trizol reagent, 200 µl of chloroform was added to the homogenized samples, which was followed by vigorous shaking for 15 seconds.

After another 3 minutes of incubation, the samples were centrifuged at 12,000 × g for 15 minutes at 4°C. Then, the top aqueous phase of the sample was transferred to a new tube. 500 μl of 100% propanol was added to the aqueous phase. The mixture was then incubated at room temperature for 10 minutes which was followed by another centrifugation at 12,000 × g for 10 minutes at 4°C. The supernatant was removed and 1 ml of RNase free 70% ethanol was added. After a brief vortexing, the samples were centrifuged at 7500×g for 5 minutes at 4°C. The wash was discarded and the RNA pellet was air dried. An appropriate amount of RNase free water was used to dissolve the RNA whose concentration was subsequently determined by NanoDrop (Thermo Scientific).

Synthesis of cDNA from miRNA

NCode™ miRNA First-Strand cDNA Synthesis Kit was purchased from Invitrogen for synthesizing the cDNA of miRNA. All experimental procedures followed the protocol provided by the manufacturer. In brief, 2.5 μg of RNA was added to Poly(A) Tailing buffer (1xmiRNA Reaction Buffer, 25 mM $MnCl_2$, 5 mM ATP and Poly A Polymerase) supplied by the kit to a final volume of 25 μl. After a gentle mixing, the samples were incubated at 37°C for 15 minutes. Immediately after the 37°C incubation, 4 μl of the Polyadenylated RNA from previous step was added to the annealing buffer. The mixture was incubated in the tube at 65ºC for 5

minutes which was followed by a chilling on ice for 1 minute. Thereafter, 10 μl of 2X First-Strand reaction mixture and 2 μl of SuperScript™ III RT/RNaseOUT™ enzyme mixture were added to the samples. The mixture was transfer to a thermal cycler for a two-step incubation, 50 ºC for 50 minutes and then 85ºC for 5 minutes. Finally, the samples were chilled on ice and stored at -20 ºC for qPCR analysis.

Synthesis of cDNA from RNA and quantitative PCR

The synthesis of cDNA from RNA used High Capacity cDNA Reverse Transcription Kit (Invitrogen). Firstly, 1 μg of purified RNA was added to RT buffer (1x RT buffer, 4mM dNTPs, 1x RT random primers, reverse transcriptase and RNase inhibitor) as provided to the final volume of 25 μl. After a gentle mixing and a short spin down, the sample was placed in a thermal cycler with a program set according to manufacturer's guideline.

The relative expression level of genes was determined by using semi quantitative PCR. 1 μl of the cDNA obtained from previous step was added to Power SYBR® Green PCR Master Mix (Invitrogen) containing corresponding set of primers for gene detection. Then the samples were loaded in triplicated into a 96-well or 384-well plate which was then placed in ABI 7900HT Fast Real Time PCR for measuring the CT values. The relative expression level of each gene was determined by comparative quantitation.

miRNA qPCR array

Cancer miRNA qPCR array plates were purchased from SBI. Reactions were set up according to the protocol provided. For each sample assayed on one qPCR plate, 500 ng total RNA was needed. cDNA of miRNA was synthesized using the compatible QuantiMir RT Kit. For each plate to be assayed by qRT-PCR, a master mix containing SYBR Green, universal reverse primer and miRNA cDNA was prepared following instructions. For each well of a 96-well qPCR plate, 29 µl master mix was loaded, to be mixed with 1 µl diluted primers from the primer plate. And then the qRT-PCR plate could be applied for qRT-PCR analysis as described above. Data was normalized to U6 control gene for further analysis.

DNA manipulation

Agarose gel electrophoresis and purification of DNA

Several types of agarose gels (typically 0.5%, 1.0%, or 2.0%, w/v) were prepared with TAE buffer containing 1X GelRed ™ staining solution (Biotium,Inc). DNA samples were firstly mixed with loading buffer and loaded on the agarose gel immersed in TAE buffer and separated at 150V for 25 minutes. The gel was placed on a trans-illuminator emitting UV light to visualize the separated DNA. Then, the gel block containing desired DNA bands was excised and purified with the QIAquick Gel Extraction Kit (Qiagen, Germany). The gel slice was weighed and an

appropriate volume of buffer QG was mixed with the gel slice in a 1.5 ml microfuge tube. The mixture was then incubated at 50°C until the gel was completely melted. The mixture was then transfer to a mirco-column and centrifuged at 13,000 rpm in a desktop centrifuge (Eppendorf, Germany) for 1 min. The flow through was discarded. The resin retaining the DNA was washed with 750 µl of buffer PE and centrifuged as above. The column-collection tube assembly was centrifuged for a further 1 min to remove the residual PE buffer from the resin. The DNA was eluted with 30 µl of NP Water and collected by centrifugation in a new clean microfuge tube.

Restriction enzymes digestion

All restriction enzymes and the respective 10x reaction buffers were obtained from New England Biolabs, USA. Restriction enzyme digestion was mainly used in DNA cloning. To digest DNA, 2 µg of plasmid DNA was mixed with 4 units of restriction enzyme, 2 µl of 10x buffer, and the volume was brought to 20 µl with Nano- water. Whenever more than two types of restriction enzymes were used, the total volume of the restriction enzymes added was kept at 1/10 of total reaction volume. All the reactions were incubated in a 37°C incubator for 2 hours.

Ligation of DNA fragments

The T4 DNA ligase (New England Biolabs, USA) was used for DNA ligation. DNA insert and vector were mixed in approximately 3:1 molar ratio (total DNA was not less than 100 ng). Then 2 µl of 10x buffer and 1 µl of T4 DNA ligase were added to the DNA mixture. The reaction volume was brought to 20 µl with Nano-Pure water and incubated at room temperature for 2 hours or at 16°C overnight.

Polymerase chain reaction

To prepare inserts for subcloning, template DNA (100 ng) was mixed with 2.5 µl of 10x PCR buffer, 0.5 µl of dNTP, 1 units of Taq polymerase(GoTaq® Flexi, Promega) and 1 µg each of specific primers; then the volume was brought to 25 µl by Nano-Pure water. Thermal cyclic reactions were done by the TaKaRa PCR Thermal Cycler Dice™ (Gradient Model) (TaKaRa, Japan). The reaction profile was 95°C for 5 min; 30 cycles of 95°C for 30 seconds, 58°C for 30 seconds (annealing temperature varied for different primers), 72°C for 1 minutes (elongation time varied depending on the size of DNA to be amplified), followed by 72°C for 7 minutes and 4°C for storage. When PCR was used to screen for positive transformants during subcloning, overnight bacterial culture from single colony (1 µl) was used as the template and the total reaction volume was 20 µl.

Preparation of competent E. coli cells

A single colony of E. coli (strain of XL1-blue or DH5α) on an LB plate was isolated and inoculated into 2 ml of LB medium which grown at 37°C for overnight. The culture was then transferred into 100 ml of LB medium and grown until the OD_{600} reached 0.3-0.5. The LB medium was then chilled on ice for 15 minutes. The bacteria were pelleted by centrifugation and the supernatant was discarded. The pellet was then resuspended with 30 ml of TFB1 solution and left on ice for 15 min. The cell suspensions were centrifuged as above and subsequently resuspended with 4 ml of TFB2 solution. After another 15 minutes incubation on ice, the TFB2-resuspended bacteria were transferred into pre-chilled 1.5-ml microcentrifuge tubes as 200 µl aliquots and stored at -80°C.

Transformation of E. coli cells

Either 1ng of plasmid DNA or all of the ligation mixture was mixed with 100 µl of competent E. coli cells and left on ice for 10 minutes. The cells were heat shocked in a 42°C water bath for 90 seconds which is following by chilling on ice for 90 seconds. The transformation mix was then mixed with 250 µl of LB medium and shaken in a 37°C environmental shaker for 30 minutes. The cells were pelleted at 3,000 rpm in a desktop centrifuge for 1 minute. Finally, 100 µl of the bacteria culture was spread on a LB plate containing appropriate antibiotics, and grown overnight in a 37°C incubator.

Small scale plasmid isolation from E. coli (mini-prep)

QIAprep Spin Miniprep Kit (Qiagen, Germany) was used for small scale plasmid isolation. A single colony of E. coli (XL1-blue or DH5α) was inoculated into 5 ml of LB medium containing appropriate antibiotics at 37°C for overnight. The bacteria were pelleted and resuspended in 250 µl S1 buffer. To lyse the bacteria, 250 µl of S2 buffer was added and the mixture was incubated at room temperature for 5 min. To neutralize the lysate and precipitate cellular proteins, chilled S3 buffer (100 µl) was added and the lysate was incubated on ice for 15 minutes. The supernatant was pipetted to QIAprep spin column and centrifuged at 13,000 rpm for 30 seconds. After discarding the flow-through, 750 of buffer PE was applied to column which was spun again as above. After removing the flow-through, the column was centrifuged for another minute to remove residual wash buffer. The DNA was eluted with 30 µl of NP Water and collected by centrifugation in a new clean microcentrifuge tube.

Results

Brucein D inhibited the growth of HCC cells both in vitro and in vivo

Considering BD's cytotoxic effect on pancreatic cancer cell lines as previously reported, we firstly investigated BD's effect on HCC cell growth by MTT assays. There were 5 HCC cell lines being tested. They are PLC, HepG2, Hep3B, Huh7, and Bel7404. The cell line MIHA is a normal human hepatocyte cell line, which serves as a normal control. MTT results (figure 1) revealed that BD suppressed cell proliferation in all the 5 human HCC cell lines in a concentration-dependent manner. However, the growth inhibitory effect of BD didn't markedly affect MIHA. By calculating the IC50 values (table 1), we also found that IC50 of MIHA was significantly higher than that of cancer cells, which further indicated BD exhibited a selective anti-cancer effect on HCC cells.

Figure 1.

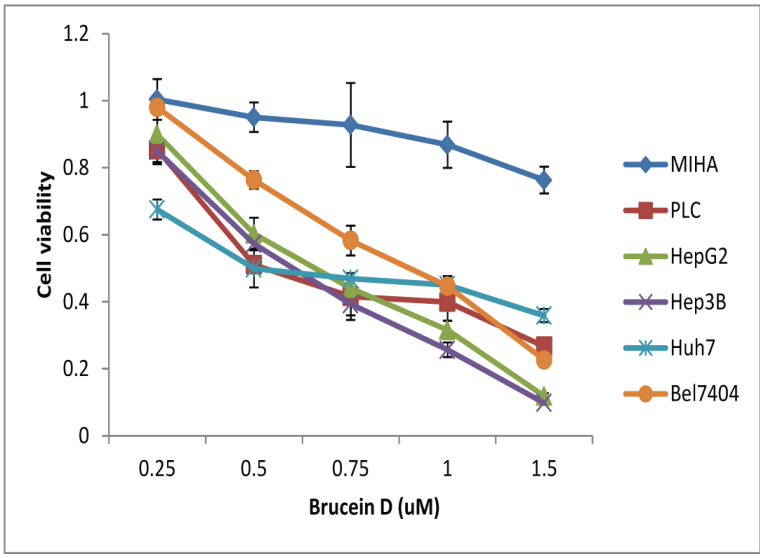

Figure 1: Brucein D inhibited HCC cell growth in vitro.

Cells were treated with BD at gradient concentrations ranging from 0.25 to 1.5 μM for 72 hours. MTT assays were applied to evaluate cell proliferation. For each cell line, cell viability was normalized to the correspondent untreated control sample. BD suppressed the growth of HCC cell lines in a concentration-dependent manner, but did not significantly affect the growth of MIHA.

Table 1. IC50 values of BD on human normal hepatocyte cell line MIHA and 5 human HCC cell lines.

Cell line	IC50 ± SD (μM)
MIHA	2.18 ± 0.08
PLC	0.14 ± 0.02
HepG2	0.56 ± 0.03
Hep3B	0.57 ± 0.04
Huh7	0.22 ± 0.03
Bel7404	0.71 ± 0.05

IC50 values were calculated by GraphPad Prism software based on MTT results as previously shown. IC50 of MIHA is much higher than that of cancer cells.

We further evaluated BD's anti-liver cancer effect in vivo (figure 2). HCC cells were subcutaneously inoculated in nude mice. When the tumors reached 5mm in diameter, mice were given BD treatment or solvent alone through i.p. injections. Tumors in the control group grew exponentially. Conversely, BD suppressed tumor growth to a relatively low level. Similar effect could be observed in both Hep3B (figure 2A) and Bel7404 (figure 2B) cell lines. These results provided evidence that BD inhibited HCC cell growth in vivo as well. Additionally, it was desirable to find that BD treatment did not result in remarkable body weight loss on nude mice (figure 2C). No other drug-induced side-effect was found either. It suggested that BD treatment did not have profound toxicity to the mice bearing tumors.

To sum up, BD exerted anti-cancer effect on HCC both in vitro and in vivo.

Figure 2.

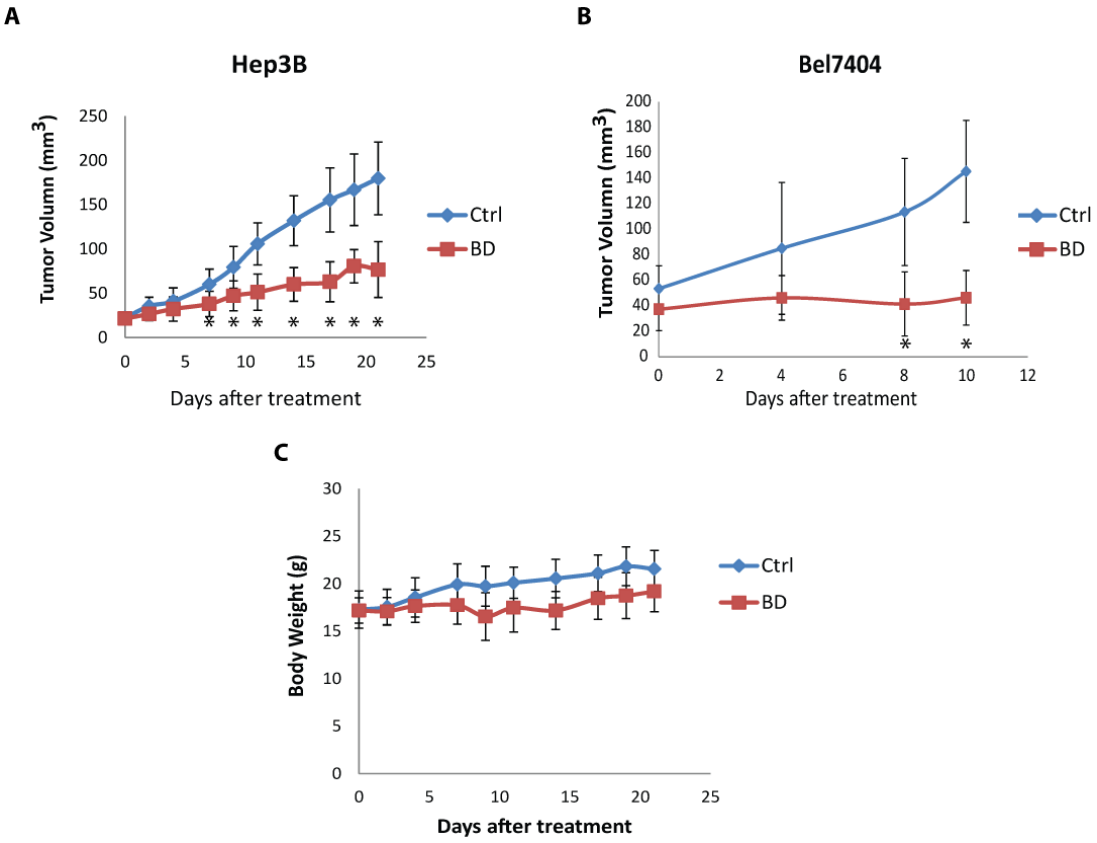

Figure 2: Brucein D inhibits HCC cell growth in vivo.

(A and B): BD inhibited the growth of HCC s.c. tumors in nude mice. Hep3B (A) and Bel7404 (B) cells were subcutaneously inoculated into nude mice. Mice were treated with either 1.5mg/kg body weight BD or control solution through i.p. injections. Schedules of treatment were every Monday, Wednesday and Friday for 3 weeks (A) or daily for 10 continuous days (B). Tumor volumes between groups were considered as significantly different when $p < 0.05$. (*, $p < 0.05$, $n = 11$ (A), $n = 4$ (B).)

(C): No significant body weight loss was caused by BD. Mice bearing Hep3B s.c. tumors were treated with BD at the dosage of 1.5 mg/kg body weight or control solution every Monday, Wednesday and Friday for 3 weeks.

BD induced apoptosis in HCC cells

The next step, we attempted to find out how BD suppressed cell growth. Previous study proposed that BD induced apoptosis in pancreatic cancer cell lines (Lau, 2009; Lau, 2010). Hence we examined whether BD had similar function for HCC cells. We conducted annexin V assays for 3 different HCC cell lines. Through flow cytometric analysis (figure 3), we found that there was a significant increase of apoptotic cells after BD treatment as compared to control samples. These results showed that BD induced apoptosis in HCC cells and implied that apoptosis probably played an important role in BD-induced growth inhibition.

Moreover, we confirmed the apoptotic activity of BD with in vivo studies. Hep3B tumor sections from the previous animal study were applied to TUNEL assay to detect apoptosis. TUNEL positively stained cells represent cells undergoing apoptosis. From IHC analysis (figure 4), we could find that, in the aspects of density and distribution, there were remarkably more positive-stained cells in BD treated samples than in control samples. The result was consistent with in vitro findings, showing that BD induced apoptosis to suppress cell growth both in vitro and in vivo.

Figure 3.

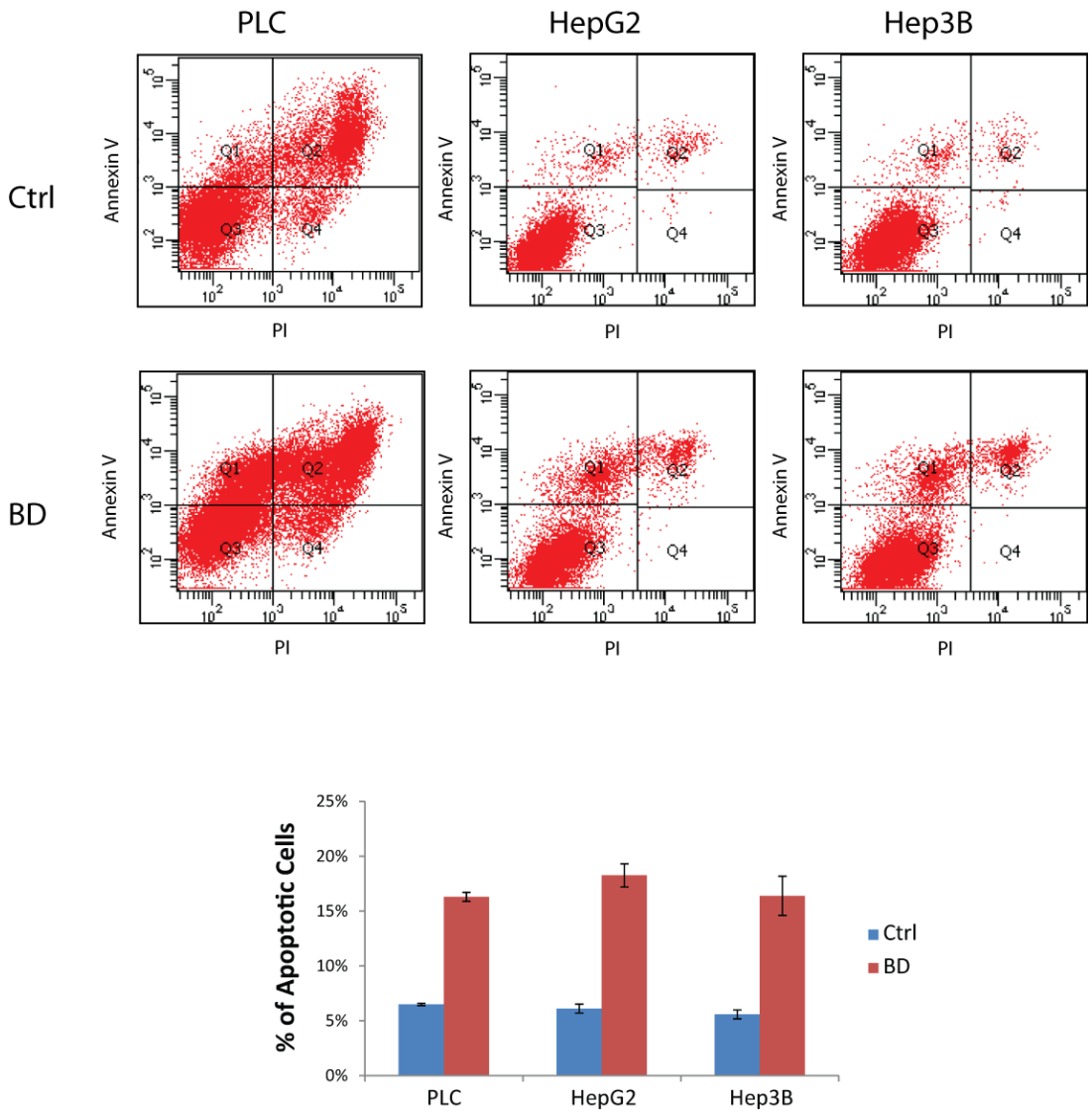

Figure 3: BD induced apoptosis in vitro.

HCC cell lines, PLC, HepG2 and Hep3B, were applied to annexin V and PI double staining after 72 hours treatment of 0.7 μM BD or control reagent. Flow cytometric analysis was carried out to detect apoptotic cells. Q1 (Annexin V + / PI -) = early apoptotic cells; Q2 (Annexin V + / PI +) = late apoptotic cells; Q3 (Annexin V - / PI -) = live cells; Q4 (Annexin V - / PI +) = dead cells (e.g. necrotic cells). A statistical analysis of the percentage of apoptotic cells (Q1+Q2) / (Q1+Q2+Q3+Q4) is shown. It revealed that BD induced apoptosis in different HCC cell lines.

Figure 4.

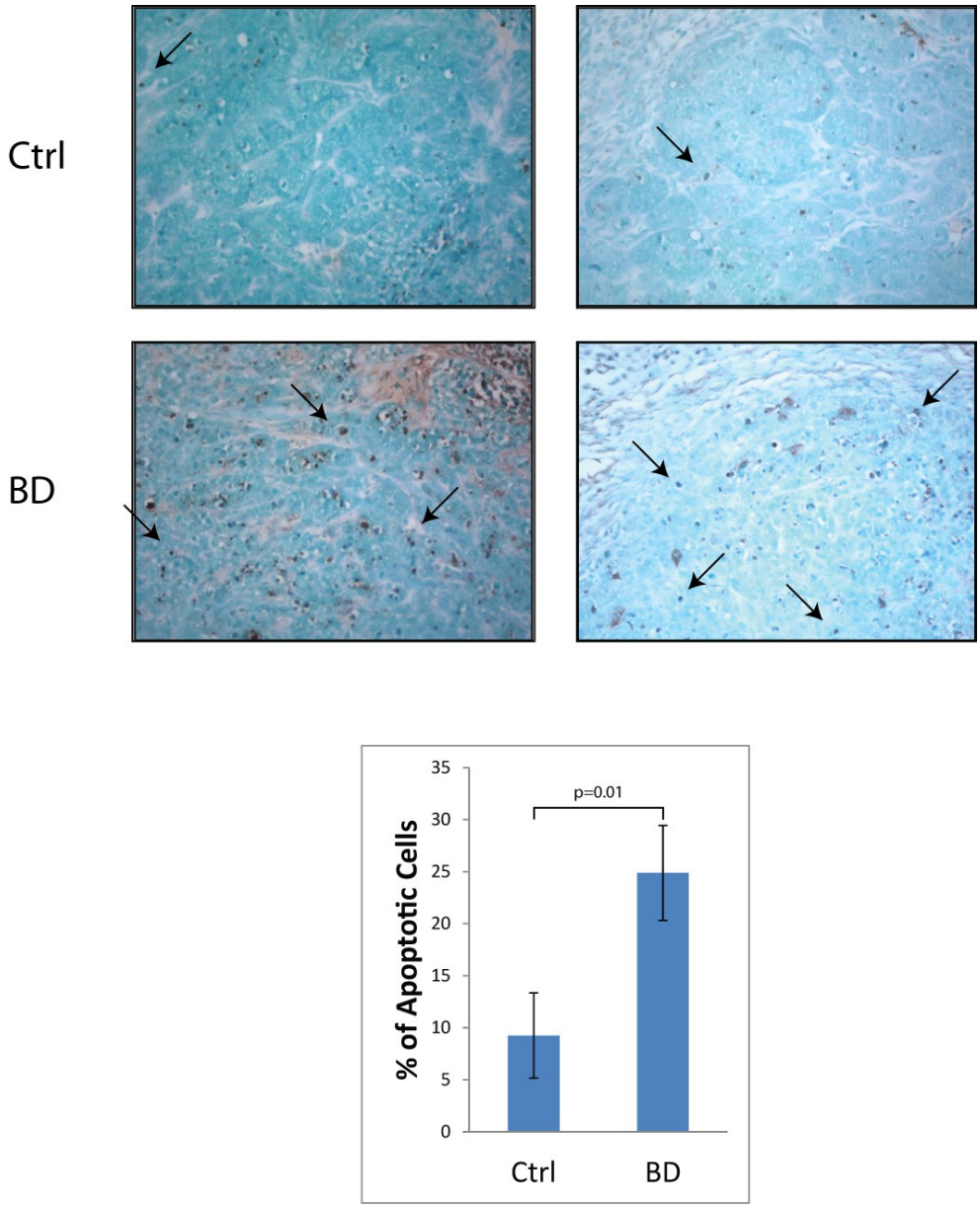

Figure 4: BD induced apoptosis in vivo.

Sections of Hep3B s.c. tumors samples from mice treated with BD or control reagent were applied to TUNEL-IHC assay. Representative images are shown. Arrows point at dark dots that are TUNEL positive-stained cells. Quantitative analysis of IHC data are presented below. Percentage of apoptotic cells were calculated as number of TUNEL-positive cancer cells / number of total cancer cells in each field at 200X magnification. More HCC cells underwent apoptosis after BD

treatment (P = 0.01, n = 5).

miR-95 is an target of BD to modulate cell growth

In order to investigate the mechanisms of BD-induced growth inhibition, we tried to find BD's downstream effectors. There is growing evidence suggesting that aberrant expression of miRNAs is associated with cancer pathogenesis. We are particularly interested in whether miRNAs are involved in the process of BD-induced cell apoptosis. To answer this question, we performed a qPCR miRNA array profiling. Figure 5 illustrates the procedure of the screening. Briefly, HCC cell line PLC was treated with either 0.7 μM BD or control reagent. Total RNA was extracted and cDNA of miRNAs was synthesized for both samples. They were then applied to the qPCR screening. This array contains primers of 95 mature human miRNAs that have published implications in cancer. U6 primer is also included as an internal control. The data analyzed by quantitative real-time PCR referred to the abundance of each miRNA in the sample tested, that was normalized to U6 control gene. By comparing the abundance of the miRNAs between the BD treated sample and the control sample, we may know the miRNAs that were up-regulated or down-regulated by BD.

Figure 5.

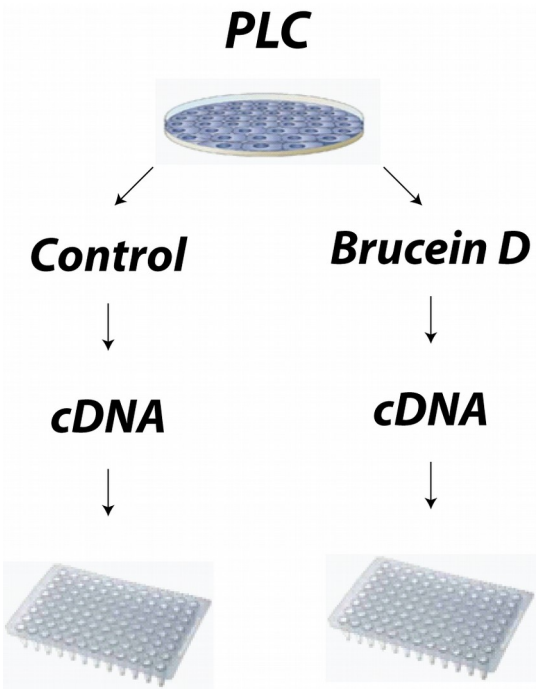

Figure 5: Flow chart of miRNA screening for BD downstream targets.

PLC cells were treated with either 0.7 μM BD or control reagent. Total RNA was extracted and cDNA of miRNAs was synthesized for both samples. Then they were applied to the qPCR analysis. This array contains primers of 95 human cancer miRNAs that have published implications in cancer. U6 primer is as an internal control. The data analyzed by quantitative real-time PCR referred to the abundance of individual miRNA normalized to U6 control gene. By comparing the abundance of the miRNAs between the BD treated sample and the control sample, we found a panel of miRNAs was significantly changed after BD treatment (fold change greater than 1.5 folds.)

A brief summary of the result of our primary screening is shown in table 2. Changed expression pattern of miRNAs were seen after BD treatment. Relative expression level of miRNAs spanned from 0.19 to 6.19. The fold of change was regarded as significant if it is greater than 1.5. Expression levels of 39 miRNAs were significantly changed after BD treatment. Among them, 25 were down-regulated and 14 were up-regulated. They were all considered as potential targets of BD.

To validate the candidate miRNAs, we individually examined the expression levels of the miRNAs from the initial screen. As figure 6 shows, miR-95, miR-153, miR-154, miR-183, miR-186, miR-196a and miR-488 were confirmed to be true positive targets. Expression of miR-95, miR-153, miR-183, miR-186 and miR-196a were decreased, whereas expression of miR-154 and miR-488 were increased. They may play a role, at least to some extents, in BD-modulated growth inhibition. Accession numbers and sequences of the 7 validated miRNAs are listed in table 3.

Table 2. Potential miRNA targets of BD identified in the primary screening.

Potential miRNA targets of BD identified in the screening (Cutoff: Fold change > 1.5)			
Fold decreased		Fold increased	
miR-200a	0.19	miR-199a+b	6.19
miR-95	0.26	miR-146a	4.62
miR-153	0.29	miR-206	3.05
miR-149	0.31	miR-154	2.35
miR-186	0.46	miR-181b	2.21
miR-196a	0.47	miR-7	2.16
miR-30b	0.47	miR-488	2.00
miR-185	0.48	miR-202	1.96
miR-219	0.49	miR-205	1.80
miR-372	0.52	miR-204	1.80
miR-181c	0.52	miR-92	1.74
miR-26b	0.52	miR-155	1.71
miR-141	0.53	miR-373	1.64
miR-126	0.54	miR-188	1.51
miR-125a	0.56		
miR-103	0.56		
miR-18a	0.57		
miR-183	0.57		
miR-151	0.59		
miR-197	0.62		
miR-9-1	0.62		
miR-200c	0.63		
miR-136	0.63		
miR-218	0.64		
miR-128b	0.65		

Figure 6

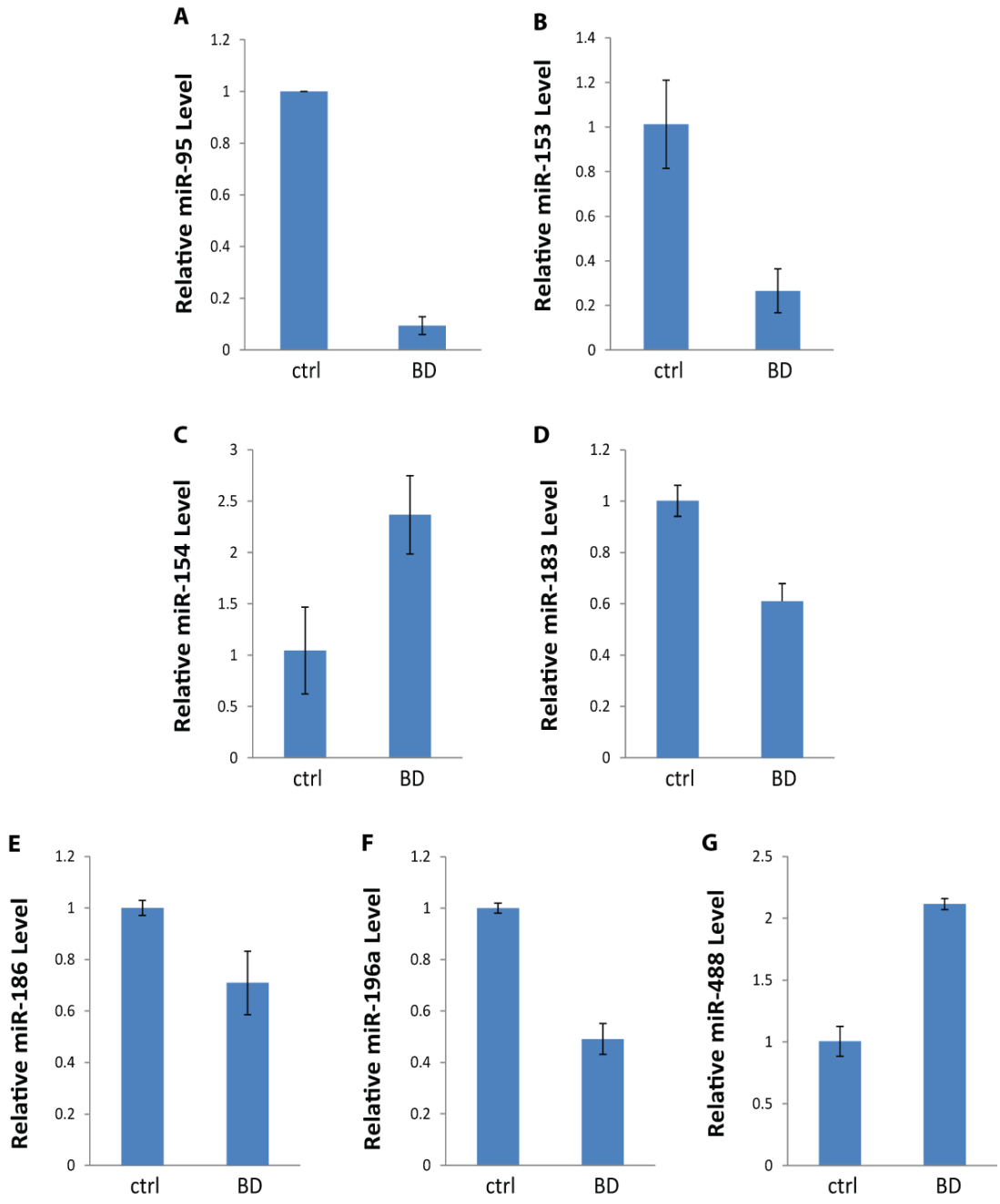

Figure 6: Validation of miRNAs as true positive targets of BD.

BD decreased expressions of miR-95, miR-153, miR-183, miR-186 and miR-196a, whereas increased expressions of miR-154 and miR-488.

Table 3. Accession number and mature sequence of the target miRNAs

MicroRNA	MirBase Accession No.	mature miRNA sequence 5' - 3'
hsa-miR-95	MIMAT0000094	UUCAACGGGUAUUUAUUGAGCA
hsa-miR-153	MIMAT0000439	UUGCAUAGUCACAAAAGUGAUC
hsa-miR-154	MIMAT0000452	UAGGUUAUCCGUGUUGCCUUCG
hsa-miR-183	MIMAT0000261	UAUGGCACUGGUAGAAUUCACU
hsa-miR-186	MIMAT0000456	CAAAGAAUUCUCCUUUUGGGCU
hsa-miR-196a	MIMAT0000226	UAGGUAGUUUCAUGUUGUUGGG
hsa-miR-488	MIMAT0002804	CCCAGAUAAUGGCACUCUCAA

To further identify which miRNA was a direct effector of BD, we carried out functional validation experiments. At this stage, our hypothesis was that if BD suppresses the expression of a miRNA to inhibit cell growth, overexpression of this miRNA would impair BD's inhibitory effect on cell growth. To justify this hypothesis, we firstly selected miR-95 for functional validation. As MTT results demonstrated (figure 7), replenishing miR-95 expression by transfection of miRNA mimic rendered HCC cells more resistant to BD treatment, as compared to negative control (NC). This growth advantage provided by miR-95 can be observed in different HCC cell lines, including PLC (figure 7A), HepG2 (figure 7B) and Hep3B (figure 7C). This finding supported our hypothesis that restoration of miR-95 expression can rescue the suppression of HCC cell growth caused by BD. However, other miRNAs that we screened, such as miR-153, failed to display similar function in neither PLC (figure 8A) nor Bel7404 (figure 8B) cells.

From these results, we believed that miR-95 was a downstream effector of BD and we proposed that BD repressed miR-95 to inhibit HCC cell growth.

Figure 7.

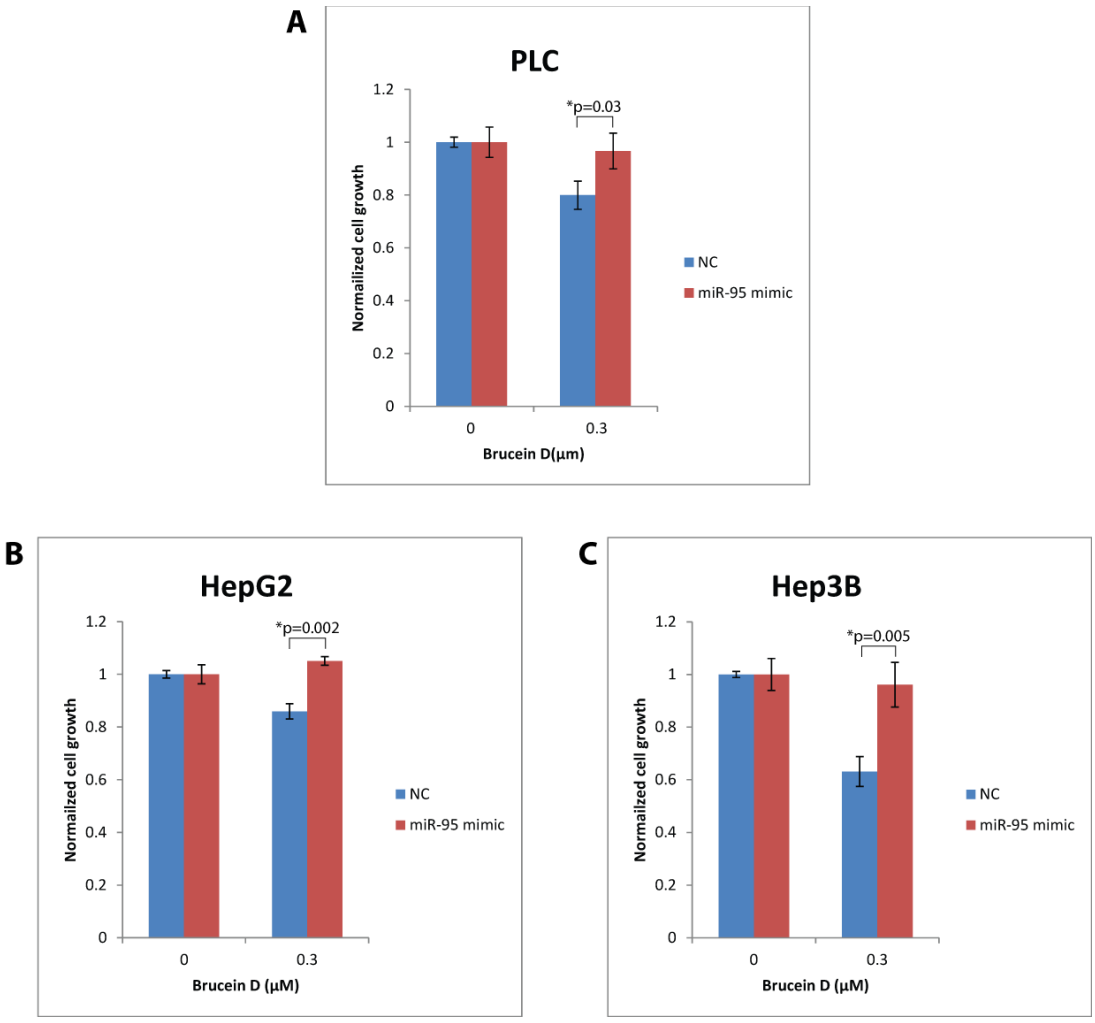

Figure 7: Overexpression of miR-95 increased resistance of HCC cells to BD.

PLC (A), HepG2 (B) and Hep3B (C) cells were transfected with either miR-95 mimic or negative control (NC) RNA. 24 hours after transfection, cells were given 0.7 μM BD treatment or control reagent for 72 hours. MTT assays were applied to measure cell growth. Cell growth rate was normalized to control reagent treated cells. After transfection of miR-95 mimic, all the 3 cell lines became more resistant to BD.

Figure 8.

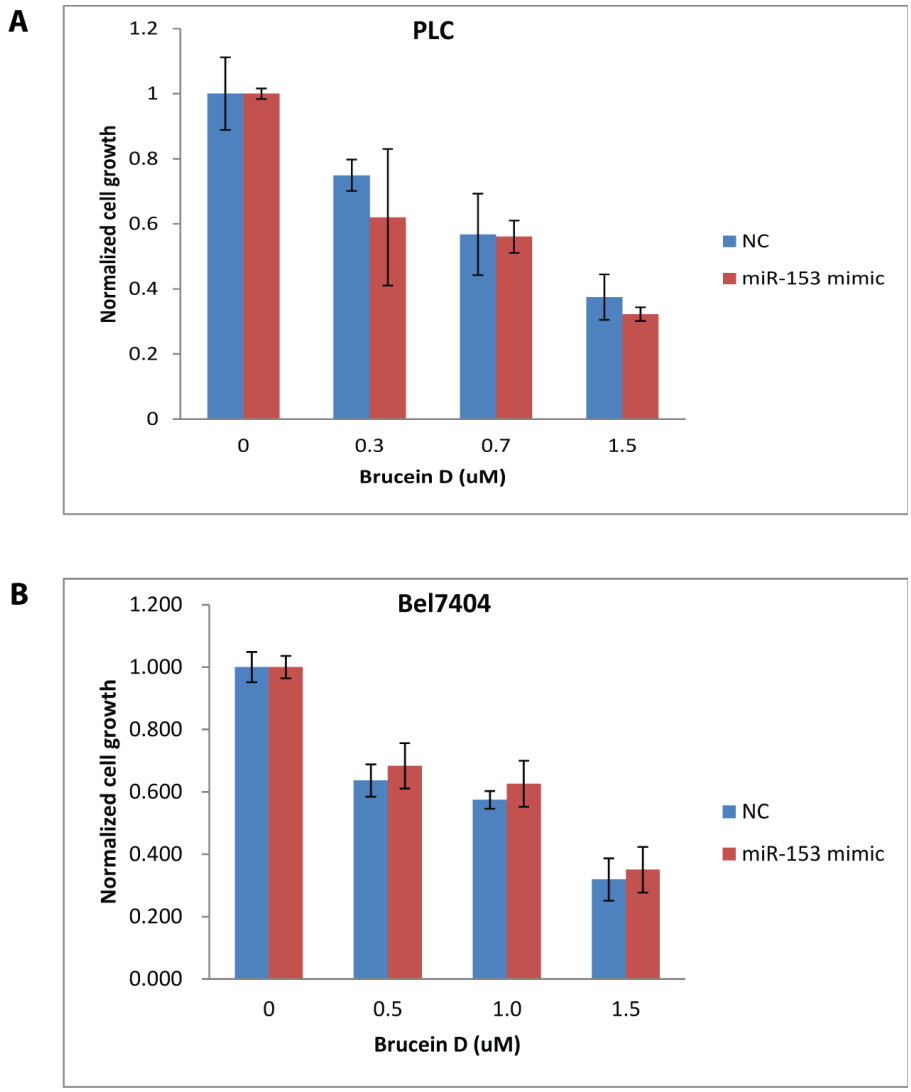

Figure 8: miR-153 mimic had no effect on sensitivity of HCC cells to BD.

PLC (A) and Bel7404 (B) cells were transfected with either miR-153 mimic or negative control (NC) RNA. 24 hours after transfection, cells were given 0.7 μM BD treatment or control reagent for 72 hours. MTT assays were applied to measure cell growth. Cell growth rate was normalized to control reagent treated cells. Transfection of miR-153 mimic failed to significantly affect cells' sensitivity to BD.

Identification of CUGBP2 as a downstream target of miR-95

Now that BD suppressed miR-95 to inhibit cell growth, the next question was how miR-95 executed its function in HCC. Firstly we wanted to find downstream target genes of miR-95. We searched databases, for instance, Target Scan and Pic Tar, to predict target genes whose 3'UTR potentially interact with miR-95. mRNAs of 6 genes (CUGBP2, SHOX2, GNAI2, SELS, NR4A2, and OAZ2) were shown as potential targets. Then we tested whether the expression of these candidate genes were correlated with the abundance of miR-95 by qPCR analysis. As a target mRNA of miR-95, it was expected that its expression would be repressed after transfection of miR-95 mimic and on the contrary would increase after transfection of miR-95 inhibitor. Among the 6 genes, only CUGBP2 fitted this model. The other 5 genes did not exhibit similar expression pattern (figure 9A). Moreover, we examined BD's effect on CUGBP2 expression. We observed an induction of CUGBP2 gene expression after BD treatment (figure 9B) where miR-95 expression was suppressed as previous shown (figure 6A). These results further proved that CUGBP2 was a downstream target of miR-95.

Figure 9.

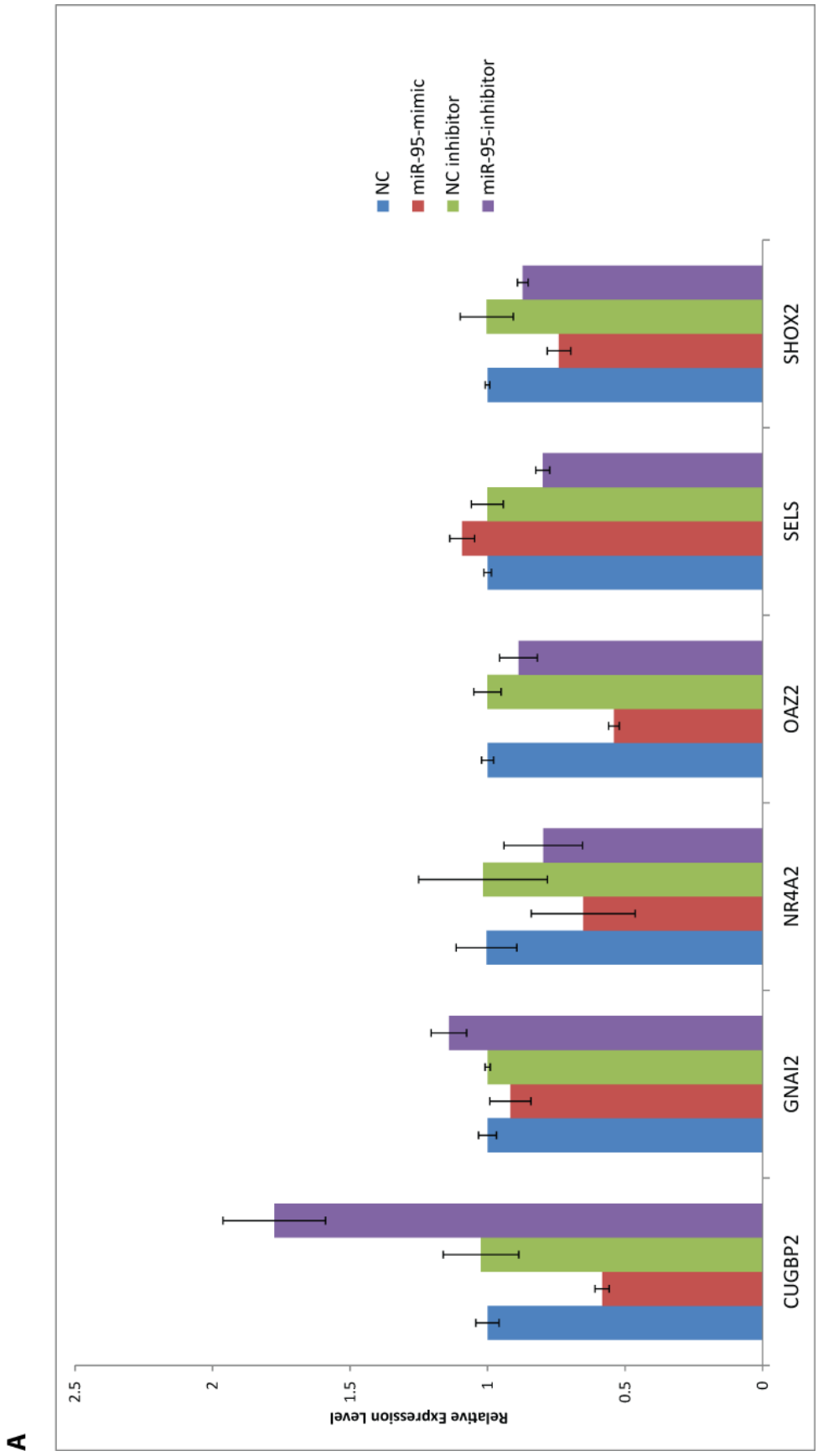
A
Relative Expression Level
2.5
2
1.5
1
0.5
0
NC
miR-95-mimic
NC inhibitor
miR-95-inhibitor
CUGBP2
GNAI2
NR4A2
OAZ2
SELS
SHOX2

B

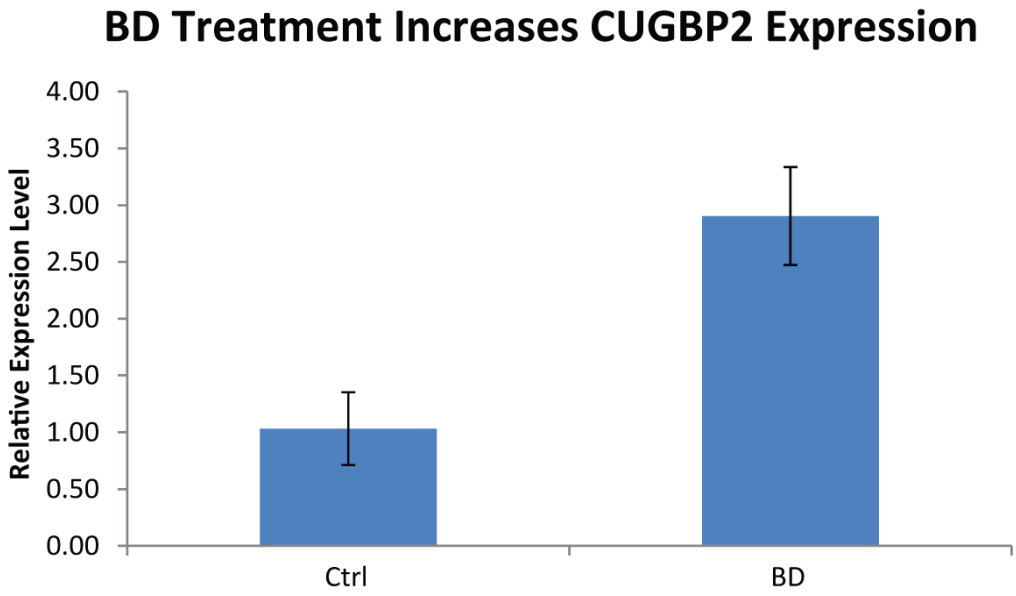

Figure 9: CUGBP2 was a downstream target of miR-95.

(A) Relative gene expression levels of 6 predicted targets of miR-95. mRNA levels of the genes were accessed by qPCR analysis in PLC cells, 48 hours post transfection of miR-95 mimic / negative control (NC) or miR-95 inhibitor / NC inhibitor. Only expression pattern of CUGBP2 matched with our expectation.

(B) CUGBP2 expression was increased after 0.7 μM BD treatment for 72 hours in PLC cells. Relative mRNA expression level was measured by qPCR analysis.

At last, we went on to investigate if miR-95 inhibited CUGBP2 mRNA through direct binding. Thus, we performed luciferase reporter assays to determine whether the predicted seed sequence on 3'UTR of CUGBP2 mRNA was a functional target site for miR-95. As illustrated in figure 10A, we constructed two reporter plasmids. Both of them had a 350 bp 3'UTR sequence of CUGBP2 mRNA. The wild-type (WT) plasmid contained the putative miR-95 seed region whereas the mutant plasmid had this region deleted. Complementary binding of miR-95 to the reporter plasmid would suppress the luciferase signals. Luciferase reporter assays revealed that miR-95 suppressed luciferase signals of WT plasmids, but did not affect luciferase signals of mutant plasmids. It indicated that miR-95 functionally interacted with 3'UTR of CUGBP2 mRNA but not the mutant one. Therefore, based on the above results, CUGBP2 was identified as a direct downstream target of miR-95.

CUGBP2 is an RNA binding protein. Some research reported that it induced apoptosis in breast cancer and colon cancer (Mukhopadhyay, 2003; Natarajan, 2008). Given the pro-apoptotic nature of CUGBP2, our proposed the mechanism of BD-modulated cell growth in HCC could be that BD repressed the expression of oncogenic miR-95 and subsequently resulted in restoring the pro-apoptotic downstream target CUGBP2 to induce apoptosis, so as to inhibit cell growth.

Figure 10.

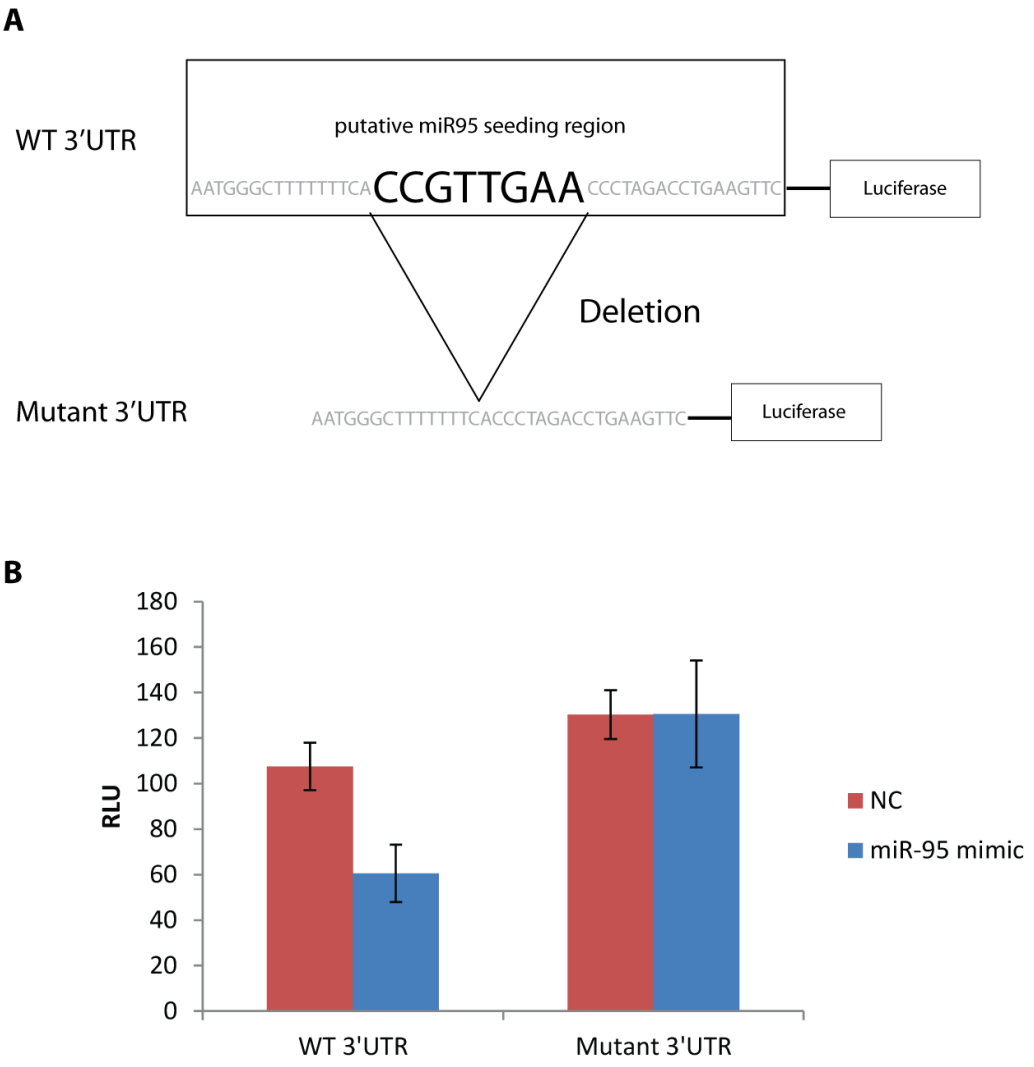

Figure 10: miR-95 directly bound to the seed sequence in 3'UTR of CUGBP2

(A) Structures of wild-type (WT) and mutant luciferase reporter plasmids. Details are described in the text.

(B) Compared to NC, miR-95 mimic suppressed luciferase signals in WT plasmids, which contained seed region in 3'UTR of CUGBP2, but not in mutant plasmids. Luciferase report assays were conducted in human embryonic kidney 293T cells 48 hours after co-transfection of reporter plasmids and miR-95 mimic / negative control (NC) RNA.

4. Discussion

With a yearly growing incidence rate worldwide, primary liver cancer, dominantly hepatocellular carcinoma (HCC), remains a difficult task in medical care. Considering its poor response to surgical resection, chemotherapy, and embolization, seeking novel and effective therapeutic methods for HCC is crucial. Brucein D (BD), a quassinoid isolated from Brucea javanica fruit, has been reported to exert cytotoxic effect in pancreatic cancer cell lines (Lau, 2009). It shows great potential of BD to be a novel therapeutic agent for cancer. However, BD's anti-cancer effect on other types of cancer still needs extensive exploration. In this study, we confirmed that BD possessed anti-liver cancer activity both in vitro and in vivo and also disclosed some underlying mechanisms of this action.

Through cell line and animal experiments, we reported for the first time that BD exhibited desirable anti-cancer effect on HCC cells. It effectively inhibited HCC cells proliferation in vitro but did not markedly suppress the growth of normal hepatocyte cell line. In a mouse model, it was able to repress the growth of HCC tumors without resulting in remarkable body weight loss. We also found that BD induced apoptosis in HCC cells both in vitro and in vivo, which could be an important way for BD to cause cell death. All these findings were consistent with previous publication about BD's effect on pancreatic cancer cells (Lau, 2009), and

further demonstrated therapeutic potential of BD to treat liver cancer.

However, how a naturally occurring compound can inhibit the growth of cancer cells remains largely unknown. With the purpose to decode the mechansims, we got started from the aspect of miRNA regulation, because more and more evidence has pointed out that deregulation of miRNAs plays an important role in cancer pathogenesis. We performed a cancer miRNA screening to search miRNAs that would be affected by BD. From primary screening, we did find an altered expression profile of miRNAs induced by BD in HCC cells. After BD treatment, 25 miRNAs were down-regulated and 14 were up-regulated. Seven of them were proved to be true positive. Among those down-regulated miRNAs, we found that overexpression of miR-95 could increase cells' resistance to BD treatment. Furthermore, we identified a pro-apoptotic gene CUGBP2 as a direct target of miR-95. These results suggested that miR-95 and CUGBP2 could be downstream effectors of BD, and we proposed one of the possible mechanisms of BD's anti-liver cancer activity was, at least in part, through inhibiting oncogenic miR-95 which degrades tumor suppressive CUGBP2, and thereby inducing apoptosis in HCC cells. Other mechanisms by which BD causes growth inhibition require further studies, especially those without involvement of miRNAs.

The finding of miR-95 as a target of BD is novel. miR-95 has been reported to

act as an oncogenic miRNA in pancreatic cancer, colorectal cancer and cervical cancer (Zhang, 2009; Huang, 2011; Cheng, 2005). But few studies have been conducted on miR-95's function in liver cancer till now. In our study, it acted like an oncogene, which was in accord with the published data regarding other cancer types. Thus far, there has been little research focusing on miRNA targets of a drug. We observed expression of a panel of miRNAs was changed after BD treatment. Interestingly, only miR-95 could reverse the inhibitory effect of BD on HCC cells, implying possibly miR-95 was a specific miRNA target of BD.

However, several questions still remained unanswered in this study. For example, how does BD regulate miR-95? If BD directly targets miR-95, the chemical structure of BD would be a crucial factor for its interaction with miR-95, which requires in-depth study. We would also like to know in which step BD suppresses miR-95, for instance, the generation of pri-miR-95 or pre-miR-95. If miR-95 is not a direct target of BD, an extensive investigation for the upstream regulators of miR-95 is needed. In addition, whether miR-95 is a specific target of BD has not yet been confirmed. At least we found in this study that expression of a panel of miRNAs was noticeably influenced by BD. If other molecules mediate BD-induced growth inhibition via miR-95, the story may be even more complex.

With regard to the identification of downstream targets for miR-95, we

suggested CUGBP2 as an effector in this setting. From published literature, CUGBP2 functions as a tumor suppressor gene, inducing apoptosis in breast cancer and colon cancer (Mukhopadhyay, 2003; Natarajan, 2008). This is in agreement with our scenario that oncogenic miR-95 inhibits expression of tumor suppressive CUGBP2. But in this study, we only showed BD can up-regulate the pro-apoptotic CUGBP2. We still lack sufficient evidence to prove that increased CUGBP2 level is a direct cause for BD-induced apoptosis. Future works could be done to examine whether silencing CUGBP2 can impair BD's impact on cell death. Moreover, the method we used to screen downstream targets for a miRNA is not comprehensive enough. miRNA-mediated gene silencing could be carried out by either cleavage of mRNA or inhibition of protein synthesis. We just focused on those target genes being degraded at post-transcriptional level because we merely relied on qPCR analysis to determine which mRNA expression matched with the expected pattern of change. This method actually resulted in precluding the real targets that were inhibited at protein synthesis level without changes of mRNA abundance. For detection of target genes that are silenced at translational level, proteomics approaches should be applied, for example, two-dimensional gel electrophoresis and mass spectrometric analysis. Nevertheless, the identification of CUGBP2 as a direct target of miR-95 has been confirmed in this study through functional assays.

In regards with the therapeutic potential of BD in cancer, it is exciting to know that BD inhibits not only pancreatic cancer cells but also HCC cells growth in pre-clinical studies. We expect that targeted therapy aiming at miR-95 or restoring CUGBP2 would sensitize patients' response to BD. Admittedly this study was largely based on in vitro manipulation and relatively lacked sufficient functional experiments. Although future investigation is needed, current results offer new insights into cancer research and development of novel therapeutic approaches. In summary, a putative pathway of BD's anti-cancer effect in HCC cells is confirmed, which might be one step further in understanding BD's mechanism in curing liver cancer.

Part II: Genome-wide RNAi screening identifies tumor metastasis suppressor genes and drug sensitivity genes in pancreatic cancer

1 Introduction

Pancreatic cancer

Overview

Ranking the fourth leading cause of cancer death in western countries, pancreatic cancer has extremely poor prognosis, with an overall 5-year survival rate of as low as 1 to 4 % (Jemal, 2007). Despite that great efforts have been made during the past decades, improvement for the outcome of this fatal disease still challenges medical world. Lack of conspicuous symptoms and efficacy screening biomarkers prevent patients with pancreatic cancer from being detected in the early stage. Due to the delayed diagnosis, pancreatic cancer often presents in advanced stages.

Currently, the only potentially radical treatment for pancreatic cancer is by surgical resection together with adjuvant chemotherapy, which could raise the 5-year survival rate to 15-20% (Ahrendt, 2002; Neoptolemos, 2004). But only a small group of patients are sustainable to accept curative therapy. The majority of patients

is unresectable at the time of presentation and thus requires palliative therapy (Andersson, 2004). The mean survival time for these patients is merely 4 months (Jemal, 2004). It should be noted that a number of patients undergoing curative operation finally develop recurrence and eventually should be given palliative care. As a prevalent palliative treatment, chemotherapy with gemcitabine is able to prolong life span to approximately 6 to 7 months and improve life quality to a certain extent (Burris, 1997; Ishii, 2005). However, the effect of chemotherapy, sometimes in combination with radiotherapy, seems far from satisfactory. Although gemcitabine serves as a first line agent for pancreatic cancer, it only gets a modest response in pancreatic cancer patients. Additionally, rapid emerging resistance to chemotherapy remains a difficult-to-tackle problem. Moreover, due to the invasive nature of pancreatic cancer, almost 100% pancreatic cancer patients develop metastasis and die (Li, 2004). The presence of metastasis implies poor response to all conventional treatment, including surgery, chemotherapy, or radiation therapy, further complicates treatment for the disease.

All these features render pancreatic cancer hopeless. We are in great need of a deeper and clearer understanding of the biological characteristics of pancreatic cancer. The investigation of novel therapeutic methods, for instance, targeted therapy or molecular therapy, is expected to bring in new light to this disease.

Pancreatic ductal adenocarcinoma (PDAC)

Pancreatic ductal adenocarcinoma is the most common type of pancreatic cancer. Histological analysis reveals a resemblance of this kind of tumor to the duct cells of pancreas. It contributes to more than 85% of pancreatic neoplasms. For simple, it may also be regarded as pancreatic adenocarcinoma or pancreatic cancer. Human pancreas also sustains other types of tumors which derive from different pancreatic cells. Different origin gives rise to varied biological behaviours. Examples include acinar-cell carcinoma which grows as zymogen granules, pancreatic endocrine tumor which produces hormone along with tumor growth, and serious cystadenoma which is featured by cystic growth. All these three types are rare events in diagnosis a pancreatic cancer.

Molecular basis of PDAC

The understanding of crucial gene mutations in PDAC is deemed valuable approach to address clinical problems. It has been shown that development of PDAC is associated with mutations of KRAS, CDKN2A, TP53, BRCA2 and SMAD4/DPC4 (Bardeesy, 2002).

KRAS

Approximately 100% of pancreatic adenocarcinoma cases bear KRAS mutation and the frequency of KRAS mutation positively correlated with disease progression

(Rozenblum, 1997). Following activation of KRAS mutation, p21 activity is induced possibly through the mitogen-activated protein kinase (MAPK) pathway (Biankin, 2001). It is well established that activation of RAS family mutations gives rise to a series of cellular responses, such as increased proliferation, invasion, and cell survival through several downstream pathways (Shields, 2000). But the targets of KRAS mutation in PDAC progression remain elusive. It has been pointed out that autocrine epidermal growth factor (EGF) promotes pancreatic cancer tomorigenesis by triggering the phosphatidylinositol 3-kinase (PI3K) pathway (Korc, 1992; Sibilia, 2000). EGF-family ligands (for example TGF-alpha and EGF) and receptors (for example EGFR and ERBB2) consistently overexpressed in PDAC (Friess, 1996).

TP53

Mutation of tumor suppressive TP53 probably contributes to the genetic instability of PDAC for the tumor has intratumoral heterogeneity and genomic rearrangements (Gorunova, 1998). Inactivation of DNA-damage response which is dependent on p53 facilitates cell survival with short telomeres (Chin, 1999). Studies on a large number of human PDAC cell lines suggested that loss of telomeres from chromosome ends was often observed, supporting the notion that pancreatic cancer genetic instability is relevant to short telomeres and telomere malfunction initiates pancreatic carcinogenesis (Gisselsson, 2001).

CDKN2A

Disturbed function of CDKN2A by mutation, deletion or promoter hypermethylation is found in 80% -95% PDAC (Rozenblum, 1997). The locus of this tumor suppressor gene (TSG) also encodes another two TSGs, INK4A and ARF. Therefore, many cases of pancreatic cancer with CDKN2A mutation also sustain loss of INK4A and ARF functions, thus impairing retinoblastoma (RB) and p53 pathways (Sherr, 2001). How these genetic bases are translated into complicated clinical aspects and subsequently guide future work on pancreatic cancer still requires active investigation.

Gemcitabine treatment in PDAC

Gemcitabine is currently a gold-standard chemotherapeutic agent for locally advanced and metastatic pancreatic cancer. It releases cancer-related pain, prevents body weight loss, improve life quality, and thus increase survival rate (Andersson, 2009).

Gemcitabine is a nucleoside analogue. It exhibits its cytotoxic activity by incorporation into DNA or RNA so as to mask chain termination (Huang, 1991; Ruiz van Haperen, 1993). Upon introduction into patients, the uptake of the drug is facilitated by nucleoside transporters, mainly by human equilibrative nucleoside

transporter-1 (hENT-1) and by human concentrative nucleoside transporter (hCNT) as well (Garcia-Manteiga, 2003). Following intracellular uptake, gemcitabine is phosphorylated by a series of kinases into difluorodeoxycytidine triphosphate (dFdCTP), which serves as a substrate of DNA and RNA polymerase, to exert its cytotoxic effect (Ruiz van Haperen, 1994). A series of actions participate in the processes of gemcitabine's uptake and metabolism before it functions as a chemotherapeutic drug.

However, gemcitabine generates only 5.4% partial response rate (Burris, 1997; Ishii, 2005), even though it proves to be a first line chemotherapy for pancreatic cancer. For many cases, patients respond well to gemcitabine at the very beginning and then suffer from resistance rapidly. It is suggested that the chemoresistance could be either intrinsic or acquired along with drug treatment. It has been proposed that there might be a subset of cells possessing resistant feature preexisting in the tumor. Alternatively, rapidly developed resistance derives from tumor stromal interactions (Kim, 2008).

Great efforts have been put to uncover the mechanisms of gemcitabine chemoresistance for years. Some explanations have been proposed, which mainly focused on gemcitabine metabolism. Decreased expression of hENT1 leading to reduced intracellular uptake of gemcitabine is one of the established mechanisms

(Mackey, 1998). Some clinical studies also confirmed the correlation between hENT1 expression level and gemcitabine treatment effect (Spratlin, 2004; Giovannetti, 2006). In addition to drug uptake, defect in drug phosphorylation is another aspect associated with gemcitabine resistance. It has been reported that low activity of MT (dCK), which mediates gemcitabine phosphorylation, is relevant to both intrinsic or acquired gemcitabine resistance (Kroep, 2002). Another study implied that overexpressed HMGA1 protein complex, which consists of transcription factors and locates downstream of RAS signaling pathway, contributes to increased gemcitabine resistance (Liau, 2008).

Metastasis

Overview

Metastasis is the spread of cancer cells from a location of origin to a secondary site, followed by the growth of tumor in the new environment. The emerging of metastasis, which contributes to more than 90% cancer mortality (Hanahan, 2011; Fidler, 2003), endows cancer to be the most deadly disease. Since Stephen Paget's 'seed and soil' theory a century before, metastasis has been drawing increasing attention from scientists. The mechanism of metastasis, however, still remains mysterious. Owing to recent technological advances, we have gained some insights into the complexity of metastasis: the understanding of the stepwise nature of the

process (Chambers, 2002; Sahai, 2007), the interactions between the tumor and the surrounding stroma(Joyce, 2009); the regulation of sets of genes and signaling pathways that determines cancer cells to metastasize or not (Fidler, 2003); the factors that drive organ specific metastasis; the evolutionary relationship between primary tumor and metastatic lesions (Hynes, 2003); But the systemic, cellular, and molecular bases of this process are far from elucidated, rendering cancers difficult to treat. A better understanding of the profound mechanism of metastasis will bring in benefits to cancer management, and cancer prevention as well.

The stepwise process of metastasis

A series of sequential steps give rise to metastasis. At the very beginning, primary tumor grows dependent on nutrients diffusion. Those aggressively growing tumors secrete angiogenic factors to stimulate the formation of a capillary network around them. This vascular network in turn nourishes the tumor. Following the continuous proliferation of primary tumor, the cascade of metastasis is triggered by the accumulative genetic changes and activated signaling pathways.

Some cancer cells acquire the ability to detach from the tumor mass and to invade the surrounding stroma. This process is characterized as epithelial-to-mesenchymal transition (EMT), which probably serves as the most actively explored feature of metastasis. EMT is the first but critical step in the long journey of a cancer

cell to colonize a new location. Epithelial cancer cells obtain features of mesenchymal cells, leading to a reduced cell–cell adhesion and apical-basal cell polarity, as well as induced cell motility. In morphological aspect, cells become spindle-like, which resembles fibroblast cells. On the molecular level, the expression of epithelial-associated markers such as E-cadherin, ZO-1, and beta-catenin reduces and on the contrary the expression of mesenchymal markers such as fibronectin, N-cadherin, and vimentin increases.

The thin-wall vessels failing to resist the penetrating of invasive tumor cells allow the entry of cancer cell into circulation. Both vascular and lymphatic systems will suffer. However, most of the circulating cancer cells will die in the blood stream. The remaining survival cells get trapped when they travel to the capillary beds of distant organs. By the similar mechanism of their entry into blood vessels, cancer cells anchored the vessel wall and exit the circulation. The above processes are named intravasation and extravasation in metastasis studies.

Upon their arrival in a new location, adapted growth of cancer cell in the new microenvironment marks the success of metastasis. It is still not an easy task, requiring the interplay between the supportive target tissues and the wandering tumor cells.

Complicated as it is, the process of metastasis is precisely orchestrated by a

network of multiple genes and signaling pathway. Failure in anyone of these steps will be rate-limiting. In addition, the coordination between metastasis promotion factors and suppression factors determines whether metastasis to proceed or not. Cancer cells must overcome all the suppressive barriers and make use of the promotion advantages to get metastatic.

Despite considerable advances in unraveling this complexity process in recent years, the exact mechanisms of metastasis in molecular and cellular levels are still largely unknown. Many widely accepted points of view are undergoing reconsideration. Tackling problems related to cancer metastasis continues to be a challenging issue. Investigations into this field have a great importance for cancer research and hopefully will guide us to more efficient management of cancers.

Metastasis of pancreatic cancer

Pancreatic cancer cells may spread by direct extension from the pancreas to adjacent structures. They may also spread to regional lymph nodes. Most common sites of distant metastatic spread include the liver and the lungs (via the bloodstream) and the peritoneum (abdominal cavity). However, tumor cells can metastasize to other parts of the body as well.

SOX9

SOX9 (sex determining region Y-box 9) is a member of the sex-determining

region Y-box (SOX) family which belongs to a superfamily of the transcription factors containing a high mobility group (HMG) box. SOX proteins regulate transcription by binding to the DNA sequence (A/T)(A/T)CAA(A/T)G through their HMG domain (Kamachi, 2000).

SOX9 is required for many important developmental processes including neurogenesis (Stolt, 2003), chondrocyte differentiation (Akiyama, 2002), male sex determination (Chaboissier, 2004), respiratory system development (Houston, 1983), bile duct development (Antoniou, 2009) and skeleton formation (Foster, 1994). Aberrant expression of Sox9 leads to a number of developmental defects and diseases.

SOX9's implication in cancer has also been intensively explored. However, its role in cancers seems controversial. It has been reported to be oncogenic in colon cancer (Blache, 2004), prostate cancer (Wang, 2008) and lung cancer (Jiang, 2010). Its interaction with TGF-beta, p63, WT-1, FGFR, and Hedgehog signaling renders SOX9 aggressive in breast cancer (Katoh, 2008; Moore, 2008; Xu, 2009; Zardawi, 2009). It inhibits PKC-alpha in the intestine epithelium to promote proliferation (Dupasquier, 2009).

On the contrary, other studies indicated an anti-oncogenic characteristic of SOX9. A study shows that promoter hypermethylation and thus loss of expression of

SOX9 is associated with progression of bladder cancer (Aleman, 2008). SOX9 also induces apoptosis in colon cancer cells (Jay, 2005) and inhibits colon cell growth by negative regulation of Wnt/beta-catenin signaling (Blache, 2004). In melanomas and retinoid-treated breast cancer cell lines, Sox9 also exerts the anti-cancer effect (Muller, 2009; Afonja, 2002; Passeron, 2009). Other evidence includes that its expression inhibits oncogenic protein CEA in colon cancer cells (Jay, 2005) and upregulates tumor suppressive CEACAM1 in normal intestine epithelium (Zalzali, 2008).

Regarding its implications in cancer metastasis, a recent publication demonstrated that cytoplasmic localization of SOX9 promoted breast cancer cell proliferation and correlated with poor prognosis of invasive breast cancer (Chakravarty, 2011). Interestingly, a research group pointed out that there was a spliced form of SOX9, named miniSOX9 (Abdel-Samad, 2011). It acted as SOX9 inhibitor to activate Wnt/beta-catenin signaling. The differential expression of miniSOX9 in tumorous and normal colon tissues suggested its oncogenic feature.

However, except for a study revealing that differential methylation of SOX9 promoter contributes to angiogenesis and higher metastatic potential in pancreatic cancer (Peter Camaj, 2010), little literature has been published on the effect of SOX9 on PDAC.

Aims of study

We hypothesized that

(1) There would be some metastasis suppressor genes, whose loss of function would result in pancreatic cancer metastasis;

(2) There would be gemcitabine sensitivity genes existing, down-regulation of which was responsible to gemcitabine resistance in PDAC.

Our objectives were to

(1) Identify metastasis suppressor genes in human PDAC;

(2) Investigate into cellular functions of the genes and understand how they modulate pancreatic cancer cell metastasis;

(3) Identify gemcitabine sensitivity genes in human PDAC.

Materials and Method

Cell culture

Mammalian Cell Culture

HPDE, Capan-2, SW1990, Bxpc3, Panc1, CFPAC1 and Panc0403 cells were obtained from the American Type Culture Collection (Rockville, MD, USA). HPDE was cultured in Keratinocyte Serum Free Medium (KSFM) (Gibco, USA) supplemented with L-glutamine, EGF, and BPE. Other cell lines were cultured in Dulbecco's modified Eagle's medium supplemented with 50 unit/ml penicillin-streptomycin (GibcoBRL, USA) and 10% (v/v) fetal bovine serum (Hyclone) in a humidified incubator at 37°C in 5% CO_2. After the cells reached about 80% confluence, the medium was removed and the cells were trypsinized with 1 ml of 0.05% trypsin-EDTA (Gibco, USA) for 2 mins. Then cell suspension was transferred to a 15-ml centrifuge tube containing 10 ml of PBS and centrifuged at 1,000 rpm at room temperature for 5 min. The cell pellet was resuspended with fresh medium and transferred to new plates and incubated as described above.

MTT Assay

MTT (3-(4,5-Dimethylthiazol-2-yl)-2,5-diphenyltetrazolium bromide was purchased from USB Chemicals Corporation. The MTT powder was dissolved in

sterile Nano-Pure water to a final concentration of 5mg/ml and sterilized by passage through a 22 μm pore PVDF filter. Before treatments, $1x10^3$ to $5x10^3$ cells were plated on a 96-well plate. When the treatment was completed, the cells were cultured in a medium containing 1mg/ml of MTT for 3 more hours. Following that, the medium was discarded and 100 μl of DMSO was added to the wells in 96-well plate. The plate was shaken at a speed of 120 rpm for 15 minutes. Finally, absorbance was measured at λ490nm. For each treatment, the samples were repeated in triplicates.

Colony formation assay

One thousand cells were seeded in a 100mm culture dish. Colonies were allowed to form for 2 weeks. Medium was changed very 3-4 days. Two weeks later, culture medium was removed and the plate was rinsed with PBS twice. Colonies were fixed by 100% methanol for 10 min and stained with coomassie blue for 5 min. Total number of colonies formed was manually counted by the naked eye examination.

Wound healing assay

Cells were cultured in a 6-well plate to be confluent monolayer. A wound was generated by gently scratching a line through the cells. Cells were allowed to migrate through the wound for 72 hours. The boundaries of the wound were

recorded every 24 hours under a microscope and the area of cell-free region was calculated by Image J.

Transwell migration chamber assay

Migration was accessed using a 24-well format cell culture insert (SPL) containing a polycarbonate membrane filter with 8 um pores. The upper chamber contained cells in DMEM without FBS, and the lower chamber contained DMEM plus 10% FBS as chemoattractant. Cells were incubated for 24 hours at 37°C in 5% CO^2 air. Non-migrated cells were scraped off the upper surface of the membrane with a cotton swab. Migrated cells remaining on the bottom surface were counted after staining with crystal violet.

Immunocytochemistry

In Day 1, appropriate amount of cells, treated or non-treated, were seeded on a poly-L-lysine coated coverslips in a 96-well plate and incubated in a humidified incubator at 37°C overnight to allow the cell to attach the coverslip. In Day 2, the cells were firstly washed with ice cold PBS twice and fixed in 4% paraformaldehyde in PBS for 15 minutes at room temperature. After washing with PBS twice, 10ml PBS containing 0.25% Triton X-100 was added to the cells for permeabilization. The cells were washed in PBS 3 times for 5 minutes before incubation with primary antibodies at 4°C overnight. The primary antibodies were diluted in a concentration

suggested by the manufacturer. In day 3, the primary antibodies were discarded and the cells were washed with ice cold PBS for 3 times. Then the cells were probed with corresponding secondary antibody in dark for 2 hours. Finally, the cells were counter stained with DAPI for 5 minutes and mounted on a slide with a drop of ProLong® Gold anti-fade reagent (Invitrogen).

Transient transfection of siRNA

DharmaFECT was purchased from Thermo Scientific. The transfection procedure was done according to the product protocol. In brief, 3000 cells were plated to each well of a 96-well plate and cultured in a 37°C overnight. On the next day, 5 µl of 2 µM siRNA was mixed with 5 µl of plain DMEM medium in a 1.5-ml eppendorf tube. In a separated tube, 0.5 µl of DharmaFECT transfection reagent was added to 49.5 µl of plain DMEM. The mixtures were gently mixed by pipetting up and down which were followed by 5 minutes of incubation at room temperature. The diluted siRNA was then added to the diluted DharmaFECT transfection reagent, mixed and incubated for another 20 minutes. When incubation was completed, 80 µl of antibiotic-free complete medium was added to the mixture for a final siRNA concentration of 100 nM. The medium from the wells of the 96-well plate was removed and replaced by the 100 µl transfection mixtures. Transfection medium was replaced with fresh culture medium 8-16 hours post transfection. The cells were

incubated at 37°C for additional 24 to 72 hours before harvest. Drug treatment could start 24 hours after transfection.

Establishment of in-vivo and in-vitro models

shRNA library introduction

A total of 2 * 10^6 capan-2 cells were transfected with one vial of the lentiviral human 50K shRNA library (SBI, SI206B-1) by polybrene according to the manufacturer's instruction. 3 days after transfection, cells were subjected to puromycin selection at the concentration of 0.5 μg/ml for 8 days. Then cells were applied for different screening schemes for the enrichment of a phenotype of interest. After harvest of cells selected, total RNA was isolated and cDNA was reverse transcribed. The shRNA templates were retrieved according to manufacturer's instruction, either by sequence analysis or microarray analysis. Target genes of corresponding shRNAs could be identified according to a gene list provided by manufacturer.

Establishment of the orthotopic pancreatic cancer mouse model

Male nude mice of 4 to 6 weeks old were supplied by the Laboratory Animal Services Center (LASEC) of the Chinese University of Hong Kong (CUHK). They were housed in pathogen-free, air-controlled conditions supplied with water, bedding, and gamma-ray-sterilized food, with 12-hour light-dark cycles. Right

before tumor implantation, pancreatic cancer cells were trypsinized and resuspended at a concentration of 5,000,000 cells per 50 µl in sterile PBS containing 10% matrigel (BD) and were kept on ice until implantation. Mice were anesthetized using ketamine/xylazine cocktail which was administrated by intraperitoneal injection at 10 µl per gram body weight. The cocktail was prepared by diluting 1 ml of ketamine stock (20 mg/ml) and 0.5 ml xylazine (100 mg/ml) into 8.5 ml PBS under sterile condition. 5-10 minutes after anesthetization, mice were positioned to the right. The surface of the abdomen was scrubbed three times by 70% ethanol. After confirmation of thorough anesthetization, an approximately 1 cm incision was made and the pancreas was gently pulled out. 50 µl of cancer cell suspension was injected into the tail of the pancreas by a 27 gauge needle. Two minutes after injection, the pancreas was gently put back into the abdominal cavity. Three sutures were made across the incision. After tumor transplantation, mice should be monitored daily for signs of illness and for infections through the surgical wounds. 2 to 3 months after transplantation, mice could be sacrificed for examination of tumor growth and formation of metastasis. All experiments were approved by the Animal Experimental Ethics Committee of the CUHK.

Package of lentivirus expressing shRNA

Lentivirus-based shRNA vectors targeting SOX9 were purchased from abm

(USA). Lentivirus was produced by co-transfection of packaging plasmids and shRNA plasmids into 293T cells using calcium phosphate methods. Transfection medium was changed 16 hour later and 293T cells were incubated for additional 72 hours. Supernatant was harvest after discarding the cell debris and was applied for overnight centrifugation at 4°C for 7680 rpm. The viral pellet was resuspended in a small volume of TBS buffer and kept at -80 °C.

Generation of stable cell line expressing shRNA

Capan-2 cells were cultured in a 24-well plate at 70% confluence. Optimized volume of lentiviral particles was added into the cells together with polybrene. Transfection medium was changed the next day. 3 days after transfection, correspondent selection agent could be given for an additional 2 weeks for selection of cells stably expressing lentiviral constructs.

DNA manipulation

Large scale plasmid isolation from E. coli (maxi-prep)

QIAGEN Plasmid Maxi Kit (Qiagen, Germany) was used for plasmid DNA preparation. An overnight culture of transformed E. coli in 500 ml of LB medium with appropriate antibiotic was centrifuged at 5000 rpm for 15 minutes. The supernatant was discarded and the pellet was resuspended in 10 ml of buffer P1. To lyse the cells, 10 ml of buffer P2 was applied to the resuspended culture and

incubated at room temperature for 5 minutes. To neutralize the lysate, 10 ml of buffer P3 solution was added into the lysate, followed by incubation on ice for 5 minutes. The cell debris was separated from the plasmid DNA solution by centrifugation at 7830 rpm for 30 min at 4°C. 10 ml of buffer QBT was added to the Maxi-prep column to activate the resin. After the N3 has gone through the column, the cell lysate from above was poured into the column until all of the lysate was drawn through the resin by gravity. To wash the DNA-bound resin, 30 ml of buffer QC was added to the column and allowed to empty by gravity, twice. To elute the DNA from the resin, 15 ml of buffer QF was loaded to the column. Following that, the eluent was mixed with 10.5 ml of isopropanol by inversion. To collect the DNA, the solution was centrifuged at 15,000 rpm for 30 min at 4°C. The supernatant was then discarded and the DNA pellet was washed with 1 ml of 70% ethanol, air-dried at room temperature and resuspended with 500 µl of TE buffer. The DNA concentration was measured by OD_{260}.

Analysis of Protein

Preparation of protein cell lysates

After the medium was discarded, the cells were washed with chilled PBS twice. Then appropriate amount of cell lysis buffer (RIPA) supplemented with protease inhibitor mixture was directly added to the cells and left it at 4 ºC for 15 minutes.

The lysed cells were scraped off from the plate and transfer to a 1.5 ml microcentrifuge tube. After 30 minutes incubation on ice, the samples were centrifuged at 13,000 rpm for 30 minutes at 4°C to remove the insoluble cell debris. The supernatant was collected and transferred to a new microcentrifuge tube.

Protein concentration determination

Bicinchoninic acid (BCA) protein assay system was used to measure the protein concentration of cell lysates. Firstly, 2 µl of protein samples were loaded into a 96-well plate together with a series of standards consisting of 0, 2, 4, 8, 16 µg of BSA. Then 200 µl of BCA reagent A and 4 µl of BCA reagent B were mixed with the samples and incubated at 37°C until the color of the mixture changed. At the end, absorbance was measured at OD_{460}. The readings of the BSA standards were plotted with linear regression as a reference, and the concentration of the sample was deduced by referring the reading of the protein sample to the BSA reference.

SDS-PAGE

Cell lysates were suspended in Proteins in Laemmli sample buffer to a concentration of 1 µg/µl and incubated at 100 ºC for 10 minutes. After that, the cell lysates were separated in 10% or 15% polyacrylamide gels. The separating gel was mixed with 40 µl of APS and 4 µl of TEMED, and allowed to polymerize at room temperature. To prepare the stacking gel, 3 ml of stacker solution was mixed with 30

µl of APS and 3 µl of TEMED. The stacking gel mixture was subsequently loaded on top of the polymerized separating gel with 14-well comb inserted. The comb was removed after the stacker was solidified. The gel was then assembled to the Mini-PROTEAN Electrophoresis System (Bio-Rad). SDS-PAGE running buffer was then filled into the tank. 10 µg of cell lysates were loaded into the wells and separated by a constant voltage of 100 V for 100 minutes.

Immunoblotting (Western blotting)

The Mini Trans-Blot (Bio-Rad) was used to transfer proteins from polyacrylamide gels to PVDF membranes (Pall, USA). First of the all, the gel holder cassette, with the black plate faced down, was put into a tank of transfer buffer. A piece of foam pad was placed on the top of the black plate with a piece of 3MM paper (Whatman, UK) was soaked in transfer buffer on it. The polyacrylamide gel and a PVDF membrane were placed on top of the 3MM paper. At the end, another piece of 3MM paper and foam pad was placed on the top of the membrane. The gel holder cassette was closed and put into the modular electrode assembly. The transfer was carried out at a constant voltage of 100V for 100 minutes.

After the transfer, the membrane was soaked in 3% milk in TBST or 5% w/v BSA in TBST for 30 minutes to block non-specific protein-binding sites. The membrane was then incubated in 2% milk in TBST containing the primary antibody

at the appropriate dilution at 4°C with shaking overnight. On Day 2, the membrane was washed twice with TBST for 15 minutes each. The membrane was then incubated in 3% milk or 2% w/v BSA in TBST containing the secondary antibody conjugated with horse reddish peroxidase (Santa Cruz) at a dilution of 1:1000 at room temperature for 2 hours. Finally, the membrane was washed three times with TBST for 10 min each, incubated in ECL solution (Millipore USA) for 3 minutes, put between two pieces of plastic film, and exposed to light sensitive films (Fuji, Japan). The exact exposure time varied depending on the intensity of the signals. The films were developed with a film-processing machine (Eastman Kodak, USA).

RNA manipulations

RNA Isolation

TRIzol® Reagent (Invitrogen) was used for RNA isolation. The samples, tissue or cells, were firstly homogenized with Trizol and incubated at room temperature for 5 minutes. For 1ml of Trizol reagent, 200 µl of chloroform was added to the homogenized samples, which was followed by vigorous shaking for 15 seconds. After another 3 minutes of incubation, the samples were centrifuged at 12,000 × g for 15 minutes at 4°C. Then, the top aqueous phase of the sample was transferred to a new tube. 500 µl of 100% propanol was added to the aqueous phase. The mixture was then incubated at room temperature for 10 minutes which was followed by

another centrifugation at 12,000 × g for 10 minutes at 4°C. The supernatant was removed and 1 ml of RNase free 70% ethanol was added. After a brief vortexing, the samples were centrifuged at 7500×g for 5 minutes at 4°C. The wash was discarded and the RNA pellet was air dried. An appropriate amount of RNase free water was used to dissolve the RNA whose concentration was subsequently determined by NanoDrop (Thermo Scientific).

Synthesis of cDNA from RNA and quantitative PCR

The synthesis of cDNA from RNA used High Capacity cDNA Reverse Transcription Kit (Invitrogen). Firstly, 1 µg of purified RNA was added to RT buffer (1x RT buffer, 4mM dNTPs, 1x RT random primers, reverse transcriptase and RNase inhibitor) as provided to the final volume of 25 µl. After a gentle mixing and a short spin down, the sample was placed in a thermal cycler with a program set according to manufacturer's guideline.

The relative expression level of genes was determined by using semi quantitative PCR. 1 µl of the cDNA obtained from previous step was added to Power SYBR® Green PCR Master Mix (Invitrogen) containing corresponding set of primers for gene detection. Then the samples were loaded in triplicated into a 96-well or 384-well plate which was then placed in ABI 7900HT Fast Real Time PCR for measuring the CT values. The relative expression level of each gene was

determined by comparative quantization.

Analysis of Clinical Samples

Clinical specimens

Pairs of pancreas normal and tumor tissues were collected from pancreatic cancer patients in Prince of Wales Hospital, Hong Kong. Samples were fixed in 3.7% paraformaldehyde for 24 hours, embedded in paraffin and sectioned as 5 um onto glass slides.

Immunohistochemistry

Histostain®-Plus Kits was used for immunohistochemistry. First of the all, the samples were deparaffinized and rehydrated by immersing the slide in following solutions and order: twice in xylene for 5 minutes, twice in 100% ethanol for 5 minutes, once in 90% ethanol for 3 minutes, once in 80% ethanol for 3 minutes, once in 70% ethanol for 3 minutes and finally in 1X PBS for 1 minutes before drying the slide. To inactivate endogenous peroxidase, the samples were incubated with 3% H_2O_2 in methanol for 5 minutes. 100 µl of serum blocking solution was applied the sample for 10 minutes to block non-specific antibody binding sites. The primary was diluted in appropriate concentration and applied to the sample in a humidified chamber at 4 °C overnight. In next day, the primary antibody was removed by rinsing in PBS twice. 100 µl of biotinylated secondary antibody was

added to each section and incubated for minutes. Sequentially, 2 drops of Reagent C was added to the sections for conjugating the streptavidin-peroxidase. At the end, the sample was covered with DAB to develop the signal. A light haematoxylin stain was applied as counterstain.

Measurement of IHC staining was based on a semi-quantitative scoring method. For the percentage (P) of positively stained cancer cells, 0 = less than 10%, 1 = 10-50%, 2 = 50-75%, 3 = more than 75%. For the intensity (I) of staining, 0 = negative, 1 = weak, 2 = moderate, 3 = strong. By multiply P and I, the scores spanned from 0 to 9, where "-" = 0, "+" = 1-2, "++" = 3-4, and "+++" = 5-9. Both "–" and "+" were identified as negative and both "++" and "+++" were identified as positive. For statistical analysis of IHC scores, Mann-Whitney non-parametric test was applied.

Results

Genome-wide RNAi screening identifies genes as metastasis suppressors in an orthotopic pancreatic cancer mouse model

In order to identify genes that play critical roles in pancreatic cancer metastasis,

we conducted an in vivo whole genome screening. We used a genome-wide lentiviral-based shRNA library (SBI) as a powerful tool which facilitated the high-throughput functional genomic studies. This library comprises of a pool of shRNAs (3-5 shRNA constructs per target gene) targeting 47,400 human transcripts. It can be introduced into a population of identical cells. Because the library is lentivirus based, the shRNA constructs can be highly efficiently integrate into genomic DNA of target cells. The endogenous and heritable expression of shRNA effectors in target cells guarantees long-term stable silencing of target gene for subsequent functional studies. And then cells containing the whole library can be applied for screening of a phenotype of interest. Cells of a selected phenotype can be harvested and the shRNA constructs inducing this phenotype can be retrieved.

Figure 11A demonstrates the strategy of our screen. To begin with, the library was transduced into capan-2 cells. As a human PDAC cell line, capan-2 is capable of forming tumors in nude mice and is previously reported possessing low metastatic potential to the liver (Suemizu, 2007). The reason why this cell line was chosen for the screening is based on our hypothesis that knocking down a metastasis suppressor gene will enable the metastasis-defective cells to spread out. The transduction of the library was carried out at low multiplicity of infection (MOI) to ensure that each cell acquired only one unique shRNA inserts. Following the infection, capan-2 cells

were selected in puromycin for 2 weeks, for the purposes that, on one hand, a pure population of transduced cells were obtained, and on the other hand cells with shRNAs targeting vital genes were excluded.

After puromycin selection, capan-2 cells bearing the entire library were transplanted into nude mice to perform the in vivo screen. Our in vivo screening system was established based on an orthotopic pancreatic cancer model. By surgical operations, cancer cells were directly inoculated into mouse pancreas where pancreatic cancer normally grew. The orthotopic model, instead of a subcutaneous model or a tail vein injection model, exhibits some advantages. Firstly, the primary site of tumor growth provides the microenvironment that best mimics the generation a spontaneous pancreatic cancer. Secondly, tumor cells in the pancreas must overcome all metastatic suppressing programs and complete all of the steps of metastasis to spread to other parts of the body. Here mice were serves as a selection system or a cell sorter to detect successfully metastasized cells. Given that liver was the most common site of pancreatic cancer metastasis, we mainly focused our attention on liver metastasis.

About two to three months after transplantation, mice would be sacrificed for a careful examination. Tumor nodules in the liver would indicate the occurrence of liver metastasis. We supposed that each liver nodule derived from a single pancreatic

cancer cell and that silencing a particular gene in the cell allowed it to spread out. Then the nodules could be harvested for the recovery of their shRNA templates, whose expression was supposed to induce metastasis. Finally the target gene of the shRNA could be decoded by sequencing analysis. Thus the gene could be identified as a metastasis suppressor gene.

In the primary screening, we used 25 nude mice for the screening. As shown in figure 11B, all of them had primary tumors grown after injection of capan-2 cells into their pancreas. Six of them generated liver metastasis in 8 to 12 weeks. The shRNAs retrieved from the metastatic liver nodules corresponded to SOX9, ABCE1, BLVRB, CNDP2, SYNJ1, and TPST2. Subsequently we carried out experiments for the validation of these candidate metastasis suppressor genes. In this study, we mainly focused on SOX9.

Figure 11.

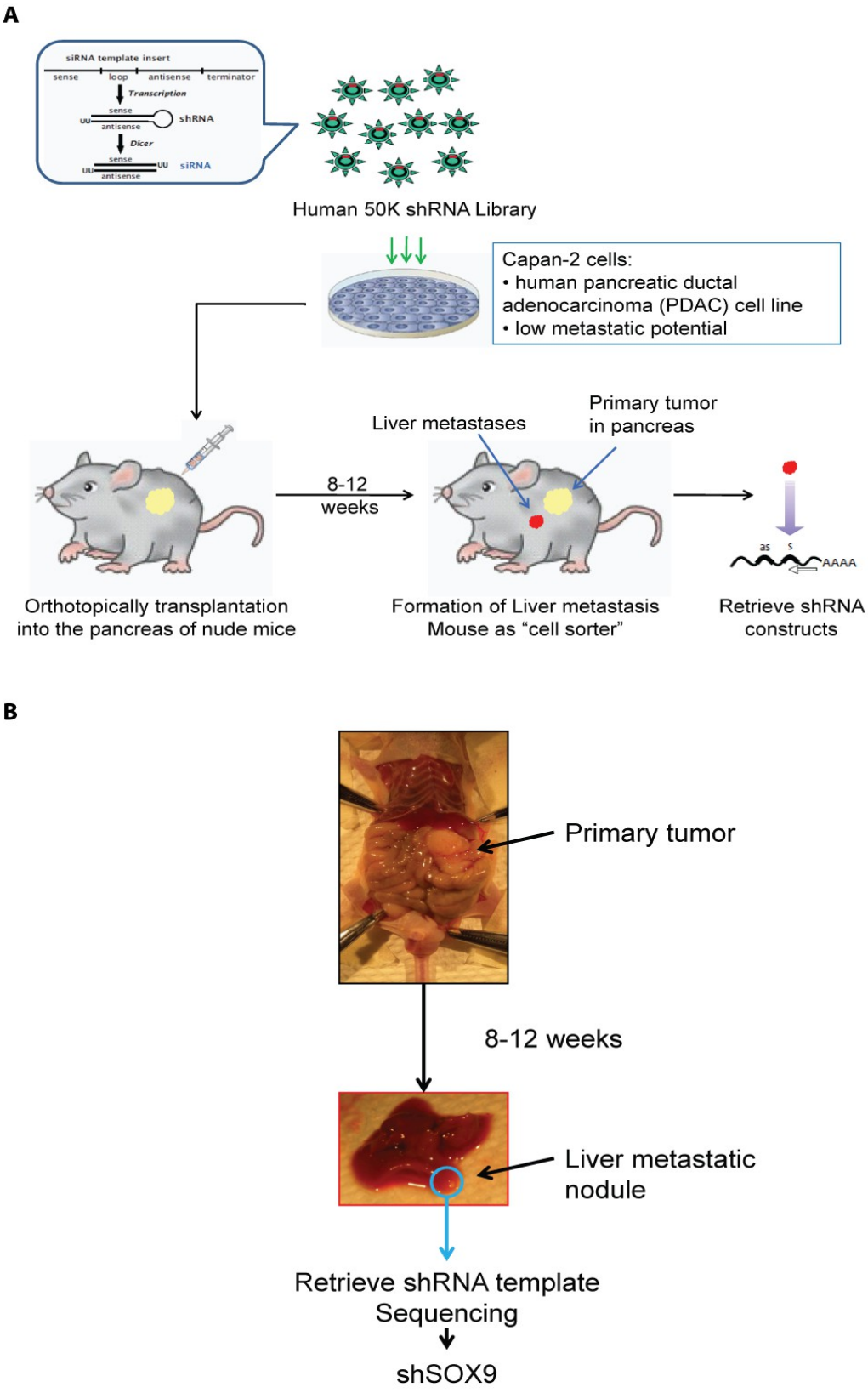

Figure 11: Genome-wide in vivo screening for metastasis suppressor genes

(A) The strategy of the genome-wide screening in an orthotopic pancreatic cancer mouse model. Details are described in the text.
(B) Primary tumors generated in all 25 nude mice in the initial screen. Six of them developed liver metastasis in 8 to 12 weeks. Arrows indicate primary pancreatic tumor and liver metastatic nodule. Retrieving shRNA constructs from liver nodules together with sequencing analysis revealed 6 genes as candidate metastasis suppressors, such as SOX9.

SOX9 is a metastasis suppressor gene in pancreatic cancer

To validate SOX9's anti-metastasis effect on pancreatic cancer, we firstly generated stable capan-2 cell lines that endogenously expressed SOX9 shRNAs through lentiviral infection techniques. Four shSOX9 constructs (a, b, c, and d) were tested in this study. The knockdown efficiency of SOX9 in these cell lines were double confirmed in mRNA level and protein level (figure 12A). Regarding to the knockdown efficacy, the stable cell line expressing shSOX9-a and its control cell line expressing shLUC were used in following experiments.

ShSOX9 and shLUC capan-2 cells were injected into the pancreas of two groups of nude mice using the same methods as in the initial screening (figure 12B). Twelve weeks after transplantation, mice were sacrificed to examine primary tumor growth and the presence of metastasis. Pancreatic tumors were successfully established in the primary site for all mice in both groups. Basically, the growth of primary tumor showed no difference between SOX9 knockdown (Kd) group and control groups (data not shown). However, different status of liver metastasis between the two groups was found. Metastatic liver nodules occurred in 7 out of 11 mice in SOX9 Kd group, while only 2 out of 10 mice were found with liver nodules in control group. It indicated that the probability of the occurrence of liver metastasis was significantly higher in SOX9 Kd group than that in control group

(figure 12B and C). It meant that down-regulation of SOX9 promoted capan-2 cells to spread to the liver. Moreover, the number of metastatic nodules was more in SOX9 Kd group (totally 10 nodules for 11 mice) than in control group (totally 3 nodules for 10 mice). In regards to the size of metastatic tumors, liver nodules of shSOX9 group were larger in size (figure 12D), which further supported the notion that silenced expression of SOX9 enhanced capan-2's ability to metastasize to the liver. Finally, histological analysis of liver sections confirmed the cells of live nodules were from primary pancreatic tumor (figure 12E). In conclusion, this validation experiment confirmed that SOX9 functioned as a metastasis suppressor gene.

Figure 12.

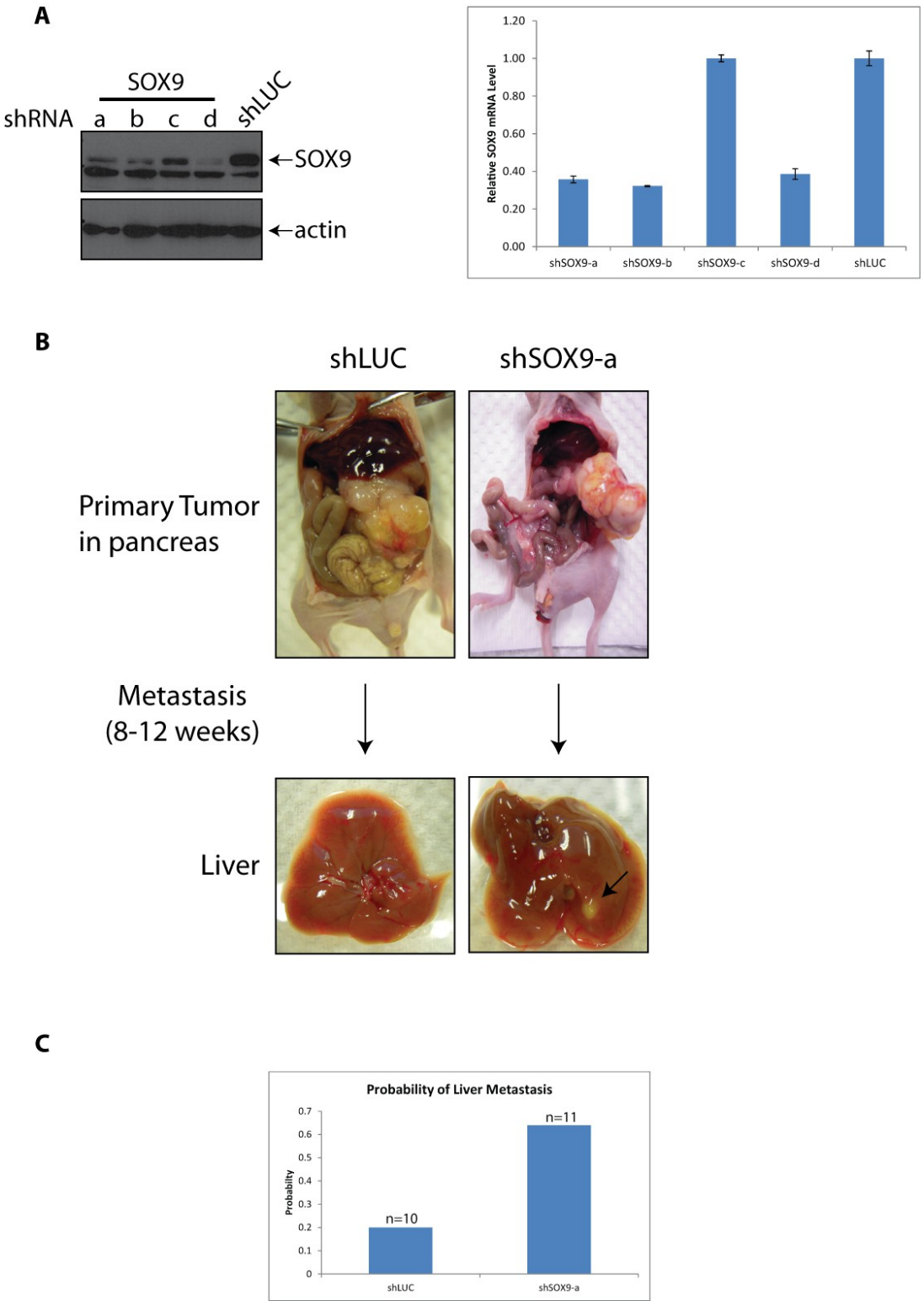
A
SOX9
shRNA a b c d shLUC
←SOX9
←actin
Relative SOX9 mRNA Level
1.20
1.00
0.80
0.60
0.40
0.20
0.00
shSOX9-a
shSOX9-b
shSOX9-c
shSOX9-d
shLUC
B
shLUC
shSOX9-a
Primary Tumor in pancreas
Metastasis (8-12 weeks)
Liver
C
Probability of Liver Metastasis
Probability
0.7
0.6
0.5
0.4
0.3
0.2
0.1
0
n=10
n=11
shLUC
shSOX9-a

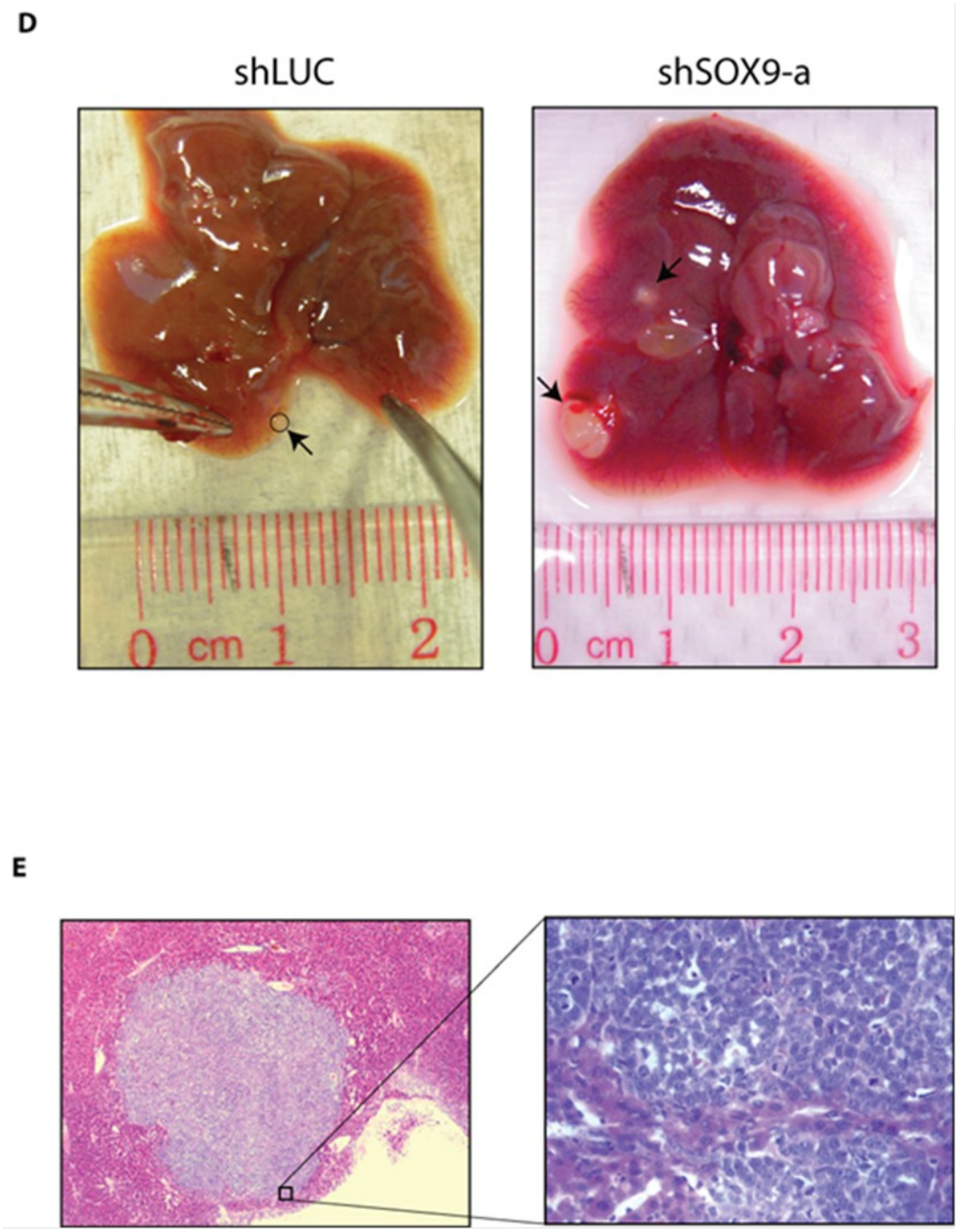

Figure 12: Validation of SOX9 as a metastasis suppressor gene in pancreatic cancer.

A. Capan-2 stable cell lines expressing shSOX9 or control shLUC were generated by lentiviral transduction. The expression levels of SOX9 were confirmed at both mRNA and protein levels. The shSOX9-a and shLUC cell lines were chosen for subsequent experiments.

B. Knocking-down of SOX9 promoted the orthotopically transplanted capan-2 cells to metastasize to the liver. In the validation experiments, 10 and 11

nude mice were used for control shLUC group and shSOX9-a group respectively. All of them had primary tumors established. 7 out of 11 mice in shSOX9 group developed liver metastasis, whereas only 2 out of 10 metastasized in control group. Primary pancreatic cancer and the liver of the representative mice are shown. Arrow points at metastatic tumor nodules in the liver.

C. Probability of liver metastasis derived from pancreatic cancer in control group (n=10) and SOX9-knockdown group (n=11). The probability was significantly higher in SOX9-knockdown group than that in control group.
D. Liver metastatic nodules of shSOX9 group were larger in size and greater in number, compared with control group.
E. H & E staining of liver sections confirmed the cells in liver nodules were from primary pancreatic tumor.

Investigation into cellular functions of SOX9

To study the potential mechanisms of SOX9 as a metastasis suppressor gene, we evaluated SOX9's effect on the following aspects, for example, cell proliferation, colony formation, and migration, which are relevant features of metastasis.

SOX9's effect on cell growth

It is proposed that genes exclusively regulating metastasis do not exist and that genes play a role in metastasis also affect tumor growth (Duffy, 2008). It has been suggested that the capability for cancer cells to metastasize are acquired from the very beginning of tumor formation (Bernards, 2002). This point of view seems reasonable, because genes that favor cancer cell proliferation may provide growth advantages for the metastatic tumors to survive in a distant location.

Based on these theories, we firstly examined whether the metastasis suppressive SOX9 had any effects on tumor growth. MTT assays revealed that down-regulation of SOX9 did not remarkably enhance pancreatic cancer cell proliferation in vitro (Figure 13A).

Then we performed colony formation assay to explore whether SOX9 affected cancer cells' ability to form colonies. This assay tests the ability of every single cell in a certain population to grow into a colony. In a highly diluted seeding condition, a cell must initiate unlimited division to give rise to a colony. Only a proportion of cells seeded possess this ability (Franken, 2006). In our studies, SOX9's effect on

this process was not obvious (figure 13B). In each 100mm culture dish, 1000 cells of each cell line were seeded. 2 weeks later, the numbers of cells to form colonies were not significantly different between SOX9 Kd and control groups. Thus in this case we failed to prove that the enhanced metastatic potential of pancreatic cancer cells was due to increased colony formation capability that supported a wandering tumor cell to colonize in a distant organ.

Figure 13.

A

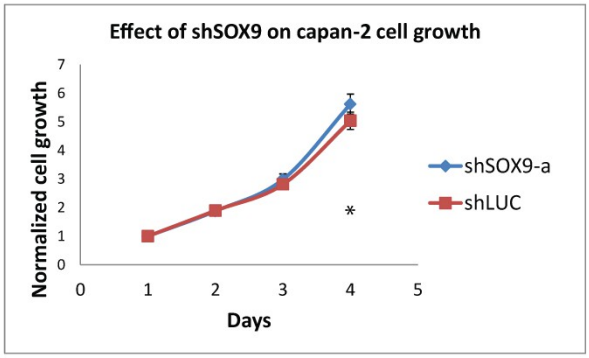

B

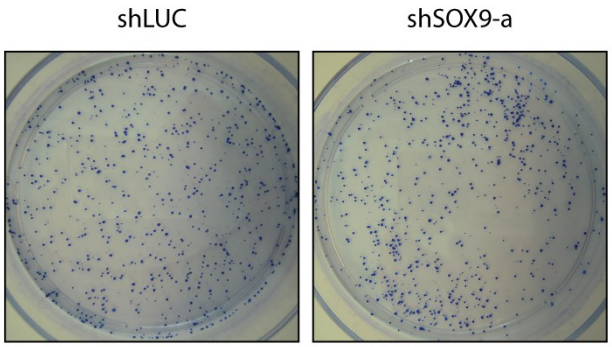

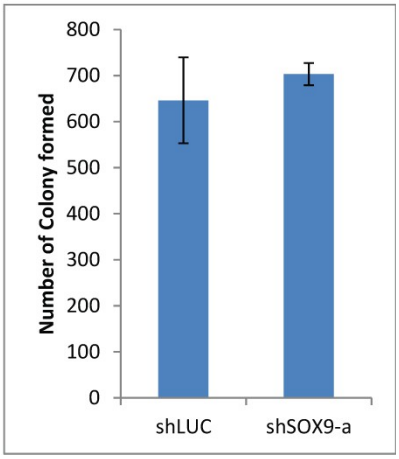

Figure 13: SOX9's effect on cell growth

(A) MTT assays showed that down-regulation of SOX9 did not remarkably enhance cell proliferation. (*, $P < 0.05$ at day 4)

(B) Colony formation assay showed no significantly difference in the capability of colony formation between SOX9 Kd and control cells. 1000 cells were seeded in a 100 mm dish. 2 weeks later, colonies derived from the cells seed were detected by coomassie blue staining. 2 independent experiments with duplicates were performed. Representative plates of the assay were demonstrated.

SOX9's effect on cell migration

High migratory and invasive activity of cancer cells is closely correlated to metastasis. Invasive capability is the major feature to distinguish malignancy from benign lesions. During invasion, proteases produced by malignant cells digest extracellular matrix and neighboring tissues. The breakdown of tissue barriers facilitated cell motility. Besides, migration behavior is essential for a metastatic cancer cell in the process of intravasation and extravasation to blood vessels or lymphatic system. It has been realized that molecules involved in these processes may be future targets of cancer therapy to prevent metastasis or suppress cancer progression. To access SOX9's contribution to cell migration and invasion, capan-2 cells expressing either shSOX9 or control shLUC were subjected to wound healing assay, trans-well chamber assay and matrigel invasion assay.

For wound healing assay, a wound was generated by gently drawing a line through a confluent mono-layer of cultured cells using a 200ul pipette tip. Cells of higher migration potential would intend to fill the gap. Real time records of cells on the boundaries revealed that the scratched area was shrunk faster in cells transduced with shSOX9 (figure 14A). Actually, both cell proliferation and migration are crucial factors affecting the healing of a wound. Given that SOX9's expression did not significantly contribute to cell growth as shown in figure 13, the efficient healing

of SOX9 Kd cells we observed could be regarded solely due to cell migratory activity. Thus we reasoned that down-regulation of SOX9 enhanced pancreatic cancer cells migration.

Trans-well chamber assay also evaluated migratory capability cells. With 10% FBS as chemo-attractant, cells capable of migrating are able to move across the 8 um pores in the membrane, while cells without migratory activity stay unchanged. As demonstrated in figure 14B, 24 hours after assay started, approximately 3 times more cells migrated through the pores in shSOX9 group than that in control group, indicating silenced expression of SOX9 endowed the low metastatic potential capan-2 cells with migration ability.

We also assayed invasion capability for these cells but failed to obtain meaningful results. Neither control nor SOX9 Kd capan-2 cells invaded the coated matrigel above the membrane of the chamber upon 10% FBS attraction. Probably down-regulation of SOX9 was not powerful enough to trigger capan-2 cells to invade. Other possibility is that SOX9 is not relevant to cell invasion.

In general, we found that down-regulation of SOX9 enhanced capan-2's ability to migrate in vitro, but did not significantly promote cell growth, which provided supportive evidence for SOX9 to be a metastasis suppressor gene.

Figure 14.

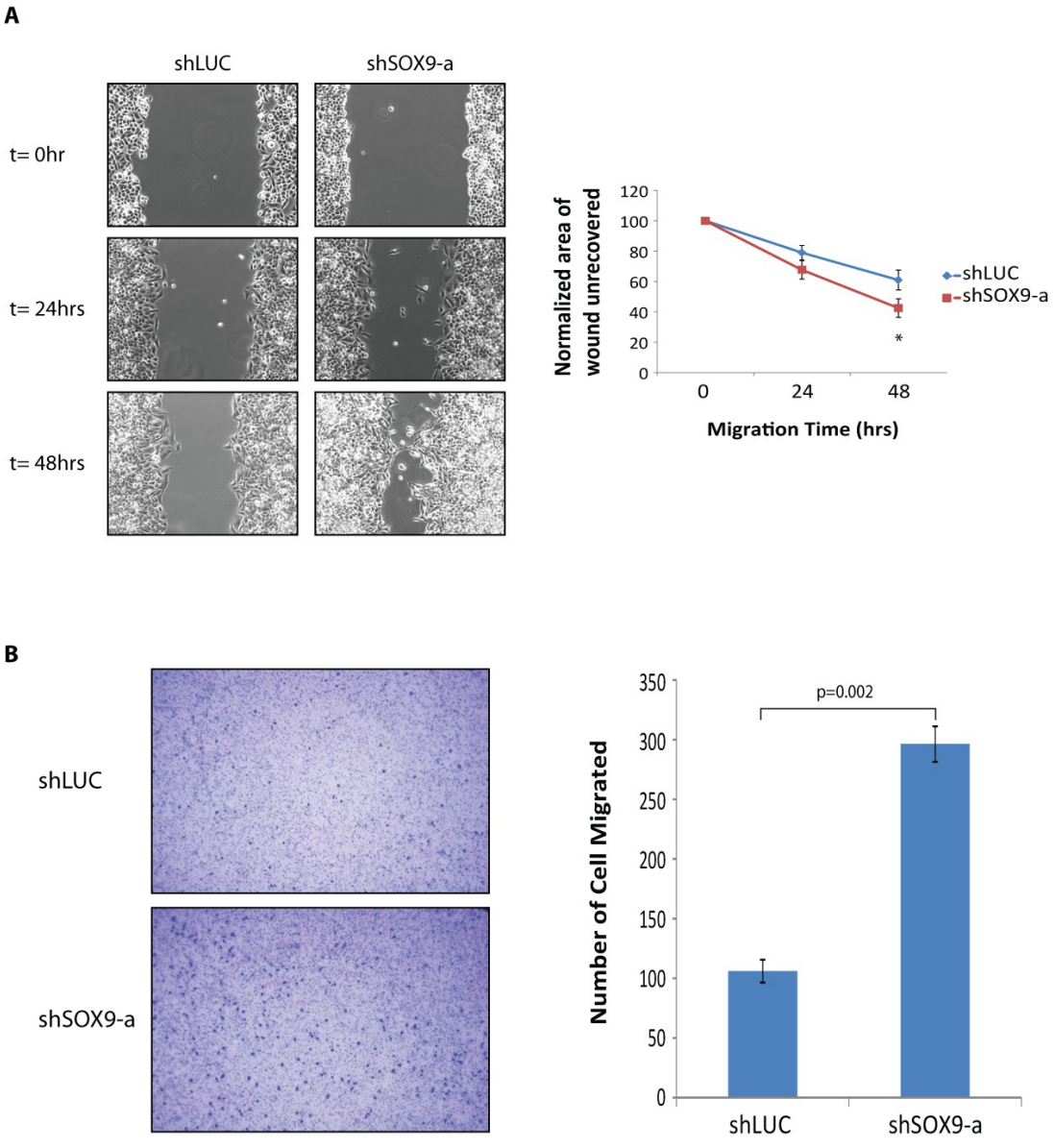

Figure 14: Down-regulation of SOX9's enhanced cell migration.

(A) Wound healing assay showed that cells with SOX9 knocked-down moved faster to fill the gap. Images of the wound were taken at 0, 24 and 48 hours after the wound generation. The area of the wounds was quantified by Image J and normalized to 0 hour. Two independent experiments with triplicates were conducted. Representative images were shown. *, $p < 0.05$.

(B) Transwell chamber assay also use for analyzing cell migration capability. 5 * 10^4 cells were seeded in the upper chamber of a cell culture insert with 8 μm pores. Inhibited expression of SOX9 promoted capan-2 cells to migrate

through the pores within 24 hours. Numbers of cell migrated were counted in each view captured under microscope. Three independent experiments with triplicates were carried out. Representative images were shown. P = 0.002.

Implication of SOX9 in human pancreatic cancer samples

To further investigate SOX9's importance in metastatic status of pancreatic cancer, we examined expression level of SOX9 in 29 human primary pancreatic tumors samples. They were from patients diagnosed as pancreatic ductal carcinoma in Princess of Wales Hospital for the past ten years. The samples were collected during surgical resection, with known distant metastatic status by follow-up observations. Patients of 14 samples had identified distant metastatic sites. Among the 14 cases, 7 metastasized to the liver, while other 7 carried metastatic sites of peritoneal, abdominal cavity, pelvis cavity, distant lymph nodes, and bowel matting. The other 15 samples had not shown any evidence of distant metastasis till the time of data analysis.

Expression of SOX9 in normal pancreatic tissue and primary pancreatic tumor tissues were accessed by immunohistochemistry (IHC) staining. As the representative images demonstrated in figure 15, normal pancreatic duct cells expressed high basal level of SOX9, which is consistent with some published studies (Furuyama, 2010; Lynn, Smith et al. 2007). Intense SOX9 stain was frequently found in non-metastatic tumor samples. On the contrary, the majority of metastatic tumor samples exhibited weak to mild SOX9 expression. Through quantitative analysis of IHC staining (table 4), 10 out of 15 non-metastatic samples were

identified as positive stain, whereas only 4 out of 14 metastatic samples were positive. This difference between groups was significant ($p = 0.044$). These results confirmed a good correlation between SOX9 expression and metastatic status, further supporting our statement that SOX9 acted as a metastasis suppressor gene.

Figure 15.

Normal Pancreatic Tissue

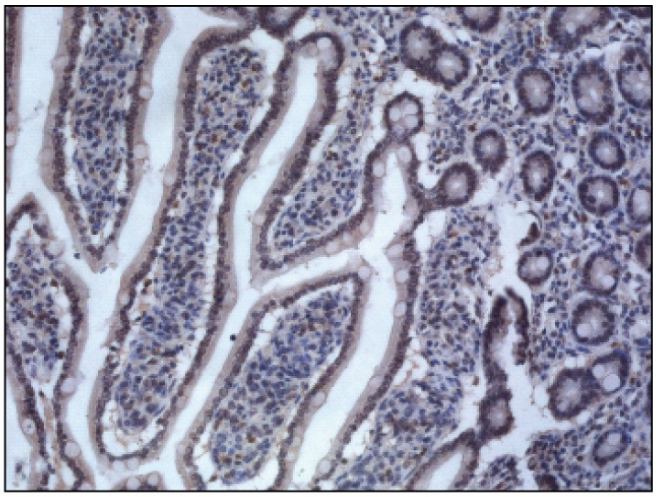

Non-Metastastic Pancreatic Tumor

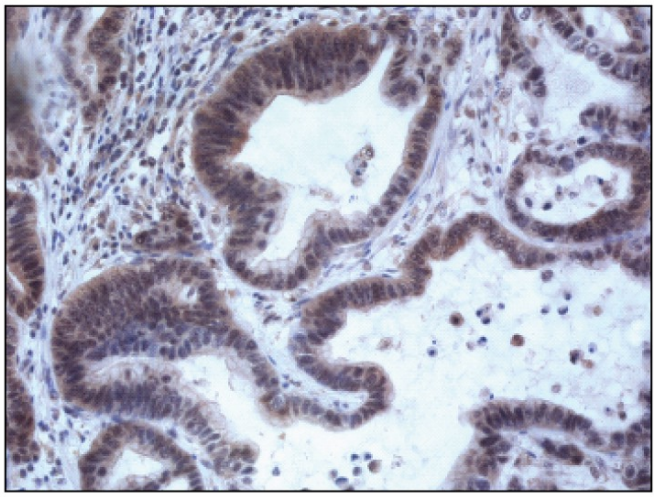

Metastastic Pancreatic Tumor

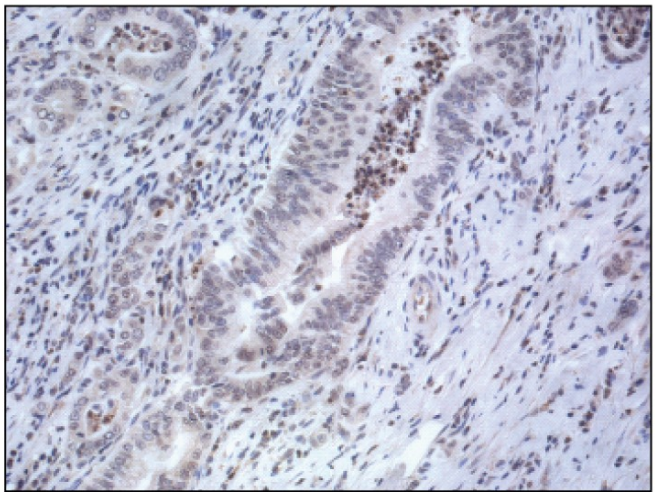

Figure 15: SOX9 expression in human pancreatic cancer samples and normal pancreatic tissues.

Primary tumor samples from 29 pancreatic cancer patients with known distant metastatic status were analyzed in this study. Immunostaining revealed SOX9 expression was high in normal pancreatic tissue. Comparing primary tumor tissues of different metastatic status, there was substantially lower expression level of SOX9 in metastatic pancreatic tumor than in non-metastatic pancreatic tumor. Representative images are shown.

Table 4. Semi-quantitative analysis of SOX9 expression in human pancreatic cancer samples.

SOX9 expression	Positive	Negative	
Non-metastatic tumor	10	5	n=15
Metastatic tumor	4	10	n=14
		P value =	0.044

Semi-quantitative analysis of IHC staining of 29 pancreatic cancer samples. IHC scoring method is illustrated in methods and materials. Statistical analysis indicated a significant difference of SOX9 expression between non-metastatic tumors and metastatic tumors.

Genome-wide RNAi screening for the identification of gemcitabine sens itivity genes

Considering the profound gemcitabine resistant problems that frustrated medical care for pancreatic cancer for decades, we performed a genome-wide RNAi in vitro screening with the purpose to identify critical genes whose inhibition could render pancreatic cancer cells resistant to gemcitabine. Figure 16 illustrates the scheme of the screen. The same cell population transduced with the lentiviral shRNA library as used in the previous screening was applied for this screen. Capan-2 cells have been reported to be sensitive to gemcitabine (Giroux V, 2006). The cells carrying the whole library were divided into two identical groups. For one of them, RNA was immediately isolated without any drug treatment. The other sample was then subjected to 2 uM gemcitabine treatment for 6 days. We expected that knockdown of particular genes would induce capan-2's resistance to gemcitabine. After 6 days of culture with the presence of gemcitabine, resistant clones would grow and growth advantages provided by shRNAs would be amplified. At that time, survival cells were harvested and RNA was isolated in the drug treated sample. Then the RNA samples of before and after gemcitabine treatment were reverse transcribed, and shRNA fragments were amplified by PCRs and labeled with biotin probes. These biotin-labeled PCR products were ready to use for hybridization of the

compatible microarray chips. The signals of the gene chip represented the abundance of shRNAs in samples. By comparing the gemcitabine treated sample to non-treated control sample, we may find shRNAs with increased fold of change as resistant clones and the correspondent genes to be gemcitabine sensitivity genes.

After data analysis, we found 30 shRNAs with fold-of-change larger than 3-fold (table 5). They were regarded as potential gemcitabine sensitivity genes. We focused our attention on one of the genes, LLGL1. The validation experiments were carried out to verify its function for gemcitabine resistance. Firstly, knockdown of LLGL1 expression was achieved by transient transfection of siLLGL1 into capan-2 cells. Quantitative realtime-PCR confirmed the knockdown efficiency of all the three siRNAs (figure 17A). We picked siLLGL1-(1) for subsequent experiments due to its significance. 24 hours after transfection of either siLLGL1 or negative control siRNA, cells were given gemcitabine at different concentrations (2uM and 8uM) for additional 72 hours. Cell proliferation was accessed by MTT assays. Figure 17B revealed an increase of cell growth in LLGL1 suppressed cells, which was consistent with the idea that inhibition of LLGL1 could provide resistance to gemcitabine treated cells.

Moreover, we investigated LLGL1 expression in several human PDAC cell lines (Capan-2, SW1990, Panc04.03, CFPAC1, Bxpc3, and Panc1) and an immortal

human pancreatic duct epithelial cell line HPDE. Varied expression level of LLGL1 could be seen in different cell lines (figure 18). It is reported that capan-2 is a sensitive cell line to gemcitabine treatment, and BxPC3 and Panc-1 are resistant cell lines(Giroux V, 2006). Their sensitivity to gemcitabine in order is: Capan-2 > Bxpc3 > Panc1. It was interested to found that LLGL1 expression levels in these cell lines are Capan-2 > Bxpc3 > Panc1, which seemed to be a desirable correlation between LLGL1 levels and gemcitabine sensitivity. In other words, the more sensitive a cell line, the higher level of LLGL1 expression it would have. This finding further supported LLGL1 to be a gemcitabine sensitivity gene.

Figure 16.

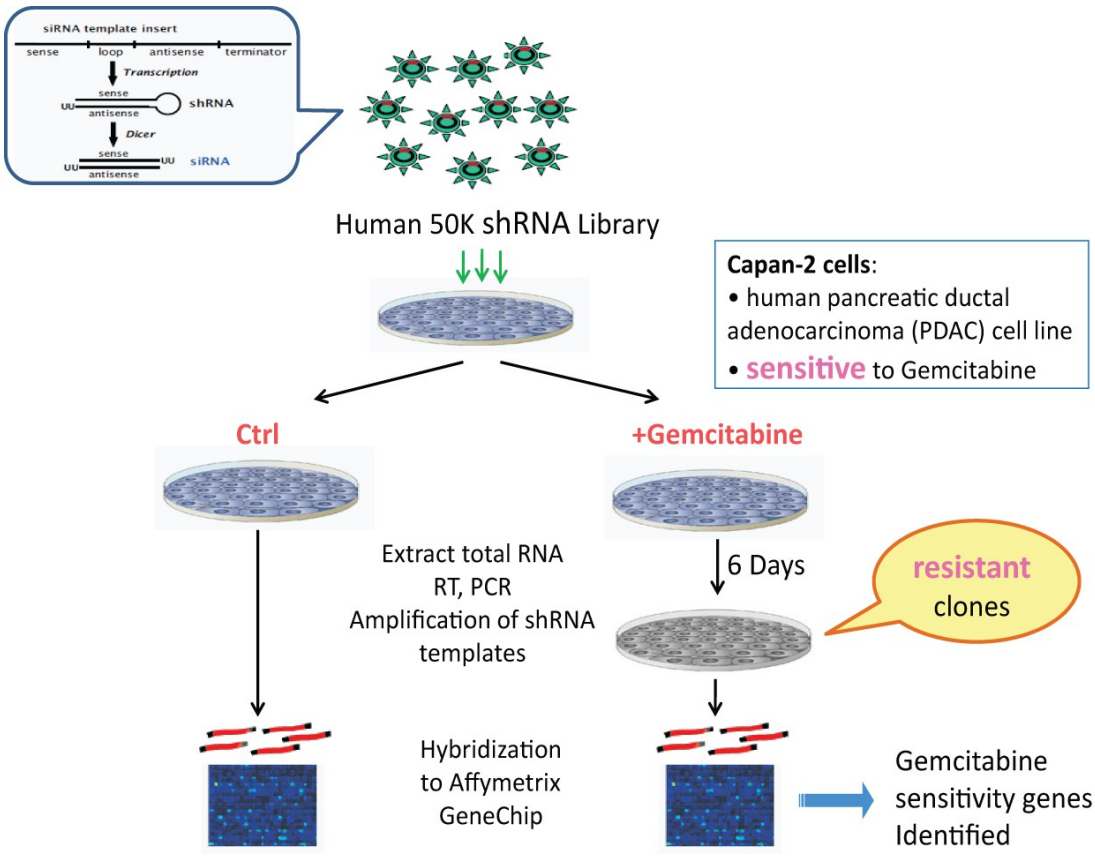

Figure 16: Scheme of an in vitro genome-wide screening for gemcitabine sensitivity genes.

Table 5. Candidate gemcitabine sensitivity genes from primary screening.

Gene Symbol	Gene Title	RefSeq Transcript ID	Fold-Change(Gem/Ctrl)
RNF126	ring finger protein 126	NM_194460	15.9575
GRIK2	glutamate receptor, ionotropic, kainate 2	NM_001166247	15.3324
LLGL1	lethal giant larvae homolog 1 (Drosophila)	NM_004140	5.96706
APC	adenomatous polyposis coli	NM_000038	5.67961
CRTC1	CREB regulated transcription coactivator 1	NM_001098482	4.96471
PRUNE	prune homolog (Drosophila)	NM_021222	4.63793
CROCC	ciliary rootlet coiled-coil, rootletin	NM_014675	4.45919
MT1M	metallothionein 1M	NM_176870	4.14549
ZNF765	zinc finger protein 765	NM_001040185	3.82651
GNPAT	glyceronephosphate O-acyltransferase	NM_014236	3.74406
PTPN2	protein tyrosine phosphatase, non-receptor type 2	NM_002828	3.66212
FCER2	Fc fragment of IgE, low affinity II, receptor for (CD23)	NM_002002	3.46774
GAS2L1	growth arrest-specific 2 like 1	NM_006478	3.34306
OBP2	odorant binding protein 2	NM_014581	3.33983
SERPINB4	serpin peptidase inhibitor, clade B (ovalbumin), member 4	NM_002974	3.3285
CD84	CD84 molecule	NM_001184879	3.24943
ATP9A	ATPase, class II, type 9A	NM_006045	3.23741
SEC14L1	SEC14-like 1 (S. cerevisiae)	NM_001039573	3.22228
BCAS3	breast carcinoma amplified sequence 3	NM_001099432	3.18156
PTGER3	prostaglandin E receptor 3 (subtype EP3)	NM_001126044	3.11788
ANO10	anoctamin 10	NM_018075	3.11598
PODXL2	podocalyxin-like 2	NM_015720	3.1088
EPOR	erythropoietin receptor	NM_000121	3.06713
TUBG1	tubulin, gamma 1	NM_001070	3.03242
NAT8	N-acetyltransferase 8 (GCN5-related, putative)	NM_003960	3.01128
DDAH2	dimethylarginine dimethylaminohydrolase 2	NM_013974	3.01043

List of candidate gemcitabine sensitivity genes identified through microarray analysis. Genes are listed in descending order according to the fold of change of individual shRNAs. The SD of fold of change of shRNAs in this screening was 1.27. ShRNAs of greater than 3-fold changes are shown.

Figure 17.

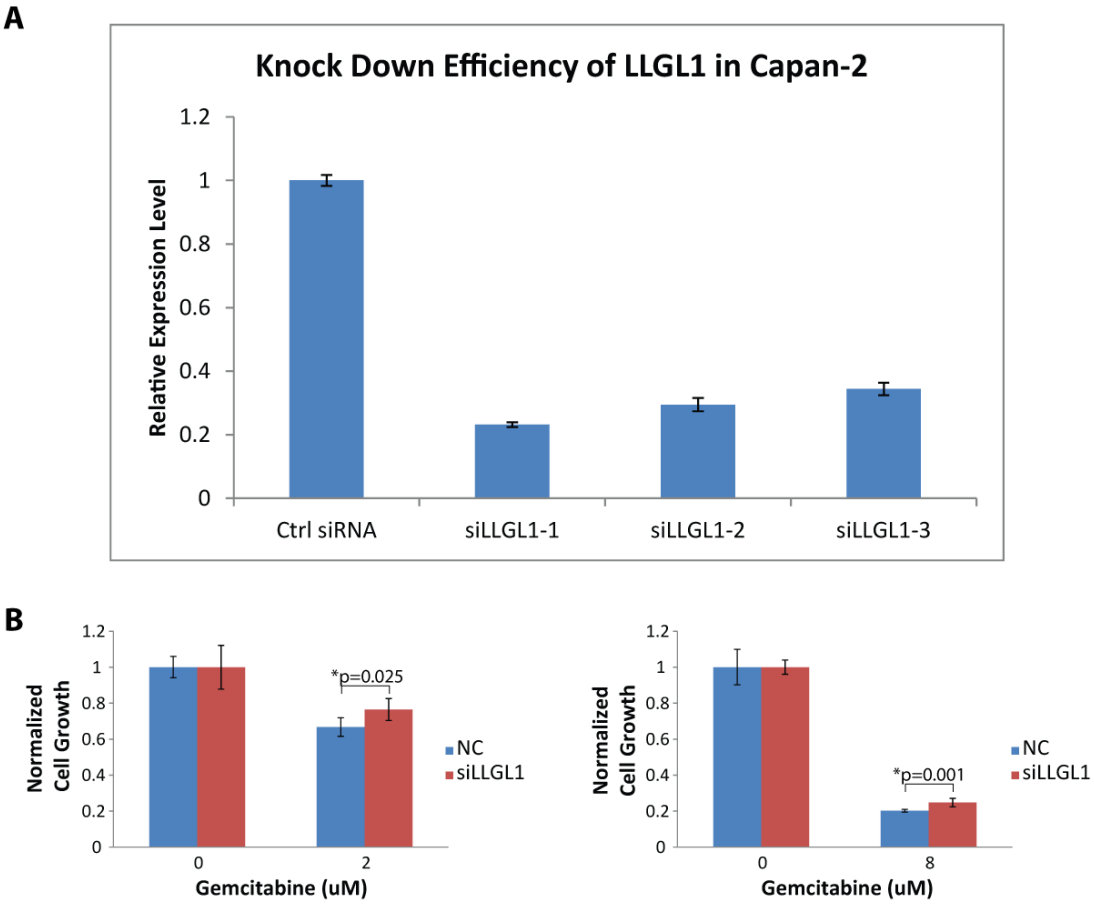

Figure 17: Validation of LLGL1 as a gemcitabine sensitivity gene

(A) Knockdown efficiency of LLGL1 by transient transfection of siRNA in capan-2 cells.

(B) MTT assays revealed that down-regulation of LLGL1 effectively induced resistance of capan-2 to gemcitabine.

Figure 18.

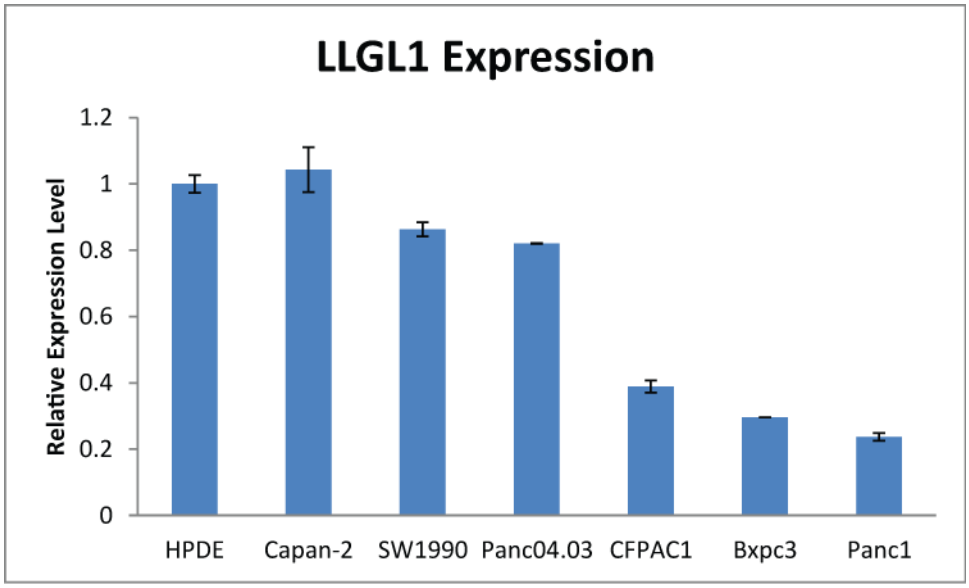

Figure 18: LLGL1 expression in human PDAC cell lines and normal pancreatic ductal cell line.

LLGL1 expression levels in PDAC cell lines were positively correlated with their sensitivity to gemcitabine. Sensitivity of cells to gemcitabine: Capan-2 > Bxpc3 > Panc1. Relative mRNA expression of LLGL1 was measured by qPCR for human PDAC cell lines (Capan-2, SW1990, Panc04.03, CFPAC1, Bxpc3, and Panc1) and a human pancreatic duct epithelial cell line HPDE.

4. Discussion

Metastasis is the major cause of cancer death and it is a complicated process. To identify novel metastasis suppressor genes, we carried out a forward whole-genome screening in a mouse model.

To begin with our work, we firstly established an in vivo screening system, which was based on an orthotopic pancreatic cancer mouse model. This model possesses advantages for many reasons. Firstly, pancreatic cnacer cells were directly transplanted in the pancreas of a mouse. Thus the model best simulated the original microenvironment for a tumor to grow, which may provide substantially more valuable data and less false positive results than in vitro assays. Secondly, tumor cells transplanted in the primary site should overcome all difficulties that suppress metastasis to disseminate. The cell line we used in the screening was capan-2, which was of low metastatic potential. Therefore capan-2 is suitable for screening a metastasis suppressor gene, based on the rationale that knockdown of a metastasis suppressor gene would facilitate cell metastasis.

Using a genome-wide loss-of-function screenitng, we found SOX9 as a potential metastasis suppressor gene. Through an in vivo validation experiment, we proved that down-regulation of SOX9 enhanced the occurrence of liver metastasis of pancreatic cancer with capan-2 cells. This indicated that SOX9 was a metastasis

suppressor gene for pancreatic cancer cell capan-2.

Capan-2 is of low metastatic potential, but it is unclear in which step of metastasis capan-2 is defective. Thus we have to investigate into SOX9's effect on various cellular functions that are relevant to metastasis. From the results we have achieved, we found in vitro that knocking-down SOX9 promoted cell migration but did not significantly favor cell proliferation or colonization. These findings suggested that probably SOX9 suppressed metastasis through modulation of cell migration. However, the mechanism underlying SOX9's function in metastasis is far from elucidated. The downstream target genes and signaling pathways of SOX9 that play a role in cell survival, EMT, invasion, and angiogenesis may also affect metastatic activity. Besides, what causes SOX9 down-regulation to induce metastasis still remains to be explored. All of these aspects can be considered as future directions.

Metastasis is a complex multi-step process. Difficulties in any steps within the process may prohibit a cancer cell to grow in a distant location. Unfortunately, current methods for the study of cancer metastasis are limited. Additionally, current research methods we used to evaluate cellular functions mainly relied on two-dimensional (2D) substrates. But the real environment of metastasis is on three-dimensional (3D) basis, where interplay between cancer cells and extracellular

matrix is important. It has been reported that some cell types have drastically different performance between 2-D and 3-D environment (Fraley, 2011). Nowadays, we are still in great need of appropriate approaches to study metastasis. If the cell line used in the screening has a known defect during the processes of metastasis, the results from the screening could provide a more specific answer for the mechanisms. Admittedly, our screening and validation were conducted on a single cell line, which was not convincing enough to show the function of SOX9 in human PDAC. Using different PDAC cell lines for validation will provide much stronger evidence to prove SOX9 as metastasis suppressor gene in human PDAC.

Fortunately, we observed a correlation between SOX9 expression level and metastatic status in clinical samples of pancreatic cancer patients. On the one hand, we confirmed the relatively high expression level of SOX9 in normal pancreas duct cells, which was concordant with data published by other research groups, implying an important role of SOX9 in maintaining normal function of pancreas duct cells. On the other hand, we observed a decreased expression of SOX9 in metastatic PDAC compared to non-metastatic PDAC. This result implied that loss of SOX9 expression was relevant to the occurrence of pancreatic cancer metastasis, which further supported our statement that SOX9 was a metastasis suppressor gene in human PDAC.

Regardless of the mechanisms of SOX9 in modulating metastasis, if a good correlation between SOX9 expression level and metastatic status really exists, SOX9 may be served as a biomarker as well to predict metastasis and prognosis for patients. However, in this situation, analysis of data from a larger sample pool is in great need for the identification of SOX9 as a biomarker.

Last but not the least, in vitro genome-wide RNAi screening revealed a novel gene to be associated with gemcitabine resistance in pancreatic cancer cells. Although gemcitabine still stands for the first choice of chemotherapeutic agent for PDAC, the noticeable problems derived from gemcitabine resistance profoundly impede our progress in improving the prognosis of pancreatic cancer. Current research into the mechanisms of gemcitabine resistance mainly focuses in the defects through steps involving in gemcitabine uptake or metabolism. Treatment strategies targeting these defects have shown limited effect in improving the outcome of PDAC. Considering this difficult situation, we attempted to discover novel genes responsible for gemcitabine resistance on a genome-wide scale.

In our screening, LLGL1 was identified as a gemcitabine sensitivity gene. LLGL1 is similar to a tumor suppressor gene in Drosophila. It has been reported that its expression is lost in several human solid tumors (Grifoni, 2004). A research group found that mutation of LLGL1 was frequently found in HCC and abnormal

expression of LLGL1 was associated with poor HCC differentiation, larger tumor size and invasive feature (Lu, 2009). But little literature has been published on LLGL1's implication in human PDAC. Here we found that LLGL1 expression level was positively correlated with PDAC cells' sensitivity to gemcitabine. And we also reported down-regulation of LLGL1 rendered capan-2 cells more resistant to gemcitabine. These results indicated LLGL1 to be the gemcitabine sensitivity gene in pancreatic cancer. Admittedly, the effect of LLGL1 knockdown on gemcitabine resistance that we obtained was far from satisfied. Possibly it is due to the unstable knockdown effect of transient transfection of siRNA. And the fluctuated knockdown efficiency limited the application of functional assays. We are going to generate a stable cell line with LLGL1 knocked down for follow-up studies. On the other hand, given the nature of microarray analysis, there were a large number of false positive results, which disturbed our decision. Currently we only pick limited targets from numerous candidate genes to perform validation experiments, which further restrained successful validation. Although the effect of LLGL1 knockdown on gemcitabine resistant was modest, it still provided some new ideas for targeted therapy in pancreatic cancer.

General conclusions

To summarize the two parts of my study,

(1) We have confirmed the anti-cancer effect of Brucein D on liver cancer through both in vitro and in vivo experiments. It further strengthened BD's therapeutic potential for cancers.

(2) We proposed a possible mechanism for BD-modulated growth inhibition. That was BD inhibits miR-95, then results in restoration of CUGBP2 and thus induces apoptosis for HCC cells. The identification of miR-95 as a target of BD is novel, which provided new insights into research of cancer therapy.

(3) We have identified SOX9 as a metastasis suppressor gene in a pancreatic cancer mouse model with capan-2 cells. And we also observed a correlation between SOX9 expression level and metastatic status of human pancreatic cancer. SOX9 may serve as a new biomarker for pancreatic cancer prognosis and has therapeutic potential for human PDAC management.

(4) We suggested LLGL1 to be a gemcitabine sensitivity gene in PDAC. It may be a novel therapeutic target for pancreatic cancer chemotherapy.

Reference

Abdel-Samad, R., H. Zalzali, et al. "MiniSOX9, a dominant-negative variant in colon cancer cells." Oncogene **30**(22): 2493-503.

Afonja, O., B. M. Raaka, et al. (2002). "RAR agonists stimulate SOX9 gene expression in breast cancer cell lines: evidence for a role in retinoid-mediated growth inhibition." Oncogene **21**(51): 7850-60.

Aguilar, F., S. P. Hussain, et al. (1993). "Aflatoxin B1 induces the transversion of G-->T in codon 249 of the p53 tumor suppressor gene in human hepatocytes." Proc Natl Acad Sci U S A **90**(18): 8586-90.

Ahrendt, S. A. and H. A. Pitt (2002). "Surgical management of pancreatic cancer." Oncology (Williston Park) **16**(6): 725-34; discussion 734, 736-8, 740, 743.

Akiyama, H., M. C. Chaboissier, et al. (2002). "The transcription factor Sox9 has essential roles in successive steps of the chondrocyte differentiation pathway and is required for expression of Sox5 and Sox6." Genes Dev **16**(21): 2813-28.

Aleman, A., L. Adrien, et al. (2008). "Identification of DNA hypermethylation of SOX9 in association with bladder cancer progression using CpG microarrays." Br J Cancer **98**(2): 466-73.

Altekruse, S. F., K. A. McGlynn, et al. (2009). "Hepatocellular carcinoma incidence, mortality, and survival trends in the United States from 1975 to 2005." J Clin Oncol **27**(9): 1485-91.

Andersson, R., U. Aho, et al. (2009). "Gemcitabine chemoresistance in pancreatic cancer: molecular mechanisms and potential solutions." Scand J Gastroenterol **44**(7): 782-6.

Andersson, R., C. E. Vagianos, et al. (2004). "Preoperative staging and evaluation of resectability in pancreatic ductal adenocarcinoma." HPB (Oxford) **6**(1): 5-12.

Antoniou, A., P. Raynaud, et al. (2009). "Intrahepatic bile ducts develop according to a new mode of tubulogenesis regulated by the transcription factor SOX9." Gastroenterology **136**(7): 2325-33.

Bardeesy, N. and R. A. DePinho (2002). "Pancreatic cancer biology and genetics." Nat Rev Cancer **2**(12): 897-909.

Bartel, D. P. (2004). "MicroRNAs: genomics, biogenesis, mechanism, and function." Cell **116**(2): 281-97.

Beasley, R. P., L. Y. Hwang, et al. (1981). "Hepatocellular carcinoma and hepatitis B virus. A prospective study of 22 707 men in Taiwan." Lancet **2**(8256): 1129-33.

Biankin, A. V., J. G. Kench, et al. (2001). "Overexpression of p21(WAF1/CIP1) is an

early event in the development of pancreatic intraepithelial neoplasia." Cancer Res **61**(24): 8830-7.

Blache, P., M. van de Wetering, et al. (2004). "SOX9 is an intestine crypt transcription factor, is regulated by the Wnt pathway, and represses the CDX2 and MUC2 genes." J Cell Biol **166**(1): 37-47.

Bosch, F. X., J. Ribes, et al. (1999). "Epidemiology of primary liver cancer." Semin Liver Dis **19**(3): 271-85.

Bosetti, C., F. Levi, et al. (2008). "Trends in mortality from hepatocellular carcinoma in Europe, 1980-2004." Hepatology **48**(1): 137-45.

Budhu, A., H. L. Jia, et al. (2008). "Identification of metastasis-related microRNAs in hepatocellular carcinoma." Hepatology **47**(3): 897-907.

Burris, H. A., 3rd, M. J. Moore, et al. (1997). "Improvements in survival and clinical benefit with gemcitabine as first-line therapy for patients with advanced pancreas cancer: a randomized trial." J Clin Oncol **15**(6): 2403-13.

Cai, Z., T. J. Liang, et al. (2004). "Effects of mutations of the initiation nucleotides on hepatitis C virus RNA replication in the cell." J Virol **78**(7): 3633-43.

Cavard, C., S. Colnot, et al. (2008). "Wnt/beta-catenin pathway in hepatocellular carcinoma pathogenesis and liver physiology." Future Oncol **4**(5): 647-60.

Chaboissier, M. C., A. Kobayashi, et al. (2004). "Functional analysis of Sox8 and Sox9 during sex determination in the mouse." Development **131**(9): 1891-901.

Chakravarty, G., K. Moroz, et al. "Prognostic significance of cytoplasmic SOX9 in invasive ductal carcinoma and metastatic breast cancer." Exp Biol Med (Maywood) **236**(2): 145-55.

Chambers, A. F., A. C. Groom, et al. (2002). "Dissemination and growth of cancer cells in metastatic sites." Nat Rev Cancer **2**(8): 563-72.

Cheng, A. M., M. W. Byrom, et al. (2005). "Antisense inhibition of human miRNAs and indications for an involvement of miRNA in cell growth and apoptosis." Nucleic Acids Res **33**(4): 1290-7.

Chin, L., S. E. Artandi, et al. (1999). "p53 deficiency rescues the adverse effects of telomere loss and cooperates with telomere dysfunction to accelerate carcinogenesis." Cell **97**(4): 527-38.

Cimmino, A., G. A. Calin, et al. (2005). "miR-15 and miR-16 induce apoptosis by targeting BCL2." Proc Natl Acad Sci U S A **102**(39): 13944-9.

Danial, N. N. and S. J. Korsmeyer (2004). "Cell death: critical control points." Cell **116**(2): 205-19.

Devarajan, E., A. A. Sahin, et al. (2002). "Down-regulation of caspase 3 in breast cancer: a possible mechanism for chemoresistance." Oncogene **21**(57): 8843-

51.

El-Serag, H. B. (2007). "Epidemiology of hepatocellular carcinoma in USA." Hepatol Res **37 Suppl 2**: S88-94.

Ferlay, J., H. R. Shin, et al. "Estimates of worldwide burden of cancer in 2008: GLOBOCAN 2008." Int J Cancer.

Fidler, I. J. (2003). "The pathogenesis of cancer metastasis: the 'seed and soil' hypothesis revisited." Nat Rev Cancer **3**(6): 453-8.

Fong, P. Y., W. C. Xue, et al. (2006). "Caspase activity is downregulated in choriocarcinoma: a cDNA array differential expression study." J Clin Pathol **59**(2): 179-83.

Foster, J. W., M. A. Dominguez-Steglich, et al. (1994). "Campomelic dysplasia and autosomal sex reversal caused by mutations in an SRY-related gene." Nature **372**(6506): 525-30.

Friess, H., P. Berberat, et al. (1996). "Pancreatic cancer: the potential clinical relevance of alterations in growth factors and their receptors." J Mol Med (Berl) **74**(1): 35-42.

Fulda, S., E. Meyer, et al. (2002). "Inhibition of TRAIL-induced apoptosis by Bcl-2 overexpression." Oncogene **21**(15): 2283-94.

Furuyama, K., Y. Kawaguchi, et al. "Continuous cell supply from a Sox9-expressing progenitor zone in adult liver, exocrine pancreas and intestine." Nat Genet **43**(1): 34-41.

Garcia-Manteiga, J., M. Molina-Arcas, et al. (2003). "Nucleoside transporter profiles in human pancreatic cancer cells: role of hCNT1 in 2',2'-difluorodeoxycytidine- induced cytotoxicity." Clin Cancer Res **9**(13): 5000-8.

Ghobrial, I. M., T. E. Witzig, et al. (2005). "Targeting apoptosis pathways in cancer therapy." CA Cancer J Clin **55**(3): 178-94.

Giovannetti, E., M. Del Tacca, et al. (2006). "Transcription analysis of human equilibrative nucleoside transporter-1 predicts survival in pancreas cancer patients treated with gemcitabine." Cancer Res **66**(7): 3928-35.

Gisselsson, D., T. Jonson, et al. (2001). "Telomere dysfunction triggers extensive DNA fragmentation and evolution of complex chromosome abnormalities in human malignant tumors." Proc Natl Acad Sci U S A **98**(22): 12683-8.

Gorunova, L., M. Hoglund, et al. (1998). "Cytogenetic analysis of pancreatic carcinomas: intratumor heterogeneity and nonrandom pattern of chromosome aberrations." Genes Chromosomes Cancer **23**(2): 81-99.

Gregory, R. I., T. P. Chendrimada, et al. (2006). "MicroRNA biogenesis: isolation and characterization of the microprocessor complex." Methods Mol Biol

342: 33-47.

Grifoni, D., F. Garoia, et al. (2004). "The human protein Hugl-1 substitutes for Drosophila lethal giant larvae tumour suppressor function in vivo." Oncogene **23**(53): 8688-94.

Gross, A., J. M. McDonnell, et al. (1999). "BCL-2 family members and the mitochondria in apoptosis." Genes Dev **13**(15): 1899-911.

Hanahan, D. and R. A. Weinberg "Hallmarks of cancer: the next generation." Cell **144**(5): 646-74.

Hengartner, M. O. (2001). "Apoptosis: corralling the corpses." Cell **104**(3): 325-8.

Homayounfar, K., B. Gunawan, et al. (2009). "Pattern of chromosomal aberrations in primary liver cancers identified by comparative genomic hybridization." Hum Pathol **40**(6): 834-42.

Houston, C. S., J. M. Opitz, et al. (1983). "The campomelic syndrome: review, report of 17 cases, and follow-up on the currently 17-year-old boy first reported by Maroteaux et al in 1971." Am J Med Genet **15**(1): 3-28.

Hu, Z., J. Chen, et al. (2008). "Genetic variants of miRNA sequences and non-small cell lung cancer survival." J Clin Invest **118**(7): 2600-8.

Huang, P., S. Chubb, et al. (1991). "Action of 2',2'-difluorodeoxycytidine on DNA synthesis." Cancer Res **51**(22): 6110-7.

Huang, Z., S. Huang, et al. "MicroRNA-95 promotes cell proliferation and targets sorting Nexin 1 in human colorectal carcinoma." Cancer Res **71**(7): 2582-9.

Hussain, S. P. and C. C. Harris (2006). "p53 biological network: at the crossroads of the cellular-stress response pathway and molecular carcinogenesis." J Nihon Med Sch **73**(2): 54-64.

Hynes, R. O. (2003). "Metastatic potential: generic predisposition of the primary tumor or rare, metastatic variants-or both?" Cell **113**(7): 821-3.

Ishii, H., J. Furuse, et al. (2005). "Impact of gemcitabine on the treatment of metastatic pancreatic cancer." J Gastroenterol Hepatol **20**(1): 62-6.

Jay, P., P. Berta, et al. (2005). "Expression of the carcinoembryonic antigen gene is inhibited by SOX9 in human colon carcinoma cells." Cancer Res **65**(6): 2193-8.

Jemal, A., F. Bray, et al. "Global cancer statistics." CA Cancer J Clin **61**(2): 69-90.

Jemal, A., R. Siegel, et al. (2007). "Cancer statistics, 2007." CA Cancer J Clin **57**(1): 43-66.

Jemal, A., R. C. Tiwari, et al. (2004). "Cancer statistics, 2004." CA Cancer J Clin **54**(1): 8-29.

Ji, J., J. Shi, et al. (2009). "MicroRNA expression, survival, and response to interferon in liver cancer." N Engl J Med **361**(15): 1437-47.

Ji, J., T. Yamashita, et al. (2009). "Identification of microRNA-181 by genome-wide screening as a critical player in EpCAM-positive hepatic cancer stem cells." Hepatology **50**(2): 472-80.

Ji, J., L. Zhao, et al. "Let-7g targets collagen type I alpha2 and inhibits cell migration in hepatocellular carcinoma." J Hepatol **52**(5): 690-7.

Jiang, S. S., W. T. Fang, et al. "Upregulation of SOX9 in lung adenocarcinoma and its involvement in the regulation of cell growth and tumorigenicity." Clin Cancer Res **16**(17): 4363-73.

Jones, P. A. (2002). "DNA methylation and cancer." Oncogene **21**(35): 5358-60.

Joyce, J. A. and J. W. Pollard (2009). "Microenvironmental regulation of metastasis." Nat Rev Cancer **9**(4): 239-52.

Kamachi, Y., M. Uchikawa, et al. (2000). "Pairing SOX off: with partners in the regulation of embryonic development." Trends Genet **16**(4): 182-7.

Katoh, M. (2008). "Cancer genomics and genetics of FGFR2 (Review)." Int J Oncol **33**(2): 233-7.

Kim, M. P. and G. E. Gallick (2008). "Gemcitabine resistance in pancreatic cancer: picking the key players." Clin Cancer Res **14**(5): 1284-5.

Korc, M., B. Chandrasekar, et al. (1992). "Overexpression of the epidermal growth factor receptor in human pancreatic cancer is associated with concomitant increases in the levels of epidermal growth factor and transforming growth factor alpha." J Clin Invest **90**(4): 1352-60.

Krepela, E., P. Dankova, et al. (2009). "Increased expression of inhibitor of apoptosis proteins, survivin and XIAP, in non-small cell lung carcinoma." Int J Oncol **35**(6): 1449-62.

Kroemer, G., W. S. El-Deiry, et al. (2005). "Classification of cell death: recommendations of the Nomenclature Committee on Cell Death." Cell Death Differ **12 Suppl 2**: 1463-7.

Kroemer, G., L. Galluzzi, et al. (2007). "Mitochondrial membrane permeabilization in cell death." Physiol Rev **87**(1): 99-163.

Kroep, J. R., W. J. Loves, et al. (2002). "Pretreatment deoxycytidine kinase levels predict in vivo gemcitabine sensitivity." Mol Cancer Ther **1**(6): 371-6.

Kumar, M., X. Zhao, et al. "Molecular carcinogenesis of hepatocellular carcinoma and intrahepatic cholangiocarcinoma: one step closer to personalized medicine?" Cell Biosci **1**(1): 5.

Lagos-Quintana, M., R. Rauhut, et al. (2003). "New microRNAs from mouse and human." RNA **9**(2): 175-9.

Larsen, F., G. Gundersen, et al. (1992). "Choice of enzymes for mapping based on CpG islands in the human genome." Genet Anal Tech Appl **9**(3): 80-5.

Lau, S. T., Z. X. Lin, et al. "Role of reactive oxygen species in brucein D-mediated p38-mitogen-activated protein kinase and nuclear factor-kappaB signalling pathways in human pancreatic adenocarcinoma cells." Br J Cancer **102**(3): 583-93.

Lau, S. T., Z. X. Lin, et al. (2009). "Bruceine D induces apoptosis in pancreatic adenocarcinoma cell line PANC-1 through the activation of p38-mitogen activated protein kinase." Cancer Lett **281**(1): 42-52.

Lavrik, I. N., A. Golks, et al. (2005). "Caspases: pharmacological manipulation of cell death." J Clin Invest **115**(10): 2665-72.

Lee, Y., M. Kim, et al. (2004). "MicroRNA genes are transcribed by RNA polymerase II." EMBO J **23**(20): 4051-60.

Li, D., K. Xie, et al. (2004). "Pancreatic cancer." Lancet **363**(9414): 1049-57.

Liau, S. S. and E. Whang (2008). "HMGA1 is a molecular determinant of chemoresistance to gemcitabine in pancreatic adenocarcinoma." Clin Cancer Res **14**(5): 1470-7.

Liu, L., J. Li, et al. (2009). "[Research progress on the regulational role of microRNA in virus infection]." Bing Du Xue Bao **25**(6): 485-9.

Llovet, J. M., A. Burroughs, et al. (2003). "Hepatocellular carcinoma." Lancet **362**(9399): 1907-17.

Lopes, R. B., R. Gangeswaran, et al. (2007). "Expression of the IAP protein family is dysregulated in pancreatic cancer cells and is important for resistance to chemotherapy." Int J Cancer **120**(11): 2344-52.

Lu, X., X. Feng, et al. (2009). "Aberrant splicing of Hugl-1 is associated with hepatocellular carcinoma progression." Clin Cancer Res **15**(10): 3287-96.

Lund, E., S. Guttinger, et al. (2004). "Nuclear export of microRNA precursors." Science **303**(5654): 95-8.

Lynn, F. C., S. B. Smith, et al. (2007). "Sox9 coordinates a transcriptional network in pancreatic progenitor cells." Proc Natl Acad Sci U S A **104**(25): 10500-5.

Mackey, J. R., R. S. Mani, et al. (1998). "Functional nucleoside transporters are required for gemcitabine influx and manifestation of toxicity in cancer cell lines." Cancer Res **58**(19): 4349-57.

McCarthy, N. J. and G. I. Evan (1998). "Methods for detecting and quantifying apoptosis." Curr Top Dev Biol **36**: 259-78.

McLaughlin, J., D. Cheng, et al. (2007). "Sustained suppression of Bcr-Abl-driven lymphoid leukemia by microRNA mimics." Proc Natl Acad Sci U S A **104**(51): 20501-6.

Meng, F., R. Henson, et al. (2007). "MicroRNA-21 regulates expression of the PTEN tumor suppressor gene in human hepatocellular cancer."

Gastroenterology **133**(2): 647-58.

Ming, L., S. S. Thorgeirsson, et al. (2002). "Dominant role of hepatitis B virus and cofactor role of aflatoxin in hepatocarcinogenesis in Qidong, China." Hepatology **36**(5): 1214-20.

Miquel, C., F. Borrini, et al. (2005). "Role of bax mutations in apoptosis in colorectal cancers with microsatellite instability." Am J Clin Pathol **123**(4): 562-70.

Moore, L. D., T. Isayeva, et al. (2008). "Silencing of transforming growth factor-beta1 in situ by RNA interference for breast cancer: implications for proliferation and migration in vitro and metastasis in vivo." Clin Cancer Res **14**(15): 4961-70.

Mukhopadhyay, D., J. Jung, et al. (2003). "CUGBP2 plays a critical role in apoptosis of breast cancer cells in response to genotoxic injury." Ann N Y Acad Sci **1010**: 504-9.

Muller, P., J. D. Crofts, et al. "SOX9 mediates the retinoic acid-induced HES-1 gene expression in human breast cancer cells." Breast Cancer Res Treat **120**(2): 317-26.

Nakanishi, K., M. Sakamoto, et al. (2005). "Akt phosphorylation is a risk factor for early disease recurrence and poor prognosis in hepatocellular carcinoma." Cancer **103**(2): 307-12.

Natarajan, G., S. Ramalingam, et al. (2008). "CUGBP2 downregulation by prostaglandin E2 protects colon cancer cells from radiation-induced mitotic catastrophe." Am J Physiol Gastrointest Liver Physiol **294**(5): G1235-44.

Neoptolemos, J. P., D. D. Stocken, et al. (2004). "A randomized trial of chemoradiotherapy and chemotherapy after resection of pancreatic cancer." N Engl J Med **350**(12): 1200-10.

Okada, M., A. Tessier, et al. (2006). "P53 mutants suppress ZBP-89 function." Anticancer Res **26**(3A): 2023-8.

Olsen, P. H. and V. Ambros (1999). "The lin-4 regulatory RNA controls developmental timing in Caenorhabditis elegans by blocking LIN-14 protein synthesis after the initiation of translation." Dev Biol **216**(2): 671-80.

Parkin, D. M. (2006). "The global health burden of infection-associated cancers in the year 2002." Int J Cancer **118**(12): 3030-44.

Parkin, D. M. and C. S. Muir (1992). "Cancer Incidence in Five Continents. Comparability and quality of data." IARC Sci Publ(120): 45-173.

Passeron, T., J. C. Valencia, et al. (2009). "Upregulation of SOX9 inhibits the growth of human and mouse melanomas and restores their sensitivity to retinoic acid." J Clin Invest **119**(4): 954-63.

Perz, J. F., G. L. Armstrong, et al. (2006). "The contributions of hepatitis B virus and hepatitis C virus infections to cirrhosis and primary liver cancer worldwide." J Hepatol **45**(4): 529-38.

Raffo, A. J., H. Perlman, et al. (1995). "Overexpression of bcl-2 protects prostate cancer cells from apoptosis in vitro and confers resistance to androgen depletion in vivo." Cancer Res **55**(19): 4438-45.

Rebouissou, S., M. Amessou, et al. (2009). "Frequent in-frame somatic deletions activate gp130 in inflammatory hepatocellular tumours." Nature **457**(7226): 200-4.

Reed, J. C. (1997). "Bcl-2 family proteins: regulators of apoptosis and chemoresistance in hematologic malignancies." Semin Hematol **34**(4 Suppl 5): 9-19.

Reed, J. C. (2000). Apoptosis. San Diego, Calif., Academic Press.

Robbins, S. L., V. Kumar, et al. Robbins and Cotran pathologic basis of disease. Philadelphia, PA, Saunders/Elsevier.

Rozenblum, E., M. Schutte, et al. (1997). "Tumor-suppressive pathways in pancreatic carcinoma." Cancer Res **57**(9): 1731-4.

Ruiz van Haperen, V. W., G. Veerman, et al. (1994). "Schedule dependence of sensitivity to 2',2'-difluorodeoxycytidine (Gemcitabine) in relation to accumulation and retention of its triphosphate in solid tumour cell lines and solid tumours." Biochem Pharmacol **48**(7): 1327-39.

Ruiz van Haperen, V. W., G. Veerman, et al. (1993). "2',2'-Difluoro-deoxycytidine (gemcitabine) incorporation into RNA and DNA of tumour cell lines." Biochem Pharmacol **46**(4): 762-6.

Sahai, E. (2007). "Illuminating the metastatic process." Nat Rev Cancer **7**(10): 737-49.

Shen, X. G., C. Wang, et al. "Downregulation of caspase-9 is a frequent event in patients with stage II colorectal cancer and correlates with poor clinical outcome." Colorectal Dis **12**(12): 1213-8.

Sherr, C. J. (2001). "The INK4a/ARF network in tumour suppression." Nat Rev Mol Cell Biol **2**(10): 731-7.

Shields, J. M., K. Pruitt, et al. (2000). "Understanding Ras: 'it ain't over 'til it's over'." Trends Cell Biol **10**(4): 147-54.

Shin, H. R., J. K. Oh, et al. "Epidemiology of cholangiocarcinoma: an update focusing on risk factors." Cancer Sci **101**(3): 579-85.

Sibilia, M., A. Fleischmann, et al. (2000). "The EGF receptor provides an essential survival signal for SOS-dependent skin tumor development." Cell **102**(2): 211-20.

Spratlin, J., R. Sangha, et al. (2004). "The absence of human equilibrative nucleoside transporter 1 is associated with reduced survival in patients with gemcitabine-treated pancreas adenocarcinoma." Clin Cancer Res **10**(20): 6956-61.

Stolt, C. C., P. Lommes, et al. (2003). "The Sox9 transcription factor determines glial fate choice in the developing spinal cord." Genes Dev **17**(13): 1677-89.

Szegezdi, E., U. Fitzgerald, et al. (2003). "Caspase-12 and ER-stress-mediated apoptosis: the story so far." Ann N Y Acad Sci **1010**: 186-94.

Tang, G. (2005). "siRNA and miRNA: an insight into RISCs." Trends Biochem Sci **30**(2): 106-14.

Tang, Y., K. Kitisin, et al. (2008). "Progenitor/stem cells give rise to liver cancer due to aberrant TGF-beta and IL-6 signaling." Proc Natl Acad Sci U S A **105**(7): 2445-50.

Tykocinski, M. L. and E. E. Max (1984). "CG dinucleotide clusters in MHC genes and in 5' demethylated genes." Nucleic Acids Res **12**(10): 4385-96.

Varnholt, H. (2008). "The role of microRNAs in primary liver cancer." Ann Hepatol **7**(2): 104-13.

Vucic, D., H. R. Stennicke, et al. (2000). "ML-IAP, a novel inhibitor of apoptosis that is preferentially expressed in human melanomas." Curr Biol **10**(21): 1359-66.

Wang, B., S. H. Hsu, et al. "TGFbeta-mediated upregulation of hepatic miR-181b promotes hepatocarcinogenesis by targeting TIMP3." Oncogene **29**(12): 1787-97.

Wang, H., I. Leav, et al. (2008). "SOX9 is expressed in human fetal prostate epithelium and enhances prostate cancer invasion." Cancer Res **68**(6): 1625-30.

Wang, X. W., K. Forrester, et al. (1994). "Hepatitis B virus X protein inhibits p53 sequence-specific DNA binding, transcriptional activity, and association with transcription factor ERCC3." Proc Natl Acad Sci U S A **91**(6): 2230-4.

Wong, R. S. "Apoptosis in cancer: from pathogenesis to treatment." J Exp Clin Cancer Res **30**: 87.

Xie, X., J. Lu, et al. (2005). "Systematic discovery of regulatory motifs in human promoters and 3' UTRs by comparison of several mammals." Nature **434**(7031): 338-45.

Xu, Z., W. Wang, et al. (2009). "Aberrant p63 and WT-1 expression in myoepithelial cells of pregnancy-associated breast cancer: implications for tumor aggressiveness and invasiveness." Int J Biol Sci **5**(1): 82-96.

Yekta, S., I. H. Shih, et al. (2004). "MicroRNA-directed cleavage of HOXB8

mRNA." Science **304**(5670): 594-6.

Zalzali, H., C. Naudin, et al. (2008). "CEACAM1, a SOX9 direct transcriptional target identified in the colon epithelium." Oncogene **27**(56): 7131-8.

Zardawi, S. J., S. A. O'Toole, et al. (2009). "Dysregulation of Hedgehog, Wnt and Notch signalling pathways in breast cancer." Histol Histopathol **24**(3): 385-98.

Zhang, Y., M. Li, et al. (2009). "Profiling of 95 microRNAs in pancreatic cancer cell lines and surgical specimens by real-time PCR analysis." World J Surg **33**(4): 698-709.